PETROLOGY, PROVENANCE AND DEPOSITIONAL ENVIRONMENT OF BHUBAN FORMATION IN AND AROUND LUNGLEI TOWN, LUNGLEI DISTRICT, MIZORAM

A THESIS SUBMITTED IN PARTIAL FULFILLMENT OF THE REQUIREMENTS FOR THE DEGREE OF DOCTOR OF PHILOSOPHY

K. LALDUHAWMA
MZU REGISTRATION NO.: 1607309
Ph.D. REGISTRATION NO.: MZU/Ph.D./1043 of 31.05.2017

DEPARTMENT OF GEOLOGY
SCHOOL OF EARTH SCIENCES AND NATURAL RESOURCES MANAGEMENT

MAY, 2024

PETROLOGY, PROVENANCE AND DEPOSITIONAL ENVIRONMENT OF BHUBAN FORMATION IN AND AROUND LUNGLEI TOWN, LUNGLEI DISTRICT, MIZORAM

BY

K. LALDUHAWMA
DEPARTMENT OF GEOLOGY

NAME OF SUPERVISOR
Dr. V. VANTHANGLIANA

NAME OF JOINT SUPERVISOR
Prof. SHIVA KUMAR

Submitted
In partial fulfillment of the requirement of the Degree of Doctor of Philosophy in Geology of Mizoram University, Aizawl.

DEPARTMENT OF GEOLOGY

PACHHUNGA UNIVERSITY COLLEGE

(A CONSTITUENT COLLEGE OF MIZORAM UNIVERSITY)

Dr.V.Vanthangliana AIZAWL-796001: MIZORAM

SUPERVISOR'S CERTIFICATE

This is to certify that **K. Lalduhawma**, a Ph.D. scholar having MZU Registration No. **1607309** and Ph.D. Registration No. **MZU/Ph.D/1043 of 31.05.2017** has completed a thesis on **"Petrology, provenance and depositional environment of Bhuban formation in and around Lunglei Town, Lunglei District, Mizoram"** under my supervision and guidance. This thesis work is a part of fulfilment of the requirements for the Degree of Doctor of Philosophy in Geology of Mizoram University, Aizawl. No part of the study has been published nor presented earlier elsewhere.

Signature and seal of Supervisors

(Dr. V. VANTHANGLIANA) (Prof. SHIVA KUMAR)

Supervisor Joint Supervisor

DECLARATION

MIZORAM UNIVERSITY

MAY, 2024

I **K. LALDUHAWMA**, hereby declare that the subject matter of this thesis is the record of work done by me, that the contents of this thesis did not form basis of the award of any previous degree to me or to do the best of my knowledge to anybody else, and that the thesis has not been submitted by me for any research degree in any other University/Institute.

This is being submitted to the Mizoram University for the Degree of **Doctor of Philosophy in Geology.**

(K. LALDUHAWMA)
Research Scholar

(Dr. JIMMY LALNUNMAWIA)
Head

(Dr. V. VANTHANGLIANA)
Supervisor

ACKNOWLEDGEMENT

First and foremost, thanks be to God Almighty, for unfailing love and guidance right from the beginning of my research till the end.

My deepest gratitude goes to my guide Dr. V. Vanthangliana, who is my classmate, roommate and friend. I knew that with his guidance my research will be accomplished. He is a man who handle everything with utmost sincerity. I am very grateful to him for his patience, motivation and immense knowledge and continuous support and guidance for my research study in the field, laboratory and in writing the thesis.

A very special thanks goes to Dr. Bubul Bharali, Department of Geology, Pachhunga University College for his immense support from the beginning of my research work till the end.

I am thankful to my former guide Prof. Shiva Kumar for taking me as his scholar and for his fruitful suggestions and motivation. I wish him a happy retired life.

I am also very thankful to ZD Laltanpuia, Senior Scientist, MIRSAC for helping me to prepare geological map of study area using ArcGIS.

I am very grateful to the Principal, Lunglei Government College, for allowing me to do the research work. I am also very grateful to all my colleagues especially to the faculty member of the Department of Geology for their inspiration and support throughout the work.

I would also like to express my gratefulness to Dr. Jimmy Lalnunmawia, Head, Department of Geology, Mizoram University, and Staffs for their co-operation and providing me necessary facilities available in the department for the completion of this work.

My sincere thanks goes to the Director, Wadia Institute of Himalayan Geology, Dehradun, Sophisticated Analytical Instruments Facility (SAIF) Guwahati, Guwahati University and Dibrugarh University, who provided me the laboratory facilities to carry out the analytical experiments in their institutes.

I extend my sincere thanks to G. Lamzamuan, Research Scholar, Mizoram University, Dr. Origen MS Dawngliana and Dr. Malsawmtluangkima Hauhnar, Assistant Professor, Department of Geology, Pachhunga University College for helping and teaching me Softwares.

Last but not the least, my sincere gratitude goes to my beloved wife Lalruatkimi Hrahsel and my children Ruth Lallawmsangi, John Lallawmzuala and Grace Lallawmawmi for their endless moral support and prayer. God bless you all.

(K. LALDUHAWMA)

TABLE OF CONTENTS

LIST OF TABLES

LIST OF FIGURES

LIST OF PLATES

CHAPTER 1

INTRODUCTION

1.1 GENERAL INTRODUCTION

Geologically, the paleogene-neogene succession of Mizoram is covered by a thick mass of sedimentary rocks which is also considered as the northern extension of the Bengal basin. The total thickness of the sedimentary succession is around 8000 meters or more and has been classified into the Barail (Oligocene), the Surma (early to Middle Miocene), and the Tipam groups (late Miocene to early Pliocene), in order of superposition. The Barail rock formation is found in the eastern part of the state, comprising layers of sandstone and shale. The Surma group of rocks is subdivided into Bhuban and Bokabil formations. The best-developed and well-exposed formation covering almost the entire terrain is Bhuban rocks which account for a thickness of about 5,000 meters. The Bhuban formation is divided into Lower, Middle, and Upper units based on variations in the sand-shale ratio. Bhuban rock is mainly composed of sandstone, shale, siltstone, and mudstone, and their combinations in varying proportions. Bokabil formation which is the younger formation of the Surma group is dominantly argillaceous with grey and brown colored sandstone, siltstone, and shale, exposed in the western part of the state. Tipam group of rocks which are composed of friable, loose, and medium-grained sandstone are mainly uncovered in the northern and north-western regions of the state. The Paleogene and Neogene age sedimentary succession of Mizoram consists of repetitive alteration of arenaceous and argillaceous rock. Important rocks commonly found in the entire area include siltstone, silty-sandstone, shale, mudstone, silt with a few pockets of calcareous sandstone, shell limestone, and intraformational conglomerate (Sarkar and Nandy, 1976). The Surma basin occupies special significance in terms of its tectonic evolution and gains importance for its oil and natural gas resources.

There are many publications regarding Bhuban sandstone in Mizoram but publications made so far focus mainly on the northern part of the state. Detail geological information based on sedimentological research which focuses on

understanding the formation of sedimentary rock and the processes occurring during their initial development is still insufficient from the southern part of the state. In addition, none of the previous workers carry out detailed petrographical and textural analysis and geochemical characterization of the area. Therefore, the primary objective of the present study included detail outcrop mapping, petrological analysis, and whole-rock geochemistry. In the present study, the various methods and techniques of sedimentary analyses like petrography and geochemistry are used to decipher the mode of formation, provenance, depositional history, tectonic setting, paleo climatic condition, and nature of weathering. Diagenesis is the method by which sediments are produced by disintegration of pre-existing rocks consolidated or lithified into sedimentary rock have also been attempted in the present study.

1.2 LOCATION AND ACCESSIBILITY OF THE STUDY AREA

Mizoram lies in the northeast of India. To the east and south lie the Chin Hills and Arakan regions of Myanmar, while to the west are the Chittagong hill tracts of Bangladesh and the state of Tripura, and the states of Assam and Manipur on the north and northeast define its borders. The state of Mizoram has a total area of approximately 21,087 square kilometers and falls in the coordinates of latitudes of $21^{o}56'$N to $24^{o}31'$N and longitudes of $92^{o}16'$ to $93^{o}26'$E.

The present study area covers the whole of Lunglei town and its surrounding areas which is about 170 km from Aizawl, the capital city of Mizoram. Lunglei town is connected by National Highway No – 54. According to the 2011 census, the total population is 57,011 and it is the second-largest town in Mizoram. It is covered within the Survey of India Topo sheet Nos. 84B/9 and 84B/13 and falls within the coordinates of latitudes $22^{o}45'0"$ N to $23^{o}0'0"$ N and longitudes $92^{o}20'30"$ E to $92^{o}51'30"$ E. The map displaying the study area's location is depicted in Figure 1.1.

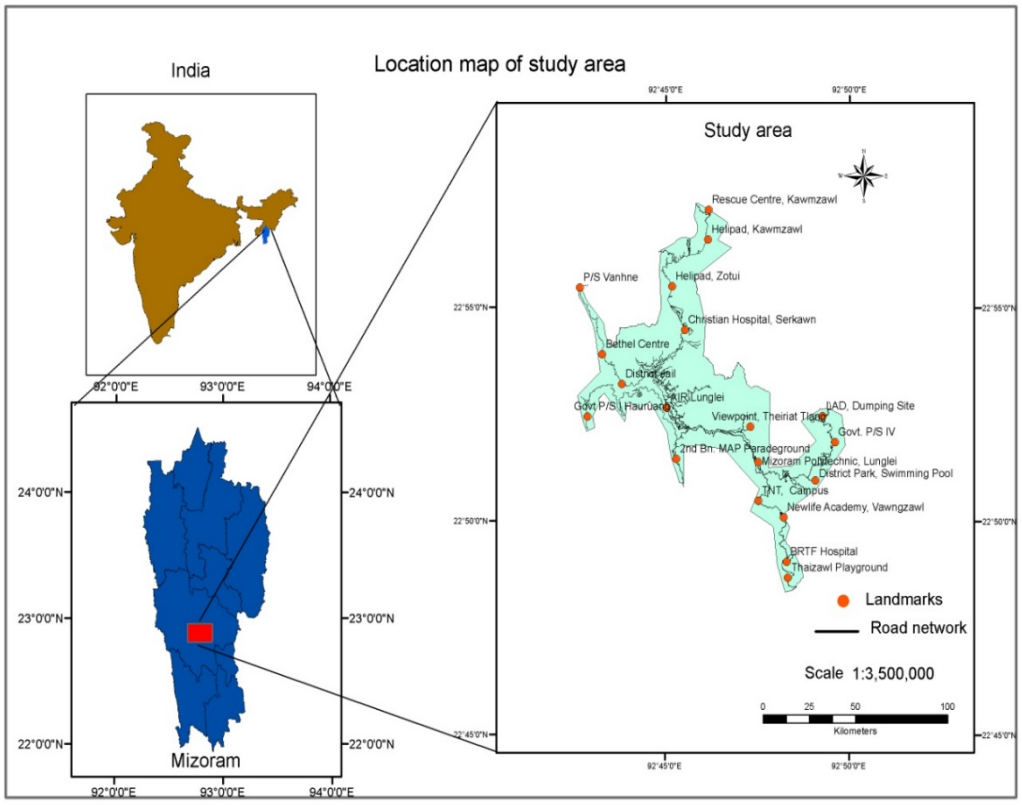

Figure 1.1: Map displaying the study area's location, Lunglei town.

1.3 CLIMATE

Mizoram witnessed a moderate climate with temperatures ranging between 21 to 35^{o}C during summer, 11 to 23^{o}C during winter, and 18 to 25^{o}C during the autumn season. The area experiences humid weather with significant rainfall during an extended summer and a short, dry winter season. Maximum rainfall occurs in the state during the southwest monsoon season, with an average of roughly 250 cm each year. The state experiences the driest months of the year in December and January, while July and August are when it receives the most rainfall. (Rintluanga, 1994).

1.4 PHYSIOGRAPHY

The Lushai hills, also known as the Mizo hills, are a group of rough, undulating mountain ranges in Mizoram that alternate between ridges and valleys with an approximate N-S to NNE-SSW trend. Due to the immature nature of the terrain some of the essential topographical characteristic features exhibit high relief with parallel to sub-parallel hill ranges and narrow valleys with several parallel

hummocks. Significant geomorphic features, such as slopes, depressions, and topographic highs, are sculpted linearly. Narrow ‘V’ shaped river valleys separate the hill ranges that are arranged linearly and create features like kneels, cols, deep gorges, and spurs due to intensive erosion during isostatic adjustment. The highly dipping fault planes interrupted by faulting that ultimately produced many steep rock scarps are found in many places. 'V' shaped, narrow valleys are interspersed with highly divided, serrated top ridges and hogback pattern ridges in numerous locations. Low linear ridges with gentle to moderate slopes formed due to gully erosion are mostly found in the western part of the state.

From the mean sea level, the average elevation of the hill ranges is about 1000 meters. The lowest point is approximately 40 meters above sea level, while the highest point reaches 2157 meters at Phawngpui, which is also known as Blue Mountain located in Lawngtlai district. Some other important high mountain ranges in the state include Lengteng (2141m), Surtlang (1967m), and Lurhtlang (1935m). In general, the elevation drops from east to west. Thus, the eastern portion of the state is home to the majority of the state's high mountain ranges. While older, more compact, and resistant formations are typically revealed in the anticlinal crests of hill ranges, younger, softer formations are typically exposed in the synclinal toughs. (Ganguly, 1975). The hilly terrains are intersected by transverse faults in many areas and are marked by steep slopes and narrow valleys.

The different types of drainage patterns include parallel, angular, and dendritic patterns. Since the trend of mountain ranges is N-S direction, most of the important rivers are flowing northerly or southerly following the trend of mountain ranges. Some of the important northerly flowing rivers include Tlawng (Dhaleswari), Tuivawl, Tuirial (Sonai), Tut, Tuichawng, Teirei, Tuirini, and Serlui. The largest of these is the river Tlawng (Dhaleswari) with a length of 185.15 km. The important southerly flowing rivers include Chhimtuipui (Koladyne), and Khawthlangtuipui (Karnafuli). Tuichang and Tiau. The biggest southerly flowing river in Mizoram is Chhimtuipui (Koladyne) with a length of 138.46 km.

1.5 SCOPE OF PRESENT WORK

The Surma succession in Mizoram is well known for its geological uniqueness. Tectonics, sedimentation patterns, development and source as well as transportation patterns of the area are of much interest. The geological knowledge of the southern section of Mizoram is far from complete. In addition, none of the previous workers carry out detailed petrographical and textural analysis and geochemical characterization of the area. No assessments have been made to deduce the tectonic setting, depositional history, and provenance characteristics of the neogene succession of the area. The hydrocarbon exploration program in different parts of the area has been unsuccessful due to a lack of proper and detail information on the structural as well as sedimentological characteristics.

Therefore, to unravel the geological history of the Surma succession within the research area it is highly necessary and required to execute a detailed geological investigation. For this purpose, during the past few decades, many sedimentologists utilized petrographic studies of sandstone to work out the tectonic setting and provenance of source areas (Pettijohn *et al*., 1972; Dickinson and Suczek, 1979; Dickinson *et al.,* 1983). In addition to petrographical studies, geochemical classification has been employed to identify the specific nature of sedimentary rock types. The present work is an integral approach that would provide a detailed understanding of mineralogical, tectonic setting, depositional history, and source area weathering as well as the provenance of neogene succession in the southern part of Mizoram.

1.6 OBJECTIVES

The present research work objectives are listed below :

1. To prepare a geological map of Bhuban formation in and around Lunglei town.
2. To establish petrochemical characteristics for sandstone, siltstone, and shale belonging to Bhuban formation.
3. To explore provenance characteristics, depositional environment, and tectonic setting of Bhuban rocks in the vicinity of Lunglei town.

CHAPTER 2

LITERATURE REVIEW

The regional geological framework of the Bengal basin including the Surma basin was first reported by Evans (1932). Later on, a basic understanding of the tectonic structure of the basin generation and sediment history was given by Evans (1964), Sengupta (1966), and Raju (1968). The Bengal basin deposition commenced during the period of the Cretaceous due to the clash between the Burma plate and the Indian plate forming a remnant ocean basin (Mitchell and Reading, 1986; Curray, 1991; Raman *et al.,* 2009). Bengal basin thus formed a large delta of thick sedimentary succession which is mostly derived from Himalayan and IBR (Uddin and Lundberg, 1999). As a result of the continuous collision between India and Eurasia, the eastern part of the Bengal basin uplifted and turned into N-S trending anticlinal hill ranges (Uddin and Lundberg, 1999). The litho unit and sedimentary succession of the eastern Bengal basin include the Oligocene Barail group and Miocene Surma group of deltaic origin (Raman *et al.,* 2009).

Due to a lack of intense research work in the Surma basin of Mizoram, the geological knowledge of the state is still highly incomplete. Geological information and data have been increasing recently due to the activities of research workers which is also still very slow. Limited geological pictures and geological information of the state are carried out by a few workers. There are many publications regarding geological investigation such as geochemical analysis, heavy mineral analysis, petrographic analysis, textural analysis, and the paleontological aspects that are carried out from the Cenozoic rocks from the northern part of Mizoram. In addition, from the southern part of Mizoram especially Lunglei district detailed geological investigation is still very less. From the different sedimentary basins of the country, petrographical and geochemical studies have been carried out by many workers. Geochemical discriminants in sandstone suits and their affinity to tectonic settings have been explored and utilized by many previous workers. Middleton (1960) was one of the first who recognize the tectonic significance of sandstone geochemistry, and grouped sandstones into three families on a tectonic basis viz. eugeosynclinal,

taphrogeosynclinal, and exogeosynclinal. The basis of this grouping mainly depends on K_2O/Na_2O and alkali/Al_2O_3 ratios within the sandstone suites. Bhatia and Crook (1986) analyzed the Rare Earth Element (REE) geochemistry of mudstone and sandstone, they reported that the ratio increases from Light Rare Earth Element (LREE) to High Rare Earth Element (HREE) and sandstone being more mature the Eu anomaly decreases. Mc Lennan *et al.* (1993) after going through the usefulness of geochemical studies to decipher provenance and tectonic setting, reported that the advantage of geochemical studies is more useful than the petrographic methods. Based on the isotope composition and whole rock geochemistry they reported five terrain types. Therefore, to understand the tectonic history and provenance characteristics the use of whole rock geochemistry and isotope composition are very useful.

Wilde *et al.* (1995) employed Cerium anomaly to ascertain eustatic sea level changes and reported that the lowering of sea level was indicated by the positive anomaly of Cerium whereas the rise in sea level was indicated by a negative anomaly of Cerium. Uddin and Lundberg (1998) set out the petrological and geochemical approach of the Surma group of rocks from the Bokabil and Bhuban sandstones. They have narrated that relative to the older sandstone the abundance of feldspars and argillite and very low-grade metamorphic rock fragments inferred the erosional unroofing and onset of uplift in the eastern Himalaya and the orogenic detritus supplied to the Bengal basin are due to the development of streams. Tiwari and Mehrotra (2000) studied paleontological characteristics of Tipam sandstone and suggested that during the time of deposition, warm and humid climates predominated. Mannan (2002) after studying mineralogical and geochemical details of Neogene sediments of the Surma basin of Sylhet, Bangladesh, suggests that due to the tectonic uplift of the Himalayas, the detrital input was intense during the Neogene period. After integrating the petrographic techniques with major and trace element analysis, he proposed that the detritus of the source area is composed of granites which are the major constituents of Himalayan rocks. Uddin *et al.* (2003) investigated the process of subsidence and sedimentation in Miocene sediments within the Bengal Basin of Bangladesh, occurring during the collision of continents,

they reported that the southward thrusting of the Shillong plateau along the Dauki fault had taken place during the post-Miocene subsidence.

Hossain *et al.* (2006) examined both major and trace elements within the Sylhet basin of Bangladesh, they suggested that in the average composition of sandstones and mudrocks of Tipam and Dupitila sandstones, strong depletion in the levels of Na_2O, CaO, and Sr, a lesser degree of depletion in the levels of Rb, Ba, Nb, K_2O, MgO and Al_2O_3, higher SiO_2 content in comparison to average upper continental crust. The provenance characteristics of Tipam sandstone of Sylhet, Bangladesh studied by Roy *et al.* (2006) concluded that igneous, metamorphic, and pre-existing sedimentary rocks with quartzose recycled orogen are the source of Tipam sandstone and the source rocks are formed under humid climatic conditions. The geochemical constitution of Miocene sandstones of the Surma group of the Bengal basin, Bangladesh was studied by Rahman and Suzuki (2007) who concluded that the sandstones are composed primarily of quartzolithic with some feldspathic and quartz arenitic sandstones. They also reported that the sandstones are composed of plentiful low-grade metamorphic, sedimentary rock fragments, low volcanic detritus, and low feldspars which indicates that they are derived from a quartzose recycled orogen region. From the Surma group of sandstones when the geochemical analysis was carried out the sandstones are reported to contain moderate to high SiO_2 content and the plotted tectonic discrimination diagrams indicate an active continental margin to passive margin.

To infer the provenance, weathering history, and tectonic settings of the source rocks, Sandstones and Shales of Surma rocks from Bangladesh were evaluated by Islam and Rahman (2009) by employing major elements of geochemical analysis. They reported that sandstones in their study area possess a high content of SiO_2 with quartzolithic composition, unsettled lithic grains, low feldspar, a high quantity of metamorphic and sedimentary rock fragments, and a fairly low quantity of volcanic rock fragments which suggest that the source rocks are originated from a recycled orogen region (fold-thrust region /collision suture zone) and the geochemical nature of the Surma rocks are indicative of active continental margin to passive continental margin tectonic settings. They also suggest

that the Himalayan rocks and materials from Indo-Burma Ranges are mainly made up of recycled materials which are the principal source of sediments and have undergone low to moderate chemical weathering.

Benthic and planktonic foraminifera of the Miocene age were reported from fossiliferous calcareous sandstone from the Upper Bhuban formation of Mizoram (Lalmuankimi *et al.* 2010). The Surma basin from the north-eastern part of Bengal basin, Bangladesh was studied by Rahman and McCann (2011) to explore the diagenetic materials of Miocene age sandstones and concluded that Fe-carbonates, quartz overgrowths, and authigenic clays are the dominant diagenetic cement and the carbonate cement isotopic composition affirmed a narrow range of δ18O values (-10.3‰ to -12.4‰) and a wide range of δ13C value (+1.4‰ to -23.1‰). The ichnofossil studies carried out by Tiwari *et al.* (2011) from Bhuban rocks of Aizawl reported conditions of high energy in the foreshore zone to low energy in the offshore zone. The geochemical approach carried out by Lalmuankimi *et al.* (2011) from the Muthi sandstone of the upper Bhuban formation revealed that the average chemical index of alteration (CIA) value was higher than the upper continental crust which indicates that in the source area high intensity of chemical weathering occurred with active continental margin tectonic setting. At the time of the formation of the upper Bhuban rocks of Mizoram, tropical to subtropical and humid climatic conditions and fresh water environment with tropical humid to subtropical climatic conditions for Tipam sediments were reported by Singh *et al.* (2011) after studying paleoecology of upper Bhuban and Tipam sediments of Mizoram.

Using grain size distribution as a parameter, Borgohain Pradip (2012) studied the Tipam sandstone of the Tipong River (Assam) and suggested a fluviatile environment of deposition. Complex provenance with high-grade metamorphic, as well as sedimentary and igneous sources and comparative short sediment transportation, was reported by Ralte (2012) after studying Tipam sandstone from the northern district of Mizoram.

Derivation of upper Bhuban shale from highly depleted, intermediate to felsic granitoid rocks was reported by Lalmuankimi (2013) after a tectonic setting and provenance study of Upper Bhuban shale by using geochemical analysis. Tectonic set up of transitional recycled orogen and derivation of Tipam sediment from middle

and upper-rank metamorphic sources was confirmed by Sarma J.N. and Chutia Ananya (2013) after obtaining petrographical data of subsurface Tipam sandstone of Upper Assam. Lallianthanga and Laltanpuia (2013) reported that the middle Bhuban and upper Bhuban formation of the Surma group of rocks exposed in and around Lunglei town is represented by a repetitive succession of Neogene arenaceous and argillaceous in varying proportions.

Classification of sandstone into litharenite and sublitharenite of an igneous and metamorphic source which originated from sediments of the Indo-Burmese Collision zone and Himalayan mountain ranges was reported by Lalnunmawia *et al.* (2014) after studying Bhuban rocks exposed along Durtlang road section, Aizawl, Mizoram. Nannofossil biostratigraphic study of Bhuban rocks of Mizoram carried out by Rai *et al.* (2014) suggested that the age of Bhuban rocks of Mizoram is of Burdigalian to late Messinian. The Ichnofacies study of Surma rocks (Bhuban formation) of Mizoram carried out by Rajkonwar *et al.* (2014) suggested sandy shifting substrate in the foreshore zone and high energy conditions of deposition for the middle Bhuban rocks. A petrochemical characteristics study of middle Bhuban rocks in and around Aizawl was carried out by Duhawma and Shiva Kumar (2014). According to their findings, abundant argillaceous matrix, calcareous, and rock fragments are the characteristic features of middle Bhuban sandstone with a maximum variation of Na_2O, K_2O, and MgO.

The Jurassic sandstone of Jhuria formation from Kachchh Basin, Gujarat was categorized into arkose, sublitheranite, wacke, and quartz arenite by Periasamy and Venkatashwarlu (2017) after employing geochemical and petrographical analysis to decipher provenance and tectonic setting. The elemental concentration and elemental ratio obtained from the tectonic discrimination diagrams suggested the derivation of Jhuria sandstone from collision setting and continental rift. By employing grain size analysis, petrographic analysis, and heavy mineral analysis an integrated approach to upper Bhuban formation to decipher provenance, tectonic setting, and paleoclimatic conditions prevailed at the time of sediment deposition was made by Bharali *et al.* (2017). They reported that the sandstones were derived from an active continental margin to recycled orogen settings and belong to litharenite and wacke.

Studies of paleogene-neogene sediments of Mizoram Foreland basin using whole rock geochemistry were carried out by Hussain, M.F. and Bharali, B. (2019). Their research revealed that the CIA and CIW values for both the Barail and Surma rock formations indicated that they originated from source rocks that had undergone moderate weathering. The shared characteristic features in the geochemistry of neogene sediments in the Mizoram foreland basin and those in the Siwalik foreland basin suggest they likely originated from the Himalayas, an area situated within an active continental margin.

Chaudhuri *et al.* (2020) examined the compositional alteration in the Mesozoic sedimentary record throughout the development of the pericratonic rift basin of Kutch using petrographical and geochemical techniques. The analysis successfully pinpointed the felsic source rocks by examining various features such as the prevalence of arkosic sandstone, zircon concentration, trace element composition, and ratios, as well as the enrichment of Light Rare Earth Elements (LREE) with a negative Europium (Eu) anomaly. "Intermediate to intense weathering in the source area with immature to mature sediments" was the hypothesis put out by the study. According to the tectonic settings investigation, the Mesozoic Era passive margin settings are where the Kutch Basin originated.

CHAPTER 3

GEOLOGICAL FRAMEWORK

3.1 REGIONAL GEOLOGY

The collision of the Indian sub-continent with Eurasia and the Burmese plate resulted in the formation of the present study area which is 2500 km long, 300 km wide east-west Himalaya and from north-south it is 1500 km long and 230 km wide fold belt of Indo-Burma ranges (IBR). The present study area is a part of the southern extent of the Indo-Burma Range (IBR) with N-S trending anticline which is formed due to the Indo-Burma oblique collision. Previous workers (Mitchell, 1993; Das Gupta and Nandy, 1995) concluded possible trench deposits of the Indo-Burmese ranges containing ophiolitic melanges that got scraped off the Indian plate. The main contributors of geologic processes and features for the area of interest include the Himalayan mountain ranges, the Bengal basin, the Surma basin, and the Indo-Burma ranges.

There are four important longitudinal litho-tectonic units generally north dipping thrust faults in the Himalayan fold belt region with constant lithologic and tectonic characteristics over long distances along strike (Gansser, 1964). These are – (i) the Tethyan Himalayan zone located in the northern extremity which consists of the marine rock beds of Paleozoic and Mesozoic ages (ii) the Central zone of higher Himalaya which is constituted of granitic plutons of neogene age (iii) Lesser Himalayan zone which is affected by a series of thrust faults resulting reverse stratigraphic succession and (iv) Foredeep folded or Siwalik range which lies in the southern margin of the Himalaya characterized by low lying hills of Miocene-Pliocene age. The southern boundary of this belt is marked by the main boundary faults.

The thick sedimentary succession of about 22 km was deposited in the Bengal basin mainly from the Himalayan fold belt and Indo-Myanmar mobile belt due to the sediment influx of the Ganga-Bramahputra meghna delta covering more than 200,000 km (Uddin and Lundberg, 1999). The sedimentary succession of the Bengal basin can be broadly classified into three major lithostratigraphic units which

are separated from one another by three major unconformities. These are – the platform shelf exhibited by the western part of Bangladesh, the folded belt exhibited by the eastern part of Bangladesh including Chittagong-Tripura, and the central subsided part with two important depressions like Sylhet trough in the north and Patuakhali depression in the south. Deltaic environment and shallow water conditions existed due to the enormous influx of sediments from the surrounding areas of the basin resulting in the subsidence of the fore-deep in the Bengal basin. Throughout geological time the Bengal Basin sediment depocentre has been changing (Uddin and Lundberg, 2004). According to them, the depocentre was on the stable shelf during the Cretaceous period but shifted eastward to Assam during the Eocene period. It shifted again towards the northeastern part (Sylhet trough) during the period of the Miocene and then throughout the basin during the Pleistocene and Pliocene. The depocentre is currently situated in the Bengal deep-sea fan and Hatia trough (Alam, 2003; Uddin and Lundberg, 2004). The gradual closure of the Bengal basin was due to the collision of plate and orogeny along the eastern and northern margins which was formed as a result of rifting from the passive continental margin (Rowley, 1996). The continuous India-Eurasia collision results from N-S trending anticlinal hill ranges towards the basin's eastern region forming the Patkoi-Naga-Manipur-Chin Hills-Arakan Yoma region with an arcuate westward convexity trending in NW-SE to its southern extremity and ENE-WSW trend to its northern side. The extent of sedimentary succession of the Bengal basin includes the Miocene Surma group of deltaic origin and the underlying Oligocene Barail group.

The Surma basin, which is also known as the northeastern extension of the Bengal basin is surrounded by the Dauki fault, running east-west, and the Disang thrust, oriented northeast-southwest, which is located to the north and northeast, the Sylhet fault, running northeast-southwest and Barisal-Chandpur high in the west and northwest, towards the south it extends upto the Arakan coastal area. The encounter between the Indian and Burma plates resulted in the deposition of Surma sediments in shallow marine to deltaic complexes at the close of the Oligocene epoch, and there were recurrent occurrences of sandstone and claystone formations that experienced

folding and faulting processes. There were fluviatile molasse deposits of the Tipam formation at the basin's western edge.

3.2 GEOLOGY OF MIZORAM

Structurally, Mizoram is a part of the Indo-Myanmar fold belt (Sarkar and Nandy, 1976). The Indian plate subducting eastward along the Arakan-Yoma suture during the Eocene epoch resulted in the arcuate shape of the fold belt (Nandy, 1982). The horizontal compression and vertical motion deformed the mobile belt into a series of sub-parallel folds (Sarkar and Nandy, 1976). The southern extension of the Surma basin exposed in Mizoram is geologically a part of the Tripura-Mizoram depositional basin. This depositional basin came into existence after the spreading of the Indian Ocean which caused plate behavioral movement in the subduction zone west of Arakan-Yoma which ultimately led to the regional uplift of the Barail succession (Evans, 1964). Crustal shortening and increase in vertical thickness of the basin were due to compressive forces which are brought about by the subduction of the Indian plate during the Eocene period which ultimately resulted in the formation of the Indo-Burman orogenic belt. The N-S trending and E-W dipping anticlines and synclines of the fold belt with slightly arcuate in shape with convexity towards the west are due to continued convergence (Ganju, 1975; Ganguly, 1975; Srivastava *et al.*, 1979). The rock formations have been intersected by multiple transverse faults running in parallel or sub-parallel directions, including NE-SW, ENE-WSW, and NW-SE. Among the transverse faults, the most prominent one is ‘The Mat River Fault’ with a trend of NW-SE having dextral slip motion in between Aizawl and Lunglei (Das Gupta, 1984; Banerjee *et al.*, 1979). This basin was represented by a repetitive succession of argillaceous and arenaceous rocks of Paleogene and Neogene sediments. Important sedimentary rocks that are typically exposed in Mizoram include 13 different types of sandstone, siltstone, mudstone, and shale. These rocks can also be added in different amounts to isolated groups of calcareous sandstone, shell limestone, and intraformational conglomerate. Neogene age thick pile of Surma group of sedimentary rocks with a total thickness of about 8000 meters or more covered the entire part of Mizoram. The Paleogene-Neogene rocks of Mizoram are sequentially divided into four groups namely the Barail Group, Surma Group, Tipam

Group, and the Alluvium based on lithostratigraphy. Table 3.1 displays the generalized stratigraphic succession of Mizoram, which was determined by Karunakaran (1974) and Ganju (1975) with minor modifications. The geological map of Mizoram according to the Geological Survey of India is given in Figure 3.1.

Table 3.1: Stratigraphic Succession of Mizoram (after Karunakaran, 1974 and Ganju, 1975).

<table>
<tr><th>Age</th><th>Group</th><th>Formation</th><th>Unit</th><th>Generalized lithology</th></tr>
<tr><td>Recent</td><td>Alluvium</td><td>-</td><td>-</td><td>Silt, clay, and gravel</td></tr>
<tr><td colspan="5">----------Unconformity----------</td></tr>
<tr><td>Early Pliocene to Late Miocene</td><td colspan="2">TIPAM (+900m)</td><td>-</td><td>Friable sandstone with occasional clay bands</td></tr>
<tr><td colspan="5">----------Conformable and transitional contact----------</td></tr>
<tr><td rowspan="7">Miocene to Upper Oligocene</td><td rowspan="7">SURMA (+5950m)</td><td>BOKABIL (+950m)</td><td>-</td><td>Shale, siltstone, and sandstone</td></tr>
<tr><td colspan="3">-------Conformable and transitional contact-------</td></tr>
<tr><td rowspan="5">BHUBAN</td><td>Upper Bhuban (+1100m)</td><td>Arenaceous predominating with sandstone, shale, and siltstone</td></tr>
<tr><td colspan="2">-Conformable and transitional contact-</td></tr>
<tr><td>Middle Bhuban (+3000m)</td><td>Argillaceous predominating with shale, siltstone-shale alternations, and shale</td></tr>
<tr><td colspan="2">-Conformable and transitional contact-</td></tr>
<tr><td>Lower Bhuban (+900m)</td><td>Arenaceous predominating with sandstone and silty-shale</td></tr>
<tr><td colspan="5">----------Unconformity obliterated by faults----------</td></tr>
<tr><td>Oligocene</td><td>BARAIL (+3000m)</td><td>-</td><td>-</td><td>Shale, siltstone, and sandstone</td></tr>
<tr><td colspan="5">----------Lower contact not seen----------</td></tr>
</table>

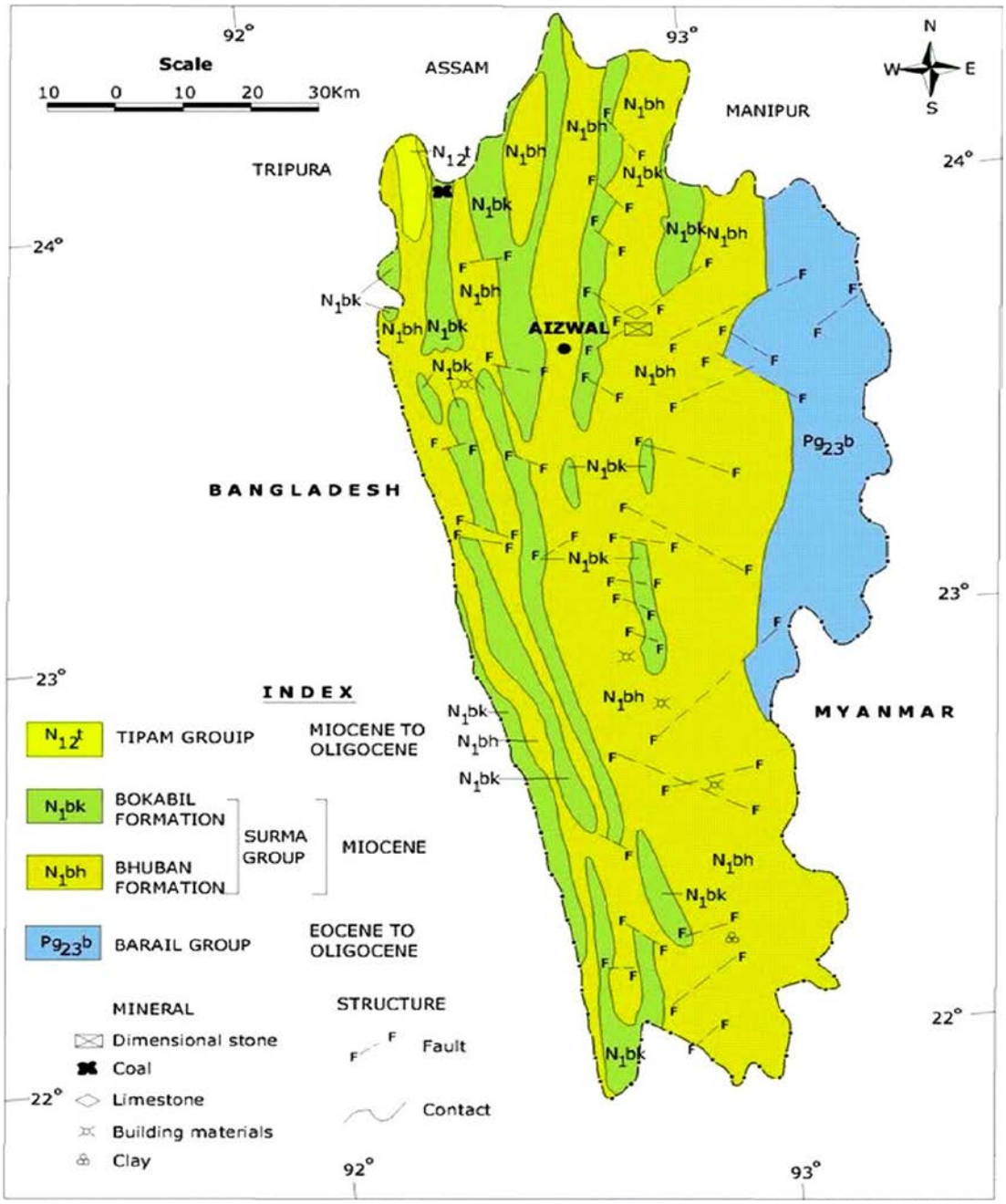

Figure 3.1: Geological Map of Mizoram according to the Geological Survey of India

3.2.1 Barail Group

In the Indo-Burmese range, arenaceous rocks of the Barail group conformably overlie the Disang group of rocks. It comprises a thick sequence of rocks of approximately 3000 m which consists of sandstone intercalated with thinly laminated shales and ranges in age from Eocene to Oligocene. Due to weathering, the

monotonous weathered shale which is interlaminated with siltstone exhibits greenish-grey, pink, violet, and white colorations. The evidence of unconformity obliterated by sub-parallel N-S trending and marginal-regional strike faults makes it difficult to recognize the lower contact of the Barail group. It contains fewer sedimentary structures when compared to the Bhuban Formation. The rocks exhibit an approximate dip of about 30^{o} to 150^{o} and are folded into a broad anticline. In the eastern region of Mizoram, the Barail group of rocks is exposed.

3.2.2 Surma Group

The most important and largest extant group of rocks in Mizoram is the Surma group which is composed of alterations of sandstone, poorly fossiliferous shale, siltstone, and mudstone in various proportions. The rocks of the Surma group extend from the Upper Oligocene to the Miocene in age. It is characterized by rapid lateral variation of facies and alternate ridge and valleys landscape. It can be divided into an Upper Bokabil Formation and a Lower Bhuban Formation.

The rocks of the Bhuban formation are the most predominant group of rocks and cover almost the whole part of Mizoram and show an alternate sequence of arenaceous and argillaceous rocks. It exhibits many sedimentary features like interference ripples, convolute laminations, slump structures, cross laminations, ridge structures, and load casts. The sandstones of the Bhuban formation are normally hard, poorly sorted, fine-grained, immature, and rich in mica. It exhibits small to medium-scale cross-stratification and ripples with sharply defined top surfaces whereas sole markings and graded bedding are less common. The Bhuban Formation is categorized into lower, middle, and upper units based on the ratio of sand to shale and the sequence of layers.

The Lower Bhuban unit has a thickness of roughly 900 meters and it is predominantly of arenaceous. The rocks are normally fine-grained, hard, moderate to poor sorted showing current bedding, grey coloration on fresh, and buff color on weathered surface. Shales in the lower Bhuban unit are thinly laminated, dark grey, and exhibit fissility in some places. Lower Bhuban rocks are normally exposed in the anticlinal cores of high amplitude fold areas.

The Middle Bhuban unit consists of about 3000 m thick succession of argillaceous rocks. It is composed of shale, siltstone, and a few clayey sandstone bands. The shales are usually laminated with ripple marks and are grey to dark grey. The siltstone/mudstone of this unit is thinly bedded to massive, jointed, hard, and exhibited grey with pale yellow color on weathering. Features such as cross-stratification and mud cracks, which show the direction of the current flowing from east to west, are secondary sedimentary features that define this region. Middle Bhuban succession normally occupies the cores of low-amplitude anticlines and on the limbs of folds.

The uppermost part of the Bhuban succession is the Upper Bhuban unit which is composed of arenaceous rocks with a thickness of about 1100 m. This unit is made up of thinly bedded and flaggy sandstone with alteration of dark grey shale which is overlain by grey, jointed, massive medium-grained with moderately hard sandstone. In the western part of Mizoram the Upper Bhuban rocks form anticlines but in the central and eastern parts, it is found in the synclinal cores area.

The Upper Bhuban formation of the Surma group is conformably overlain by the Bokabil formation. The thickness of Bokabil formation is about 950 m which is a monotonous repetitive succession of arenaceous and argillaceous sequences. This formation is characterized by soft, grey, laminated claystone with large-scale facies variation from shale/claystone alteration to fine sandstone. It is mainly exposed in the western and northwestern parts of Mizoram occupying the cores of the synclinal area.

3.2.3 Tipam Group

The Tipam group of rocks which are formed as a result of stream deposition unconformably overlies the Boikabil formation of the Surma group but has some gradational contact with the underlying rocks. It consists of friable coarse ferruginous sandstone with occasional clay bands. The thickness of the Tipam group of rocks is approximately 900 m and originated during the period of Late Miocene to Early Pliocene. It is mainly exposed in the extreme northwest region of Mizoram.

The Recent Alluvium is composed of silt, clay, and gravel and is formed due to the action of rivers.

3.3 GENERAL GEOLOGY OF THE STUDY AREA

The current research area falls within the boundaries outlined by the Survey of India Toposheets Nos. 84B/9 and 84B/13 and fall within the coordinates of latitudes $22^{o}45'0"$ N to $23^{o}0'0"$ N and longitudes $92^{o}20'30"$ E to $92^{o}51'30"$ E. The area is composed of anticlines and synclines with a serial trend of NW-SE and plunging in the N-S direction. High to moderately dipping eastern limb of anticlines are overturned whereas due to the severe weathering and erosion of highly sheared rock, sharp ridgelines, and vertical cliff faces are the characteristic features of the western part.

Lallianthanga and Laltanpuia (2013) reported that the study area is constituted by a repeated succession of Neogene arenaceous and argillaceous in various proportions belonging to the Middle Bhuban and Upper Bhuban formation of the Surma group. With gradational and transitional contact the upper Bhuban formation is underlain by the middle Bhuban formation. Shale and siltstone are important rocks whereas sandstone occurs in thin layers in the middle Bhuban formation. The dominant rock type of the upper Bhuban formation is sandstone. Sandstones exposed in the study area vary from fine grey, fine to medium brown color alternated with various proportions of clay and silt size particles of shales. The southern part of the town and its adjoining areas are dominated by argillaceous rocks of the Middle Bhuban formation which is characterized by occasional sandstone beds with thick shale beds. Most of the shales are grey, olive green to yellowish brown, and exhibit spheroidal pattern and fissility. Frequent occurrences of silty shale beds and silty sandstone beds with thin lamination of sandstone beds are encountered throughout the middle Bhuban formation.

The Upper Bhuban formation is mainly encountered in the upper part of the main anticline and the northern part of the town. It is dominated by a thick succession of sandstone sequences that conformably overlie the middle Bhuban formation. The sandstone beds are alternated with shale beds, range in thickness

from massive bed to thin bed, and are mostly brown, grey to dark grey. Rocks exposed in the upper Bhuban formation gently plunge towards the north and run parallel to the fold axial line. Trace fossil remains and bioturbated shales indicate a high rate of deposition in this area. Stratified brown to grey sandstones with various thicknesses inferred that the sediment is supplied from a mixed source with a frequently fluctuated environment and shallow depositional environment. Localities like Zotlang, some parts of Pukpui, Zohnuai, Serkawn, and Ramzotlang are situated along the anticlinal crest of the town and are characterized by fragile, coarse grain, highly porous and weakly cemented buff sandstone representing the youngest formation in the study area. The main town area is characterized dominantly by a sandstone sequence dipping moderately towards the east and the western side is marked by a ridgeline with a steep cut slope. The lithologically transitioned rocks which are considered to be middle Bhuban formations are exposed in the main town area and western part of the town and its adjoining areas. The lithological succession is more argillaceous with grey and olive green splintery shales. This area is characterized by a massive bedded formation of sandstone and occasional alternation of sandstone bed with shale bed. Trace fossils which are indicative of changes in paleo-environmental condition at the time of deposition are found in many places. In certain sandstone strata, bioturbated preservations in the form of burrows have been found. These findings suggest and bolster the hypothesis of a shallow deposition area that offers both oxidizing conditions and a conducive environment for life, where sunlight penetration is possible. Sandstones are generally massive, but their sedimentary structures like ball and pillow structures, ripple marks, load casts, burrows, raindrop structures, cross laminations, lenses, etc. are extraordinarily well preserved (Figures 3.3 – 3.14). In the extreme southern part of the town area i.e. Hrangchalkawn-Zobawk; a grey color, very fine to fine-grained massive sandstone bed with occasional alternation with shale beds is encountered along the roadside section. Figure 3.2 illustrates the geological map of the area under examination.

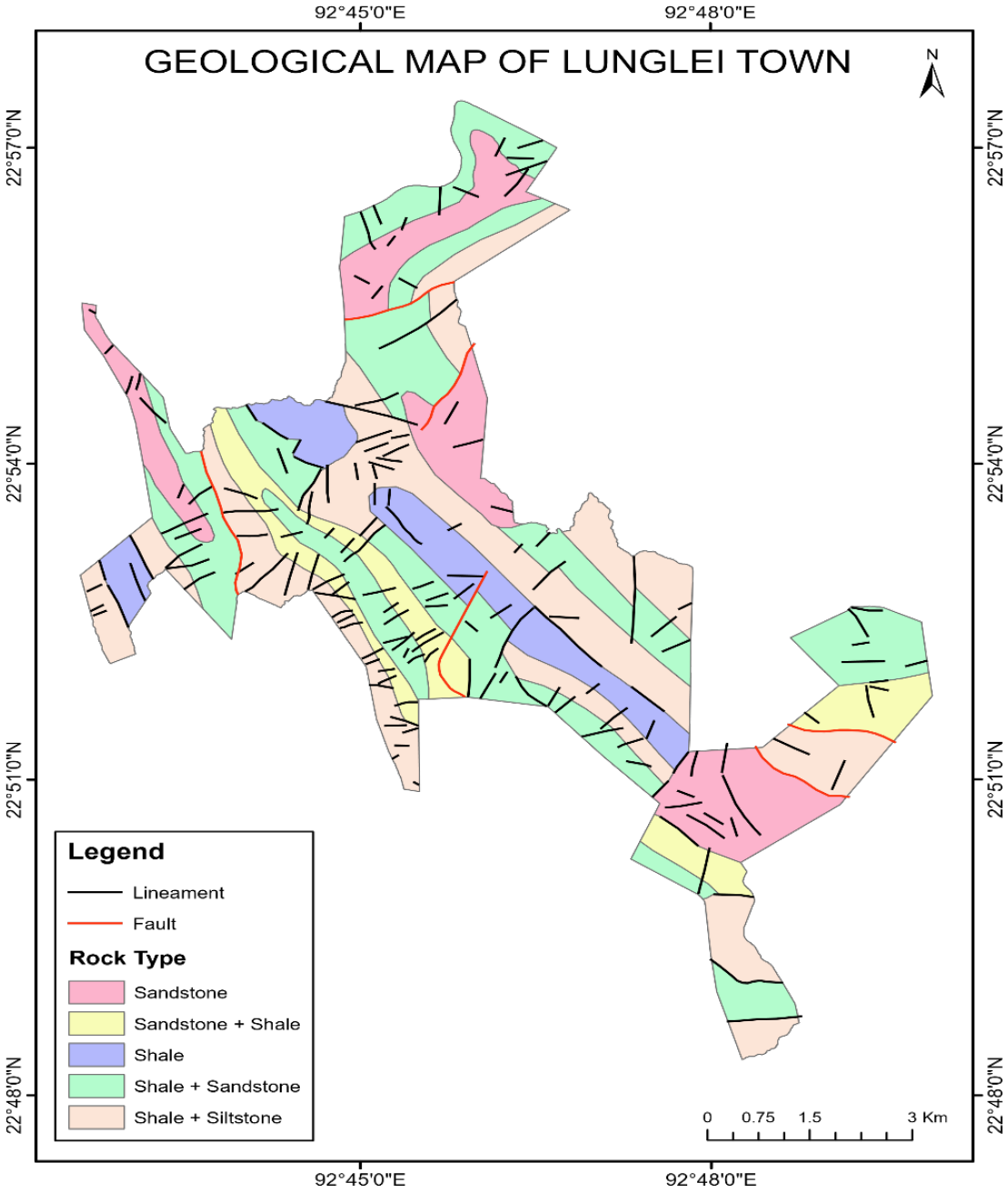

Figure 3.2: Geological map of the study area, Lunglei town.

.

Figure 3.3: Crumpled siltstone bed overlain by fine-grained sandstone exposed along the road section at Rahsiveng, Lunglei.

Figure 3.4: Massive sandstone bed at Lungpuizawl in the southern part of Lunglei Town.

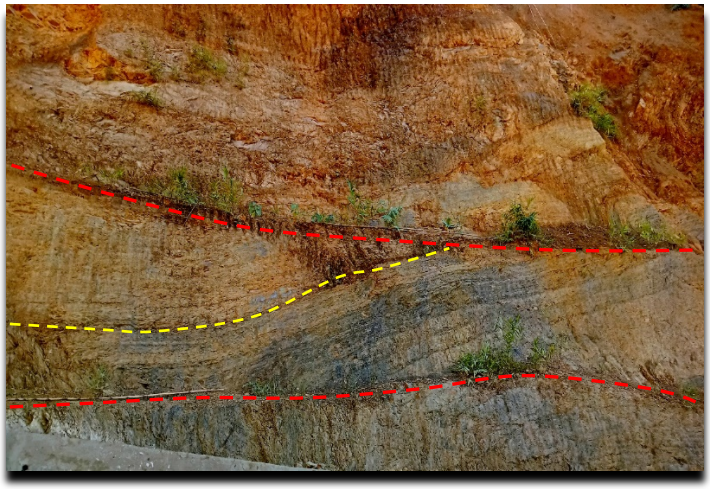

Figure 3.5: Disturbed thick shale bed at Zobawk, Lunglei. Reactivation surface and unconformity is also seen.

Figure 3.6: Thinly bedded intercalation of sandstone and shale exposed along Sazaikawn to Luangmual Road, Lunglei.

Figure 3.7: Interbedded shale, siltstone, and sandstone outcrop at Lungmual, Lunglei.

Figure 3.8: Fine-grained sandstone bed overlain by shale and siltstone at Pukpui, Lunglei.

Figure 3.9: Intercalation of shale and silty sandstone outcrop at Farm veng, Lunglei Town.

Figure 3.10: Massive sandstone bed at Zohnuai quarry.

Figure 3.11: Sandstone bed at Venghlun, Lunglei Town. The sandstone bed is gradually thinning upwards with an increase in shale content.

Figure 3.12: Medium-grained sandstone bed exposed along the flanks of Lunglei anticline (Melte Quarry).

Figure 3.13: Ball structure in sandstone bed at Vanhne in the north western part of Lunglei Town.

Figure 3.14: Burrow marks preserved in grey sandstone bed at Ramthar Quarry.

CHAPTER 4

METHODOLOGY

4.1 INTRODUCTION

In the present sedimentological research, the different methodologies employed can be broadly categorized into three categories such as – Literature Survey, Geological Field Work, and Laboratory Analysis.

4.2 LITERATURE REVIEW

Previous literature on the area is very important because it provides information about the various outlooks of geology and research activities carried out in the study area. It is very helpful to find out the strengths and weaknesses of the previous works. The collected literature survey was mainly obtained from Research papers, Journals, scientific reports, theses, and the Internet. After carefully studying and reviewing, the collected literature is used for the current research to make conclusions and for interpretation of generated data.

4.3 GEOLOGICAL FIELDWORK

For the present research, detailed geological fieldwork was carried out in the study area for the recognition of sedimentary structures, lithology, and facies variation. The main task of fieldwork is the preparation of a geological map and collection of representative un-weathered fresh samples. The samples collected in the study area are documented by measuring dip and strike with the help of Brunton Compass and their latitude and longitude with the help of GPS. The different outcrops of sedimentary strata and other structures encountered during the fieldwork are also authenticated in the form of field photographs. After a detailed field investigation, 37 fresh and un-weathered representative sandstone samples and 15 shale samples are collected for detailed analytical studies in the laboratory. The fresh sandstone and shale samples collected were accurately marked and labelled for studies in the laboratory.

4.4 LABORATORY ANALYSIS

Laboratory analysis includes the following:

a) Petrological Analysis
b) Geochemical analysis

Thin section analysis was done in the Department of Geology, Mizoram University, and Geochemical analysis was done at Wadia Institute of Himalayan Geology, Dedradun, Uttarakhand. The observed laboratory data integrated with field observations are used to explore provenance characteristics, paleoclimatic conditions, depositional environment, and tectonic setting of Bhuban rocks in the study area.

4.4.1 Petrological Analysis

Petrological analysis was carried out by preparing thin section slides from the representative samples collected from the studied area which were photographed, studied, and analyzed using Leica DM2700 P, petrological magnifying tool equipped with Leica DFC420 camera, Leica picture examination computer program (LAS-v4.6). Modal analysis was done using the PETROGLITE Stepping stage at the Department of Geology, Mizoram University. The Gazzi-Dickinson (1966) point-counting method was employed for modal analysis of the collected sandstone samples. A total of 400 points have been counted for each thin section. Primary essential detrital components like quartz, feldspar, and lithic fragments recorded were used for the classification of sandstones and the elucidation of provenance, tectonic settings, and intensity of weathering of Bhuban sandstone. Other detrital components taken into consideration include micas, specifically biotite and muscovite.

4.4.2 Geochemical Analysis

The Geochemistry Division at the Wadia Institute of Himalayan Geology in Dehradun, Uttarakhand, India conducts analyses on rock samples, focusing on major, trace, and rare earth elements. Analysis of Major oxides is done with XRF while analysis of Trace and REE is done with ICP-MS. For geochemical analyses, the

samples which are found containing no microfossils are selected. Major oxide concentrations are analyzed using the X-ray Fluorescence Spectrometer (XRF) technique applied to pressed pellets. Measurement of LOI is done by heating the samples at 950°C in an aliquot of rock powder about 5 gm. Analysis of Trace and Rare Earth Elements is carried out with the Perkin Elmer SCIEX ICP-MS. The rock samples crushed to 200 mesh are used for the preparation of sample solution which is followed by the open acid digestion method by using 10 ml of $HF+HNO_3$ (2:1) acid mixture. To ensure thorough digestion of the solution, employ an open Teflon crucible on a hot plate, repeating the process 3 to 4 times. The solution is used for $HClO_4$ treatment to attain a complete absence of moisture. Again, the solid substance was dissolved in 10 ml of nitric acid solution with a concentration of 20%. Then, distilled water was added to the solution to bring its total volume to 100 ml. By using a peristaltic pump with a cross-flow nebulizer the final sample is then passed through argon plasma. The analytical instruments' precision falls within an acceptable range, with major elements having an accuracy of around ±2-3%, trace elements ±5-6%, and rare earth elements (REE) ranging from ±1-8%.

Fifteen shale samples of Lunglei town were analyzed at the Sophisticated Analytical Instrumentation Facility (SAIF) at Guwahati University where the PANalytical X'pert Powder was used for the powder diffraction. Empyrean Power X-ray Diffractometer is manufactured by PANalytical and covers an extensive range of X-ray diffraction, scattering, and imaging applications, making it an invaluable tool.

Solid samples in the form of dry Powder of 300 mesh about 3g of sample on a glass slide of size 2cm x 3.5 cm and thickness 0.2cm with a uniform layer of size 2cm x 1.5cm on one side is required. The output consists of an X-ray Diffractogram, Peak Position, d values, and relative intensity data. Phase Identification, Quantitative analysis of minerals, Grazing incidence XRD of thin film, determination of unit cell parameters, particle size measurement. With a robust 4 kW X-ray generator and impressive specifications such as $-111 < 2\theta < 168°$ usable range, 0.0001° smallest addressable increment, and < 0.0002° angular reproducibility, the Empyrean delivers accurate and reliable results.

CHAPTER 5

PETROGRAPHY

5.1 INTRODUCTION

Petrographic analysis of sedimentary rock is extremely useful for determining the diagenetic history of the sediments, provenance, tectonic setting of the source area, and the environment of deposition of sediments. Using the framework mineral composition of sandstone, Crook (1974) has proposed the method of establishing the tectonic setting and ever since has gone through several appreciable modifications.

For the reconstruction of the tectonic setting of the geological past and the provenance of terrigenous deposits, petrographical evidence as well as geochemical analyses of sandstone have been extensively used. In petrographical analysis, different ternary plots like QmLt, QmPK, QFL, etc. are extremely useful in deducing tectonic settings and understanding the interactivity of plates in the ancient geologic past (Ingersoll, 1978; Dickinson and Suczek, 1979; Dickinson *et al.*, 1983). The paleo climatic conditions that prevail at the time of deposition can also be obtained by petrographical analysis (Suttner and Dutta, 1986). The nature of the source rocks and their existence can be ascertained by the mineral compositions, rock fragments, and other constituents. Therefore, the nature of grain, inclusions, and extinction pattern of quartz are used as inferences to provenance. Various kinds of feldspars and lithic fragments are also used as a guide in provenance determinations.

Since the petrological characteristics of sandstone can reveal information about the tectonic history, provenance, weathering conditions, diagenesis, etc. a detailed petrographic study of Bhuban sandstones was carried out in and around Lunglei town. Thus, detailed thin-section studies under the microscope have been conducted to decipher the textural characteristics, mineralogical composition, provenance, sandstone classification, tectonic history, and paleoclimatic conditions at the time of deposition.

5.2 PETROGRAPHIC ANALYSIS

A total number of 37 (thirty-seven) samples of Bhuban sandstone collected from the study area are accounted for petrographic analysis. The different varieties of quartz, feldspars, and rock fragments are thoroughly examined for primary detrital components for the petrographic analysis. Other detrital components include micas like muscovite and biotite. Cementing materials identified during petrographic analysis are argillaceous, siliceous, calcite, and ferruginous cement. The petrographic study reveals that the framework grains are represented by moderately sorted, angular to sub-rounded {Plate 5.1 (B)}, and medium to fine-grained textures {Plate 5.1 (A)}. The detailed mineralogical compositions are described as follows:

5.2.1 Quartz

Among the representative sandstone samples collected from the study area, quartz is the most abundant detrital component comprising an average of 65.79% in the Upper Bhuban Formation (UBF) and 66.23% in the Middle Bhuban Formation (MBF). Though some rounded grains are encountered, most of the grains are angular to sub-rounded (Plate 5.1 B) in shape and have partial or incomplete crystal outlines (subhedral) with some inclusions. Among the detrital quartz identified, monocrystalline quartz (both undulatory and non-undulatory) and polycrystalline quartz (both 2-3 and >3 crystal units per grain) are ubiquitous. Quartz grains can be widely categorized into two classes namely monocrystalline quartz and polycrystalline quartz (Conolly, 1965; Blatt, 1967).

The monocrystalline quartz comprises an average of 63.69% in UBF of which, undulose quartz constitutes 5.09% and non-undulose quartz constitutes 58.60%. Similarly, monocrystalline quartz makes up 63.82% of MBF of which, undulose quartz constitutes 4.78% and non-undulose quartz comprises 59.04% on average. The undulose monocrystalline quartz {Plate 5.1 (C)} is recognized by its wavy extinction. In the present study area, the undulose quartz modal percentage varies from 2.10% - 15.40% in UBF and 1.40% - 11.50% in MBF, the grains exhibit angular to sub-angular shape, sutured grain boundaries and are found to break into smaller grains because of less stability. The non-undulose monocrystalline quartz

(unit quartz) is again recognized by its distinctive characteristic features of invariable extinction under a crossed polarizer. The concentration of non-undulose quartz or unit quartz (Plate 5.1 C) is very high in comparison with all other constituents and the modal percentage varies from 52.08% - 66.61% in UBF and 50.21% - 66.11% in MBF (Table 5.1). Most of the grain exhibits medium to fine grain, straight and concavo-convex contact, and at places sutured grain boundaries {Plate 5.1 (D & E)}.

In the present study, the polycrystalline quartz in UBF is 2.11% of which polycrystalline quartz 2-3 constitute 1.46% and polycrystalline quartz > 3 accounts 0.65 %. Whereas the concentration of polycrystalline quartz in MBF is 2.42% of which polycrystalline quartz 2-3 constitute 1.78% and polycrystalline quartz > 3 constitute 0.64 %. The crystal units per grain in polycrystalline quartz are normally specified by straight, sutured, and curved internal boundaries. The polycrystalline quartz in the studied samples is perhaps derived from metamorphic or igneous sources. Polycrystalline quartz 2-3 {Plate 5.1 (F)} is mainly distinguished if the number of composite crystals in a single grain varies from 2-3 whereas polycrystalline quartz > 3 {Plate 5.2 (A)} is identified if the composite crystal exhibits several microcrystalline units more than 3 with sutured grain contact. Most of the quartz grains are medium to fine-grained and roundness varies from angular to sub-angular with few sub-rounded grains. In a few samples, quartz overgrowth {Plate 5.2 (B)} and floating of framework grains {Plate 5.2 (C)} in the cement and matrix are observed. The modal percentage of different quartz and other components is shown in Table 5.1.

5.2.2 Feldspar

Felspar present in the Bhuban sandstones of the study area are readily recognized by their special characteristics of twinning under cross Nicols. Plagioclase feldspar {Plate 5.2 (D)} can be easily recognized by lamellar twinning. Microcline and orthoclase {Plate 5.2 (E)} are also commonly observed, the former can be identified by cross-hatched twinning and the latter by Carlsbad twinning (simple twin). Perthite {Plate 5.2 (F)} which is formed as a result of intergrowth between plagioclase feldspar and K-feldspar is also observed at places. Most of the

feldspar grains identified in the present studied Bhuban sandstones are angular to sub-angular in shape and are easily recognized by their weathered nature. Orthoclase of untwined variety are also seen and they are recognized by their cloudy appearances. In the present study, the total concentration of feldspar is 2.10% in UBF and 1.65% in MBF. Plagioclase feldspar constitute 0.54% in UBF and 0.48% in MBF and its modal percentage range varies from 0.00% - 1.60% in UBF and 0.00% - 1.20% in MBF whereas orthoclase feldspar constitute 1.56% in UBF and 1.18% in MBF and its modal percentage range varies from 0.00% - 6.50% in UBF and 0.00% - 4.60% in MBF.

5.2.3 Rock Fragments

In petrological analyses of sedimentary rocks, lithic fragments derived from sedimentary, igneous, and metamorphic rocks are very essential components because they provide signs of tectonic setting and provenance of the source area. In the present study, the concentration of rock fragments is 7.17% in UBF and 8.43% in MBF. Rock fragments are normally identified by their well-known grain boundaries and most of them are fine-grained with a dirty appearance in shades of brown. Both sedimentary and metamorphic rock fragments are identified in the studied samples where the former is identified by their sedimentary character and the latter is identified by preferred orientation and high-order interference color. Important rock fragments reported include chert, shale, slate, and schist {Plate 5.3 (A)}.

5.2.4 Mica

The modal percentage of mica varies from 0.20% - 18% in UBF and 0.50% - 11.40% in MBF and the average concentration is 5.10% in UBF and 4.01% in MBF. Mica commonly occurs as elongated, slender, flaky minerals showing cleavages. Muscovite and biotite are the two important mica observed in the present study area. However, chlorites which are formed as a result of alteration of biotite are also frequently observed. Biotites are mainly specified by their straight extinction, pleochroism, and brown color. On the other hand, muscovites are specified by their silvery white and red-green interference color. Muscovite being more resistant to

chemical alteration is more common than biotite. Authigenic and bended mica flakes are also commonly observed {Plate 5.3 (B)}.

5.2.5 Cement

Secondary minerals that are formed after the deposition and during diagenesis of sandstone that bind the framework grains are called cement. The average percentage of cement in the present study is 11.09% in UBF and 9.47% in MBF. The common cementing materials in the examined sandstones are mainly siliceous, calcareous, ferruginous, and argillaceous cement {(Plate 5.3 (C)}. Quartz overgrowths are shown by siliceous cement. The percentage of argillaceous cement is very high in comparison with other types of cement observed. Erosional features and penetration of grain boundaries by the cementing material are also observed. In some samples, argillaceous cements are coated by ferruginous cement which indicates that argillaceous cement is precipitated first and then ferruginous cement.

5.2.6 Matrix

The fine-grained siliceous and argillaceous groundmass which are without grain boundaries confined in sedimentary rocks are called matrix. In the present study, the concentration of the matrix varies from 0.00% - 18.30% in UBF and 2.77% - 17.55% in MBF, and the average percentage of the matrix is 8.76% in UBF and 10.20% in MBF. They are mainly formed by the precipitation of clay minerals and alteration of framework grains and therefore consist of authigenic and detrital grains.

5.2.7 Accessory Minerals

Other minerals like chlorite, glauconite, sillimanite, zircon, and rutile are reported but they are not counted since their proportions are negligible.

5.3 X-RAY DIFFRACTION ANALYSIS

X-ray Diffraction (XRD) stands as a widely employed technique crucial for identifying and quantifying crystalline substances, notably aiding in discerning the mineral composition of rocks, particularly finer clay sediments. Its utility extends to both qualitative and quantitative analysis of rock minerals, offering insights into the

structural and chemical attributes of ultrafine minerals like clay, which are smaller than 2 μm in diameter.

Fifteen representative shale samples from Lunglei town are used as the basis for X-ray diffraction investigations. Documenting the clay and non-clay mineralogy of the shales of Lunglei town was the goal of the analyses. Figure 5.1 displays the X-ray diffractograms of the separated clay fraction (< 2 pm) of selected shale samples. In all the samples, Quartz, cristobalite, and muscovite are the main minerals showing intense peaks. Among the clay minerals, chlorite and illite are prominent although overshadowed by the intense peak of quartz. The diffraction patterns also indicate the presence of albite, corrensite, faujasite-Na, anorthite/anorthoclase, caldecahydrite, garronite, microcline, vermiculite, sanidine, clinochlore, lizardite orthoclase, and atalpulgite in a smaller amount. In terms of mineralogical abundances and assemblages, the shales are comparatively uniform. The sediments may have originated from a homogenous source because of the mineralogical homogeneity. The XRD bulk mineralogical results of Lunglei town shales are shown in Table 5.4.

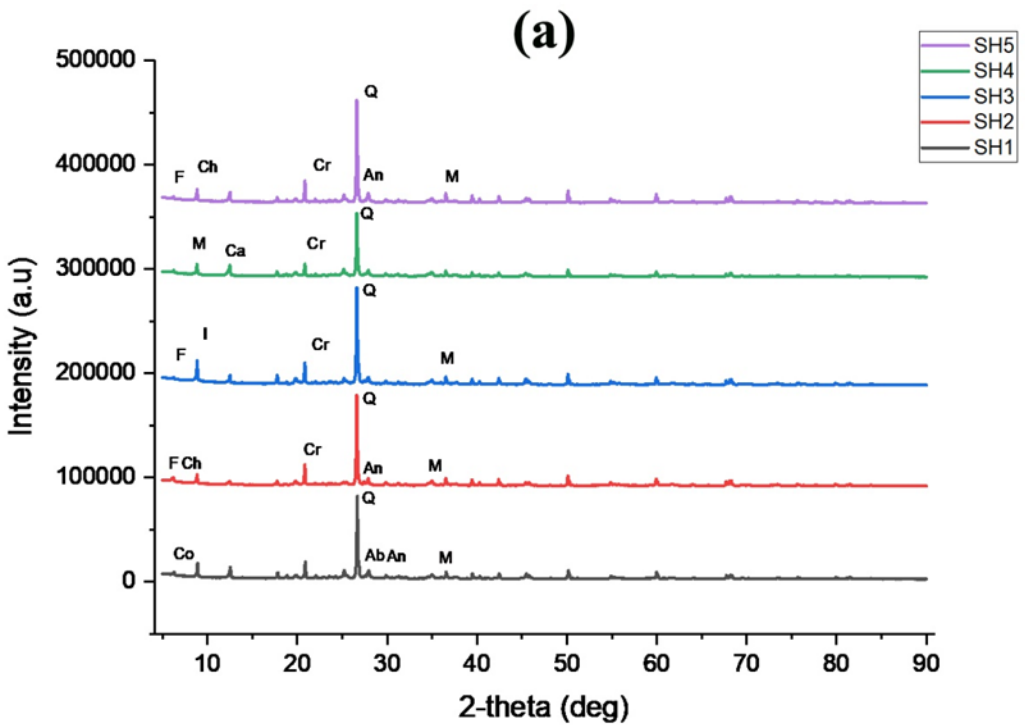

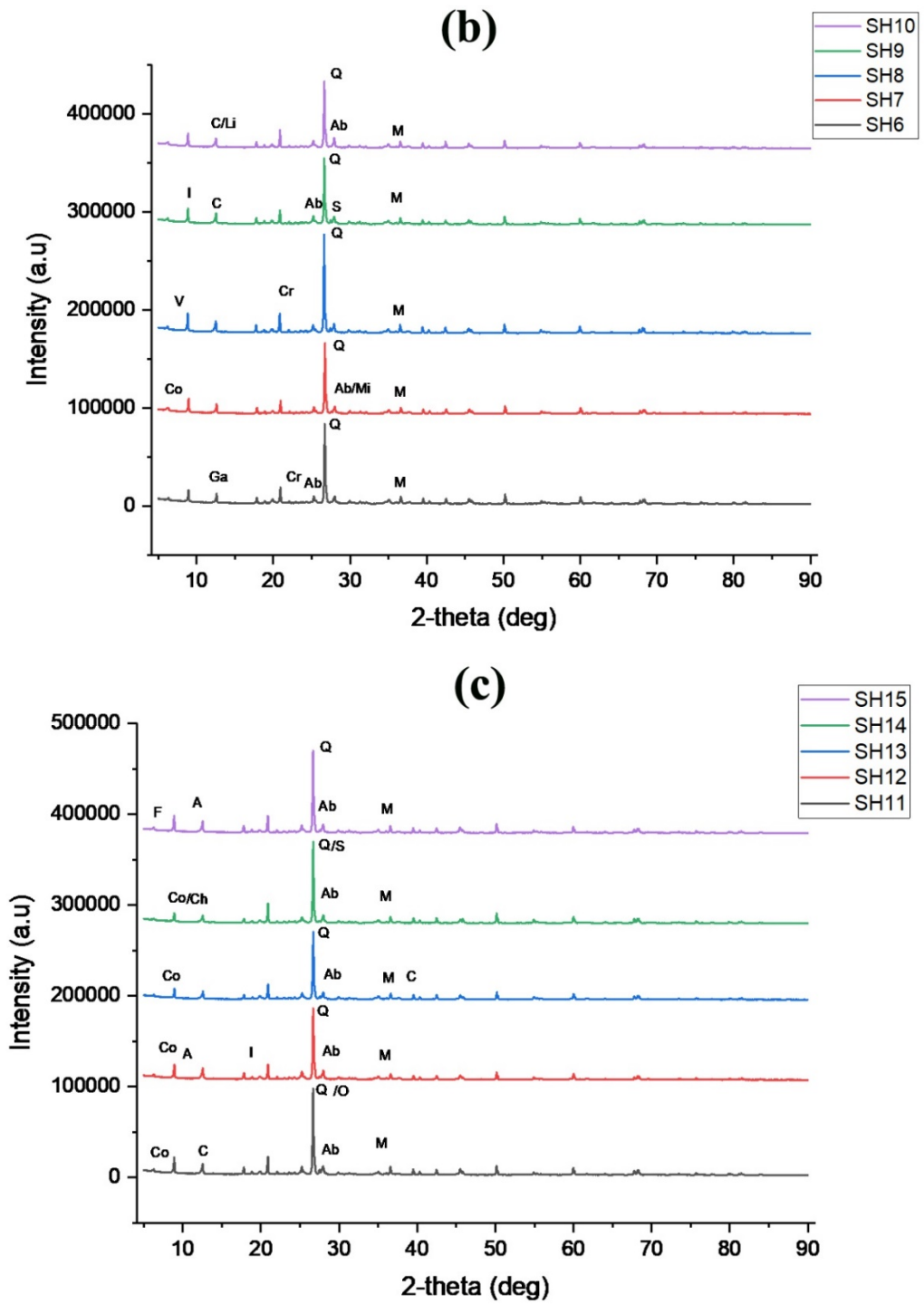

Figure 5.1: Average mineral composition of Shales from Lunglei town. (Where, Q=Quartz, M=Muscovite, Ab=Albite, Co=Corrensite, F=Faujasite-Na, Cr=Cristobalite, Ch=Chlorite, I=Illite, An=Anorthite/anorthoclase, Ca=Caldecahydrite, Ga=Garronite, Mi=Microcline, V=Vermiculite, S=Sanidine, C=Clinochlore, Li=Lizardite, O=Orthoclase and A=Atalpulgite)

Table 5.1: Modal composition of Bhuban sandstones, Lunglei Town, Mizoram.

UPPER BHUBAN FORMATION														
Sl. No.	**Sample No.**	**Monocrystalline Quartz**			**Polycrystalline Quartz**			**Total Quartz**	**Feldspar**		**Rock Fragments**	**Cement**	**Mica**	**Matrix**
		Q_{Mu}	**Q_{Mnu}**	**Q_{Mt}**	**Q_{P2-3}**	**$Q_{P>3}$**	**Q_{Pt}**	**$Q=(Q_{Mt} + Q_{Pt})$**	**$P_{Ca/Na}$**	**FK**				
1	LS-1	3.80	66.03	69.83	0.20	0.00	0.20	70.03	0.50	0.00	8.54	7.43	6.40	7.10
2	LS-2	2.60	57.14	59.74	3.70	0.50	4.20	63.94	0.80	0.70	9.80	6.46	5.80	12.50
3	LS-3	5.40	66.61	72.01	0.90	0.00	0.90	72.91	0.90	0.90	7.60	7.39	6.10	4.20
4	LS-4	2.90	54.15	57.05	0.60	0.00	0.60	57.65	0.30	0.90	9.50	8.35	7.20	16.10
5	LS-5	6.30	61.36	67.66	1.30	0.20	1.50	69.16	0.00	0.20	8.30	7.44	6.00	8.90
6	LS-6	3.10	64.73	67.83	2.90	1.30	4.20	72.03	0.70	2.30	2.70	18.97	3.30	0.00
7	LS-7	3.60	65.11	68.71	0.20	0.00	0.20	68.91	0.50	0.50	7.90	9.94	5.60	6.65
8	LS-8	4.50	66.21	70.71	0.50	0.00	0.50	71.21	0.50	0.50	5.60	13.51	6.30	2.38
9	LS-9	3.50	57.05	60.55	0.70	0.00	0.70	61.25	0.50	0.00	7.80	13.65	5.50	11.30
10	LS-10	6.60	52.28	58.88	1.50	0.20	1.70	60.58	0.50	0.90	8.10	12.33	6.60	10.99
11	LS-11	4.00	53.75	57.75	0.50	0.00	0.50	58.25	0.00	0.00	7.60	9.55	8.70	15.90
12	LS-18	2.50	59.36	61.86	3.30	0.80	4.10	65.96	0.20	3.80	2.20	9.34	0.50	18.00

Where:

Q_{Mu} - Monocrystalline undulatory quartz, Q_{Mnu} - Monocrystalline non-undulatory quartz, Q_{Mt} -Total Monocrystalline quartz, Q_{P2-3} - Polycrystalline quartz with 2-3 grain per quartz, $Q_{P>3}$ - Polycrystalline quartz with >3 grains per quartz, Q_{Pt} -Total polycrystalline quartz, Q - Total number of quartz, $P_{Ca/Na}$ - Plagioclase feldspar, F_K - Potash feldspar.

13	LS-19	2.30	63.84	66.14	1.30	1.80	3.10	69.24	0.70	1.50	11.10	6.92	1.30	9.24
14	LS-26	4.10	59.39	63.49	1.30	0.00	1.30	64.79	1.60	6.50	10.30	8.77	0.80	7.24
15	LS-27	6.10	52.08	58.18	0.50	0.00	0.50	58.68	0.80	2.70	1.50	18.32	18.00	0.00
16	LS-28	6.10	52.53	58.63	3.40	2.30	5.70	64.33	0.50	5.20	1.90	12.01	4.40	11.66
17	LS-29	10.30	55.14	65.44	1.30	0.50	1.80	67.24	0.50	3.40	7.50	13.59	0.20	7.57
18	LS-30	6.50	52.48	58.98	1.70	0.00	1.70	60.68	0.50	0.70	6.10	11.52	2.20	18.30
19	LS-33	2.10	58.66	60.76	1.00	0.20	1.20	61.96	0.50	0.20	12.60	11.23	6.40	7.11
20	LS-34	15.40	54.10	69.50	2.40	5.10	7.50	77.00	0.30	0.30	6.80	15.00	0.60	0.00

MIDDLE BHUBAN FORMATION														
Sl. No.	Sample No.	Quartz type						Total Quartz	Feldspar		Rock Fragments	Cement	Mica	Matrix
		Monocrystalline Quartz			Polycrystalline Quartz									
		Q_{Mu}	Q_{Mnu}	Q_{Mt}	Q_{P2-3}	$Q_{P>3}$	Q_{Pt}	$Q=(Q_{Mt} + Q_{Pt})$	$P_{Ca/Na}$	F_K				
1	LS-12	1.40	62.06	63.46	0.80	0.00	0.80	64.26	0.00	0.00	5.00	11.44	4.20	15.10
2	LS-13	2.70	63.39	66.09	2.50	0.50	3.00	69.09	1.20	0.20	6.40	13.28	3.00	6.83
3	LS-14	3.10	65.21	68.31	1.80	0.50	2.30	70.61	0.50	0.00	12.40	7.90	3.30	5.29
4	LS-15	1.70	66.11	67.81	1.40	0.20	1.60	69.41	0.00	0.00	9.80	6.29	0.50	14.00
5	LS-16	3.60	65.42	69.02	2.10	0.70	2.80	71.82	0.00	0.70	13.50	5.61	4.60	3.77
6	LS-17	3.89	62.18	66.07	2.33	1.55	3.88	69.95	0.52	0.00	8.60	5.55	3.50	11.88
7	LS-20	7.30	61.08	68.38	2.40	0.20	2.60	70.98	0.50	4.30	9.10	7.23	2.10	5.79
8	LS-21	2.00	65.24	67.24	0.70	0.70	1.40	68.64	0.70	0.70	12.50	9.99	4.70	2.77
9	LS-22	2.10	64.45	66.55	1.80	0.50	2.30	68.85	0.50	3.10	9.00	0.00	1.00	17.55
10	LS-23	11.50	52.82	64.32	3.20	1.00	4.20	68.52	1.20	2.50	3.30	14.09	1.20	9.19
11	LS-24	2.00	53.72	55.72	2.00	2.30	4.30	60.02	0.50	1.00	4.60	16.84	5.60	11.44
12	LS-25	5.20	55.28	60.48	0.50	0.00	0.50	60.98	0.50	0.00	5.80	11.95	11.40	9.37
13	LS-31	6.90	55.46	62.36	1.10	0.20	1.30	63.66	0.20	4.60	11.00	3.54	1.10	15.90
14	LS-32	10.60	50.21	60.81	2.50	1.90	4.40	65.21	0.60	1.20	9.20	10.46	7.40	5.93
15	LS-35	3.80	53.46	57.26	3.00	0.50	3.50	60.76	0.70	1.00	8.26	14.78	2.90	11.60
16	LS-36	9.40	53.06	62.46	1.10	0.00	1.10	63.56	0.00	0.00	5.20	7.23	6.60	17.41
17	LS-37	4.00	54.47	58.47	1.00	0.20	1.20	59.67	0.50	0.70	9.70	14.78	5.10	9.55

Table 5.2: Recalculated values of modal data in percentile.

Litho-Unit	Sample No	Quartz (Total)	Felspar (Total)	Rock Fragment (Total)	(Q_{tot}+F+RF)	Total Quartz %	Total Felspar %	Rock Fragments %
UPPER BHUBAN FORMATION	LS-1	70.03	0.50	8.54	79.07	88.56	0.63	10.80
	LS-2	63.93	1.50	9.80	75.23	84.97	1.99	13.02
	LS-3	72.91	1.80	7.60	82.31	88.57	2.19	8.58
	LS-4	57.65	1.20	9.50	68.35	84.34	1.76	13.89
	LS-5	69.16	0.20	8.30	77.66	89.05	0.26	10.68
	LS-6	72.03	3.00	2.70	77.73	92.03	3.86	3.47
	LS-7	68.91	1.00	7.90	77.81	88.56	1.29	10.15
	LS-8	71.21	1.00	5.60	77.81	91.51	1.29	7.19
	LS-9	61.25	0.50	7.80	69.55	88.06	0.72	11.21
	LS-10	60.58	1.40	8.10	70.08	86.44	2.00	11.55
	LS-11	58.25	0.00	7.60	65.85	88.45	0.00	11.54
	LS-18	65.96	4.00	2.20	72.16	91.40	5.54	2.40
	LS-19	69.24	2.20	11.10	82.54	83.88	2.67	13.44
	LS-26	64.79	8.10	10.30	83.19	77.88	9.74	12.38
	LS-27	58.68	3.50	1.50	63.68	92.14	5.50	2.35
	LS-28	64.33	5.70	1.90	71.93	89.43	7.92	2.64
	LS-29	67.24	3.90	7.50	78.64	85.50	4.96	9.53
	LS-30	60.68	1.20	6.10	67.98	89.26	1.77	8.97
	LS-33	61.96	0.70	12.60	75.26	82.32	0.93	16.76
	LS-34	77.00	0.60	6.80	84.40	91.23	0.71	8.05

Litho-Unit	Sample No	Quartz (Total)	Felspar (Total)	Rock Fragment (Total)	(Q_{tot}+F+RF)	Total Quartz %	Total Felspar %	Rock Fragments %
MIDDLE BHUBAN FORMATION	LS-12	64.26	0.00	5.00	69.26	92.78	0.00	7.21
	LS-13	69.09	1.40	6.40	76.89	89.85	1.82	8.32
	LS-14	70.61	0.50	12.40	83.51	84.55	0.60	14.66
	LS-15	69.41	0.00	9.80	79.21	87.62	0.00	12.37
	LS-16	71.82	0.70	13.50	86.02	83.49	0.81	15.69
	LS-17	69.95	0.52	8.60	79.07	88.46	0.66	10.87
	LS-20	70.98	4.80	9.10	84.88	83.62	5.66	10.72
	LS-21	68.64	1.40	12.50	82.54	83.15	1.70	15.14
	LS-22	68.85	3.60	9.00	81.45	83.50	4.42	11.04
	LS-23	68.52	3.70	3.30	75.52	90.73	4.90	4.36
	LS-24	60.02	1.50	4.60	66.12	90.77	2.27	6.95
	LS-25	60.98	0.50	5.80	67.28	90.63	0.74	8.62
	LS-31	63.66	4.80	11.00	79.46	80.11	6.04	13.84
	LS-32	65.21	1.80	9.20	76.21	85.56	2.36	10.75
	LS-35	60.76	1.70	8.26	70.72	85.91	2.40	11.67
	LS-36	63.56	0.00	5.20	68.76	92.43	0.00	7.56
	LS-37	59.67	1.20	9.70	70.57	84.55	1.70	13.74

Table 5.3: Percentile values of Quartz (monocrystalline), Feldspar (F), and Rock fragments (RF) of Bhuban sandstones, Lunglei Town, Mizoram (in percentile).

Litho Unit	Sample No.	Qmt	F	RF	(Qmt+F+RF)	Qmt %	Feldspar %	RF %
UPPER BHUBAN FORMATION	LS-1	69.83	0.50	8.54	78.87	88.53	0.63	10.27
	LS-2	59.74	1.50	9.80	71.04	84.09	2.11	13.79
	LS-3	72.01	1.80	7.60	81.41	88.45	2.21	9.33
	LS-4	57.05	1.20	9.50	67.75	84.20	1.77	14.02
	LS-5	67.66	0.20	8.30	76.16	88.83	0.26	10.89
	LS-6	67.83	3.00	2.70	73.53	92.24	4.08	3.67
	LS-7	68.71	1.00	7.90	77.61	88.53	1.29	10.17
	LS-8	70.71	1.00	5.60	77.31	91.46	1.29	7.24
	LS-9	60.55	0.50	7.80	68.85	87.94	0.73	11.32
	LS-10	58.88	1.40	8.10	68.38	86.10	2.05	11.84
	LS-11	57.75	0.00	7.60	65.35	88.37	0.00	11.62
	LS-18	61.86	4.00	2.20	68.06	90.89	5.88	3.23
	LS-19	66.14	2.20	11.10	79.44	83.25	2.77	13.97
	LS-26	63.49	8.10	10.30	81.89	77.53	9.89	12.57
	LS-27	58.18	3.50	1.50	63.18	92.08	5.54	2.37
	LS-28	58.63	5.70	1.90	66.23	88.52	8.61	2.86
	LS-29	65.44	3.90	7.50	76.84	85.16	5.08	9.76
	LS-30	58.98	1.20	6.10	66.28	88.98	1.81	9.20
	LS-33	60.76	0.70	12.60	74.06	82.04	0.95	17.01
	LS-34	69.50	0.60	6.80	76.90	90.37	0.78	8.84

Litho Unit	Sample No.	Qmt	F	RF	(Qmt+F+RF)	Qmt %	Feldspar %	RF %
MIDDLE BHUBAN FORMATION	LS-12	63.46	0.00	5.00	68.46	92.69	0.00	7.30
	LS-13	66.09	1.40	6.40	73.89	89.44	1.89	8.66
	LS-14	68.31	0.50	12.40	81.21	84.11	0.62	15.26
	LS-15	67.81	0.00	9.80	77.61	87.37	0.00	12.62
	LS-16	69.02	0.70	13.50	83.22	82.93	0.84	16.22
	LS-17	66.07	0.52	8.60	75.19	87.87	0.69	11.43
	LS-20	68.38	4.80	9.10	82.28	83.10	5.83	11.05
	LS-21	67.24	1.40	12.50	81.14	82.86	1.73	15.40
	LS-22	66.55	3.60	9.00	79.15	84.08	4.55	11.37
	LS-23	64.32	3.70	3.30	71.32	90.18	5.19	4.62
	LS-24	55.72	1.50	4.60	61.82	90.13	2.43	7.44
	LS-25	60.48	0.50	5.80	66.78	90.56	0.75	8.68
	LS-31	62.36	4.80	11.00	78.16	79.78	6.14	14.07
	LS-32	60.81	1.80	9.20	71.81	84.68	2.51	12.81
	LS-35	57.26	1.70	8.26	67.22	85.18	2.53	12.28
	LS-36	62.46	0.00	5.20	67.66	92.31	0.00	7.68
	LS-37	58.47	1.20	9.70	69.37	84.28	1.73	13.98

Table 5.4: The minerals composition of characterized d-valve (Å) calculated obtained from the diffractogram of Lunglei town.

Sample/ Elements	SH-1	SH-2	SH-3	SH-4	SH-5	SH-6	SH-7	SH-8	SH-9	SH-10	SH-11	SH-12	SH-13	SH-14	SH-15
Quartz	3.34	3.34	3.34	3.34	3.34	3.34	3.34	3.34	3.34	3.34	3.34	3.34	3.34	3.34	3.34
Muscovite	2.56	2.56	2.56	3.35	2.56	2.56	2.56	2.56	2.56	2.56	2.56	2.56	2.56	2.56	2.56
Albite	3.19	-	-	-	-	4.03	3.18	-	3.18	3.18	3.18	3.18	3.18	3.18	3.18
Corrensite	14	-	-	-	-	-	14	-	-	-	14	14	14	14	-
Anorthoclase	3.21	3.25	-	-	-	-	-	-	-	-	-	-	-	-	-
Anorthite	3.24	-	-	3.2	-	-	-	-	-	-	-	-	-	-	-
Cristobalite	-	4.03	4.03	4.03	4.03	4	-	4	-	-	-	-	-	-	-
Chlorite	-	14	-	-	14	-	-	-	-	-	-	-	-	14	-
Faujasite	-	14.2	14.2	-	14.2	-	-	-	-	-	-	-	-	-	-
Illite	-	-	10.2	-	-	-	-	-	9.96	-	-	9.96	-	-	-
Caldecahydrite	-	-	-	7.1	-	-	-	-	-	-	-	-	-	-	-
Clinochlore	-	-	-	-	-	3.57	-	-	7.12	7.12	-	-	2.54	-	-
Lizardite	-	-	-	-	-	-	-	-	-	7.28	-	-	-	-	-
Microcline	-	-	-	-	-	-	3.29	-	-	-	-	-	-	-	-
Sanidine	-	-	-	-	-	-	-	-	3.24	-	-	3.24	-	3.24	-
Garronite	-	-	-	-	-	7.14	-	-	-	-	-	-	-	-	-
Vermiculite	-	-	-	-	-	-	-	14.3	-	-	-	-	-	-	-
Orthoclase	-	-	-	-	-	-	-	-	-	-	3.18	-	-	-	-
Attapulgite	-	-	-	-	-	-	-	-	-	-	-	14.6	-	-	14.6
Gismondite	-	-	-	-	-	-	-	-	-	-	-	-	-	4.28	-
Adularia	-	-	-	-	-	-	-	-	-	-	-	-	-	-	3.3

PLATE: 5.1

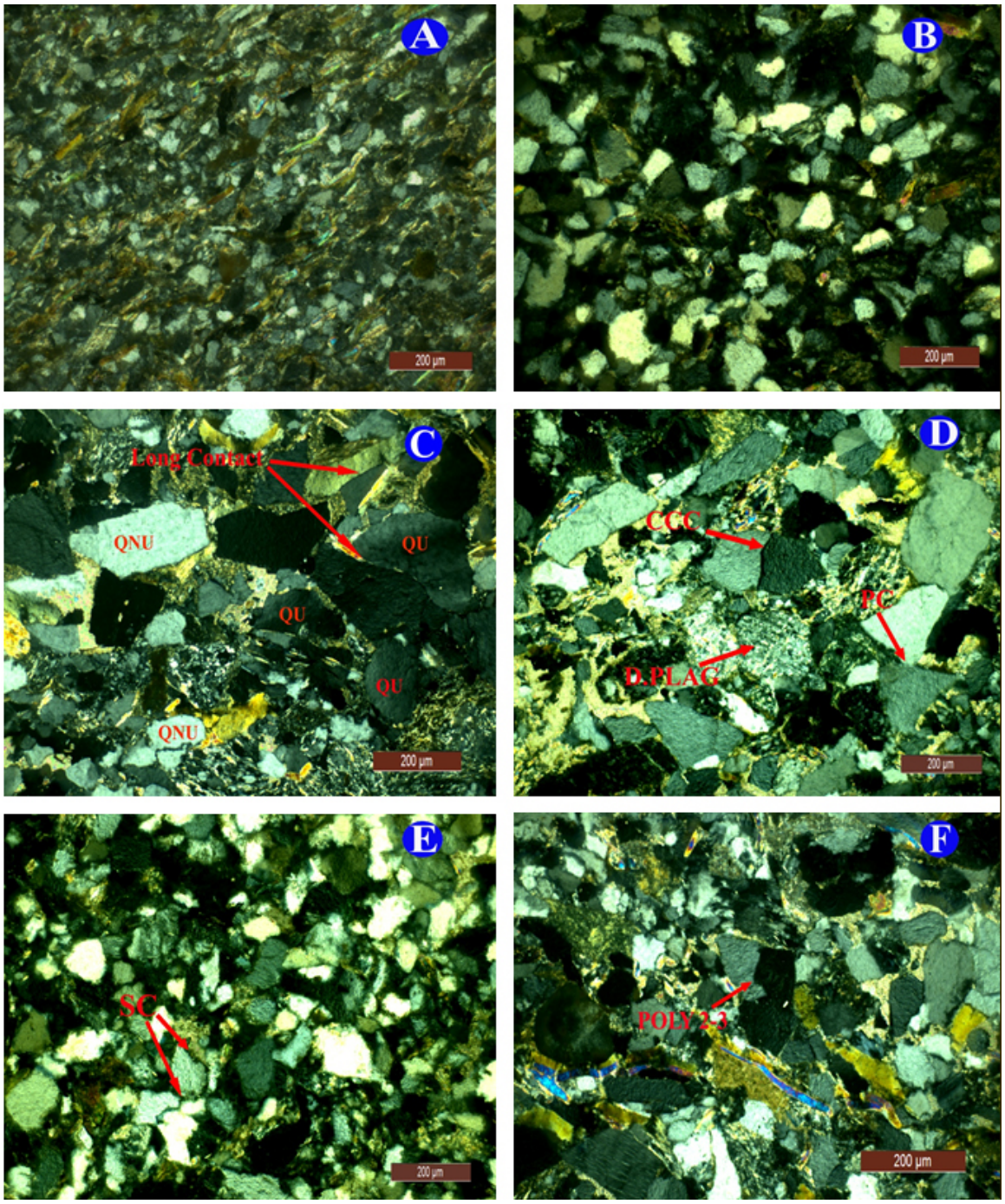

Where, A: Fine-grained sandstone B: Angular to sub-angular sandstone
C: QNU (Quartz non-undulatory), QU (Quartz undulatory),
D: CCC (Concavo-convex contact), PC (Point contact)
D.PLAG (Dissolution of Plagioclase), E: SC (Suture contact),
F: POLY 2-3 (Polycrystalline quartz 2-3)

PLATE: 5.2

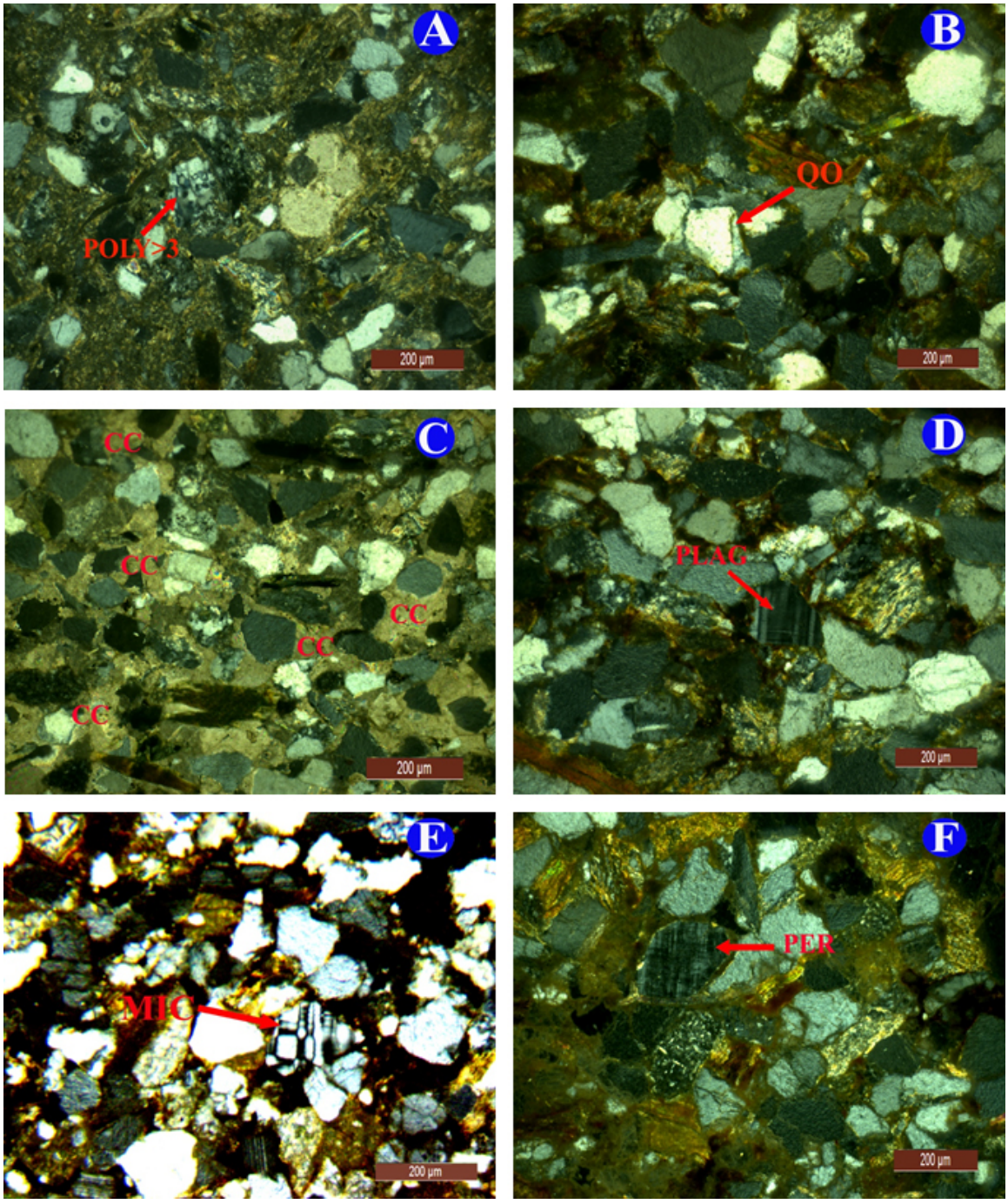

Where, A: POLY>3 (Polycrystalline quartz >3), B: QO (Quartz overgrowth)
C: CC (Calcite cement), D: PLAG (Plagioclase), E: MIC (Microcline)
F: PER (Perthite)

PLATE: 5.3

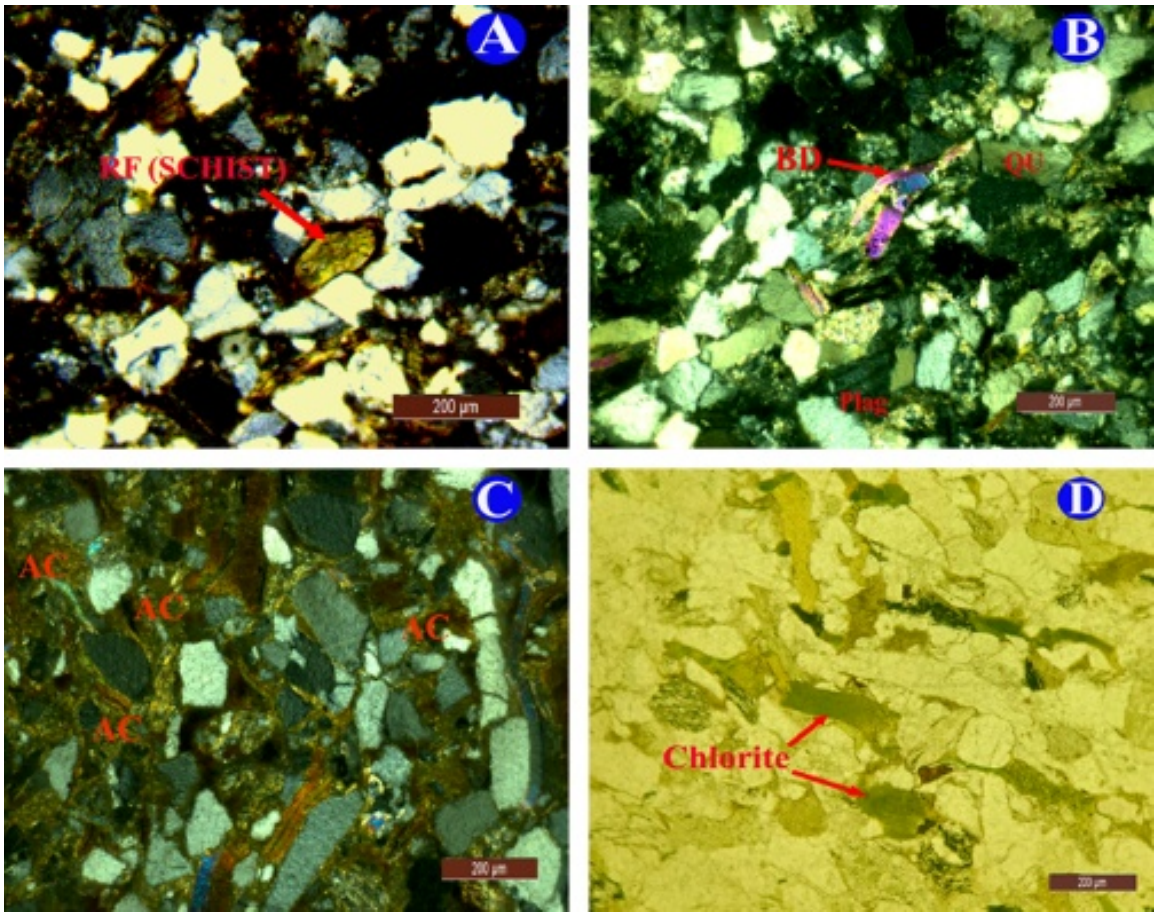

Where, A: RF (Rock Fragment, Schist), B: BM (Bended Mica)
C: AC (Argillaceous Cement), D: Chlorite

CHAPTER 6

GEOCHEMISTRY

6.1 INTRODUCTION

Clastic Sedimentary rocks are produced by the weathering, erosion, transport, and deposition of older rocks. They are a valuable source of knowledge about past orogenic processes and may contain detritus that explains the development of orogenic settings (Johnsson, 1993). During the weathering process, the minerals in pre-existing rock crumble, dissolve, and are carried by various agents to generate sediments (Krishnamurthy *et al.,* 1986; Laird *et al.,* 2003; Rose *et al.,* 2004). According to Dickinson and Suczek (1979) and Johnsson (1993), the chemical makeup of sandstone can be utilized to identify connections between tectonic setting and provenance.

Thin section analyses of sedimentary rock can reveal the environment of depositional, diagenesis, provenance, and transportation of sediments (Dickinson and Suczek, 1979; Ingersoll and Suczek, 1979; Dickinson, 1985). As the sediments have undergone extensive burial and compaction for a long period, it is plausible that the framework grains can be altered. The accuracy of geochemical data, as opposed to thin section study, provides accurate information on sedimentary rocks (McLennan *et al.,* 1993; Kroonenberg, 1994; Armstrong and Altrin, 2014). The primary determining factor for the chemistry of sedimentary rocks is the chemical makeup of the source rock. However, different variables such as weathering, erosion, hydraulic sorting, deposition, transit, burial, and diagenesis can significantly alter the composition of clastic sedimentary rocks (Bhatia and Crook, 1986; Johnsson, 1993; Cullers and Podkovyrov, 2000).

The depositional environment, which is mostly governed by subsidence rate, affects chemical changes during deposition. According to Johnsson (1993), the composition of the source rock, chemical weathering, abrasion, sorting during transit, and diagenesis are the most significant contributors. Three key interconnected factorstectonic context, climate, and depositional characteristics affect these variables. Each of these variables influences the traits of the others, resulting in

various clastic compositions. Lithics are chemically broken down and separated from relict quartz as sediments and are transported far from the source area. As a result, vast mud-rich deltas typical of passive continental margin slope settings, quartz-rich sandstones typical of continental interiors and passive margin platforms are produced. In contrast, the sediments are transported for a shorter distance in a magmatic arc depositional environment. Because of this, there is a lesser chance that sediments will physically sort or undergo chemical changes, which may result in the formation of sandstone that contains a high proportion of lithic fragments.

Chemical weathering indices combined with the bulk chemistry of the principal element oxides into a single metric, are frequently used to characterize the weathering profile of a source rock (Jason *et al.,* 2003). It can be challenging to relate the chemical compositions of the sediments to the source rock due to these intricate interactions (Johnsson, 1993). However, it has been noted that the composition of sandstones and their origin is closely associated with tectonic settings (Dickinson and Suczek, 1979; Dickinson *et al.,* 1983). Thus, it appears that these components often behave in the same way in any given situation, despite the complexity of the interactions between them. Moreover, these elements have different effects on sediment composition depending on the tectonic setting (Seiver, 1979), resulting in compositional groups that are comparable and consistent throughout.

The rare earth elements (REE, from La-Lu) can be distinguished by their single oxidation state: REE (III), except for cerium and europium. Over the past few decades, REEs have emerged as significant geochemical tracers that can be used to comprehend and explain the chemical development of the earth's continental crust (Goldstein and Jacobsen, 1988; McLennan, 1989; Dupre *et al.,* 1996). The source rock characteristics of the sediments are reflected by certain elements such as REE, Zr, Hf, Th, and Sc if they are present in the terrigenous sediments. The abundance of these elements is not appreciably changed by weathering, transportation of sediment, diagenesis, or metamorphism; Taylor and McLennan (1985), McLennan (1989), and McLennan and Taylor (1991).

Bhatia (1983) has classified the tectonic setting for sandstones into an oceanic arc, continental arc, active, and passive continental margin based on unique Th/La, Th/Sc, and other elemental pairs. According to Nesbitt (1979) and Cullers *et al.* (1987), the effects of chemical weathering on trace element distributions suggested that the typically immobile elements might also be somewhat redistributed.

Based on recent research, it has been suggested that REE patterns and Eu anomalies in sediments can be affected by chemical weathering processes. To some extent, the concentration of rare earth elements and high field strength elements (HFSE) is also influenced by the fractionation of heavy mineral assemblage and the degree of diagenesis (Ohr *et al.,* 1994).

According to several studies (Middleton, 1960; Bhatia, 1983; McLennan, 1989), the geochemical composition of sedimentary rocks is a multiplex function of factors such as the source material, weathering, transportation, physical sorting, and diagenesis. Due to their relatively low mobility during sedimentary processes and their residence times in seawater, many trace elements, including the rare earth elements (REE; for example, La, Ce, Nd, Gd, Yb), Y, Th, Zr, Hf, Nb, and Sc are best suited for discriminations of provenance and tectonic setting (Holland, 1978; Taylor and McLennan, 1985). They are therefore more helpful in differentiating tectonic environments and source-rock compositions than the major elements due to their low mobility, which causes them to be transferred quantitatively into clastic sediments during weathering and transportation, reflecting the identity of the parent rocks (Bhatia and Crook, 1986; McLennan, 1989; Condie, 1993).

6.2 WHOLE ROCK GEOCHEMISTRY

6.2.1 Major Oxides

Tectonic settings, depositional environment, and provenance of Bhuban sandstones in the study area are determined by analyzing major oxide concentrations. The concentration of major elements in Bhuban sandstones in the study area is represented in Table 6.1. UCC normalized major elemental spider diagram {(Figure 6.2 (B)} demonstrated the depletion of Na_2O, CaO, and K_2O. Depletion of Na_2O can be explained by the comparatively smaller content of Na-rich plagioclase in

comparison to k-felspar in the petrographic observation. The concentration of Na_2O and K_2O and the ratio of K_2O/Na_2O all greater than 1 (>1) are also consistent with the petrographic data. This observation also supports the frequent occurrence of mica as void fillings and patchy distribution in the Bhuban sandstones of the study area. The depletion of CaO in the spider diagram may be attributed to the absence of calcite cement in the majority of the samples. The concentration of SiO_2 in UBF and MBF varies from moderate to high (UBF: 51.77-74.32 wt. % with an average of 69.46 wt. %, MBF: 67.52-74.17 wt. % with an average of 71.89 wt. %) and a negative correlation (R_{UBF}: 0.28, R_{MBF}: -0.52) with Al_2O_3 which may be due to the differentiation of clays and quartz grains during the sedimentation processes {Figure 6.2 (A)}. In comparison to UCC (Rudnick and Gao, 2003, 2005), SiO_2 is slightly enriched. Al_2O_3 concentrations range from UBF: 8.68-13.48 wt. % with an average of 11.67 wt. % and MBF: 10.24-13.46 wt. % with an average of 12.04 wt. % which is slightly less than the UCC values. The concentration of Na_2O (UBF: 0.67-1.77 wt. % with an average of 1.31 wt. % and MBF: 0.21-1.83 wt. % with an average of 1.22 wt. %) is also lower than the UCC values. The low values of Na_2O/K_2O ratio (UBF = 0.57 avg.; MBF = 0.56 avg.) are consistent with the petrographic data in which the K-feldspar dominates over plagioclase. When correlating major oxides against Al_2O_3, Bhuban sandstones of Lunglei show a negative correlation with SiO_2 suggesting that most of the silica content in sandstones are detrital quartz. A positive correlation is observed in K_2O (R_{UBF} = 0.89, R_{MBF} = 0.52) and Fe_2O_3 (R_{UBF} = 0.94, R_{MBF} = 0.63) and TiO_2. The association of these major oxides with micaceous or clay minerals in the rock is strongly supported by the positive correlation of these major oxides against Al_2O_3. According to Feng and Kerrich (1990), the positive correlation of K_2O with Al_2O_3 implies the enrichment of clay minerals and also reflects the impact of weathering. Moreover, Fe_2O_3 (R_{UBF} = 0.56, R_{MBF} = 0.05) is showing a moderate to weakly positive correlation with TiO_2. However, a discernible trend is not observed in MgO, P_2O_5, CaO, MnO, Na_2O and P_2O_5. Occasionally, other sedimentation processes like diagenesis resulted in the enrichment of Fe_2O_3. The lower concentrations of Cr, Ni, and V, which indicate an early diagenetic and syngenetic precipitation of Fe-oxides, further support this. The higher Al_2O_3/TiO_2 ratio (UBF = 20.81 avg. and MBF = 21.14 avg.) suggests that the sediments were most likely

derived from a continental source (Fyffe and Pickerill, 1993). According to the UCC normalized pattern {Figure 6.2 (B)}, samples like MgO, CaO, Na_2O, and K_2O are showing depletion.

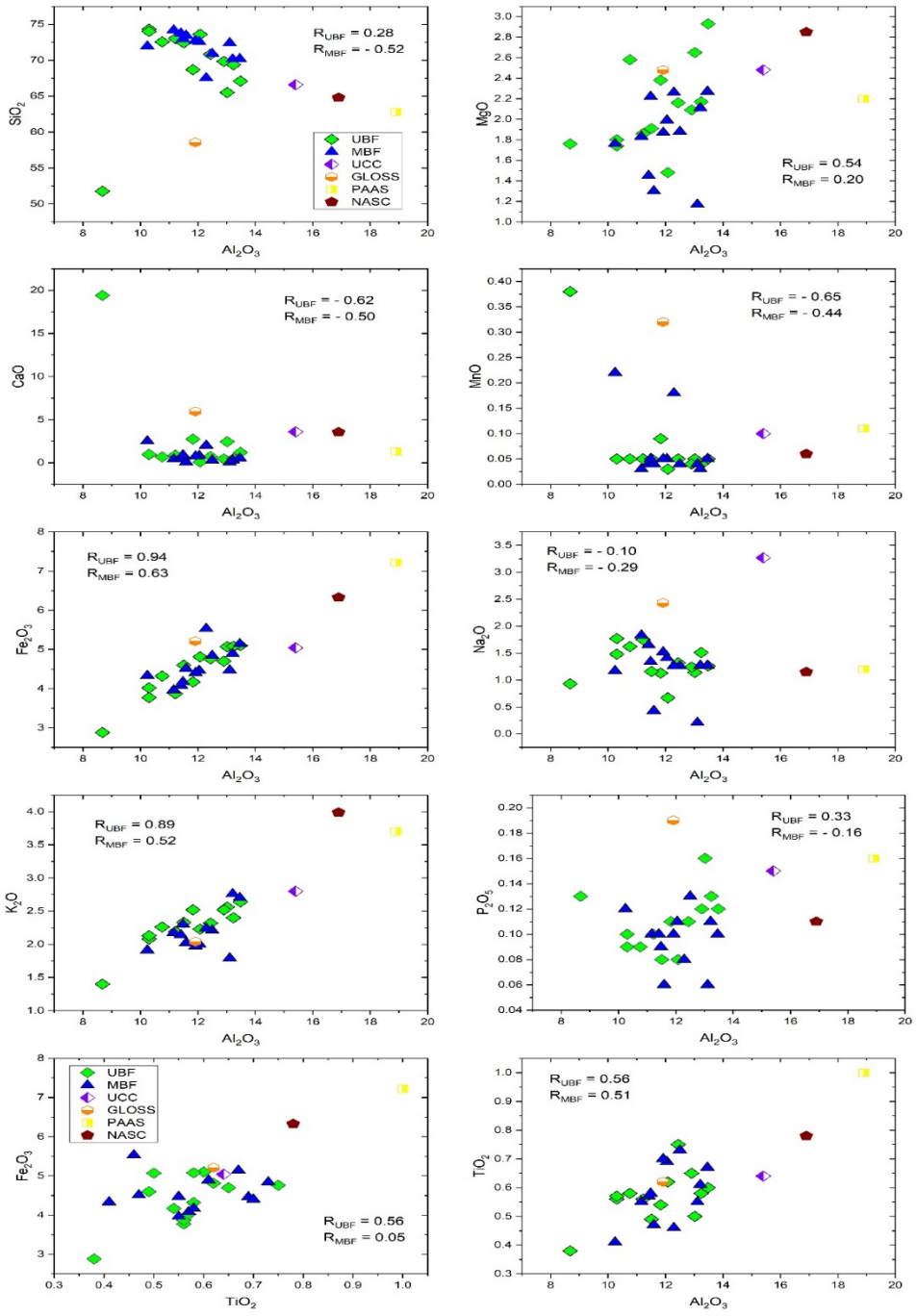

Figure 6.2 (A): Correlation between various Major Oxides of Bhuban sandstones, Lunglei town.

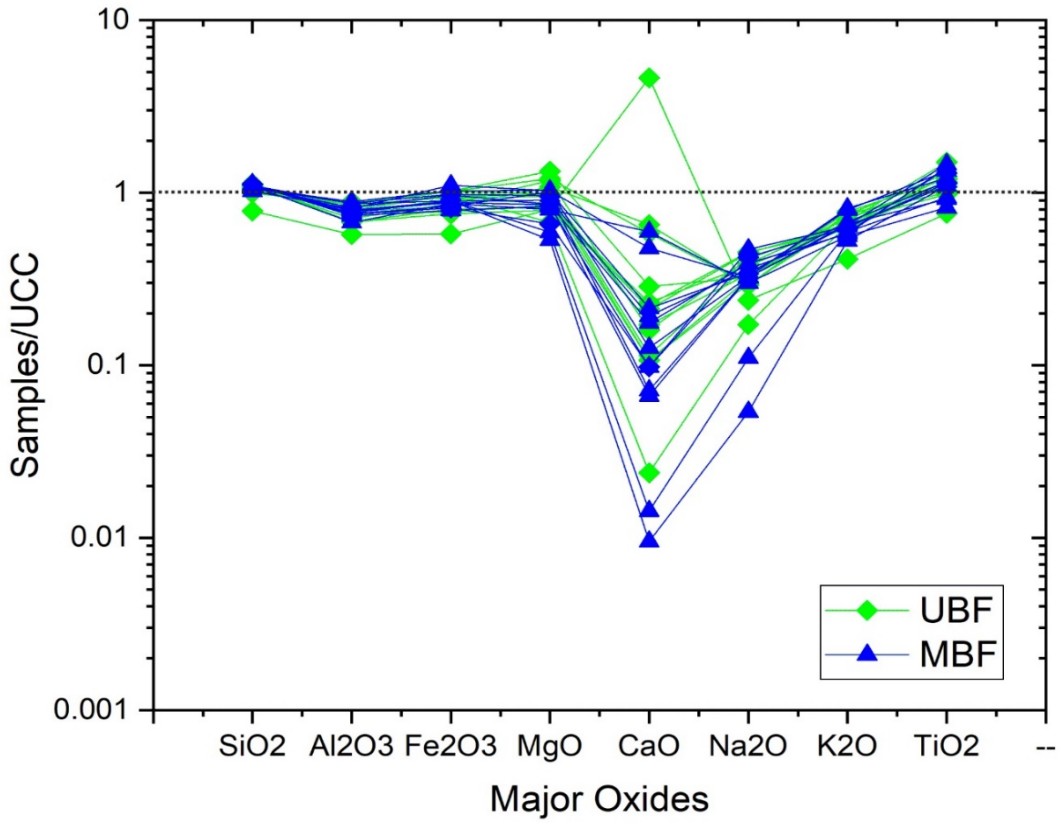

Figure 6.2 (B): UCC normalized the major elemental spider diagram of Bhuban sandstones, Lunglei town (UCC values after Taylor and McLennan, 1993).

6.2.2 Trace Elements

The concentration of trace elements (in parts per million) in the Bhuban sandstones of Lunglei is represented in Table 6.2. The UCC normalized trace element pattern {Figure 6.2 (D)} shows narrow compositional changes for Nb, Pb, Zr, Mg, La, Ce, Sc, Ni, and Cr. In comparison with UCC, the Bhuban sandstone samples are enriched in Si, and Rb, as well as depletion of Ca, Th, Na, Ba, and Fe. The zircon content of sediments is increasing in tandem with their compositional maturity. In the present study, the concentration of zircon is close to the UCC suggesting that the Bhuban sandstones in the study area are immature which is consistent with the petrographic analysis. Among the High Field Strength elements (HFSE), the depletion of Th, Y, and Ti may be associated with the source rocks. In the present studied samples, K-felspar, mica, and clay minerals are ubiquitous in most of the thin sections. Thus, the common occurrence of these minerals that

frequently host rubidium can account for the high Rb level in the Bhuban sandstone. Al_2O_3 exhibits a positive correlation with certain trace elements {Figure 6.2 (C)} such as Rb (R_{UBF}: 0.87, R_{MBF}: 0.58), Nb (R_{UBF}: 0.49, R_{MBF}: 0.43), and V (R_{UBF}: 0.88, R_{MBF}: 0.67) demonstrating the relationship between these elements and clay minerals such as kaolinite, chlorite, and illite. A strong positive correlation between Rb and K_2O (R_{UBF}: 0.98, R_{MBF}: 0.98) also suggested that the concentration of Rb is controlled by K_2O. However, other elements did not show a discernible trend as the samples are scattered. Lower concentrations of calcic plagioclase or their removal during the sedimentation processes are suggested by the depletion of CaO as well as the weak negative correlation of Sr against Al_2O_3 (R_{UBF}: - 0.32, R_{MBF}: - 0.37).

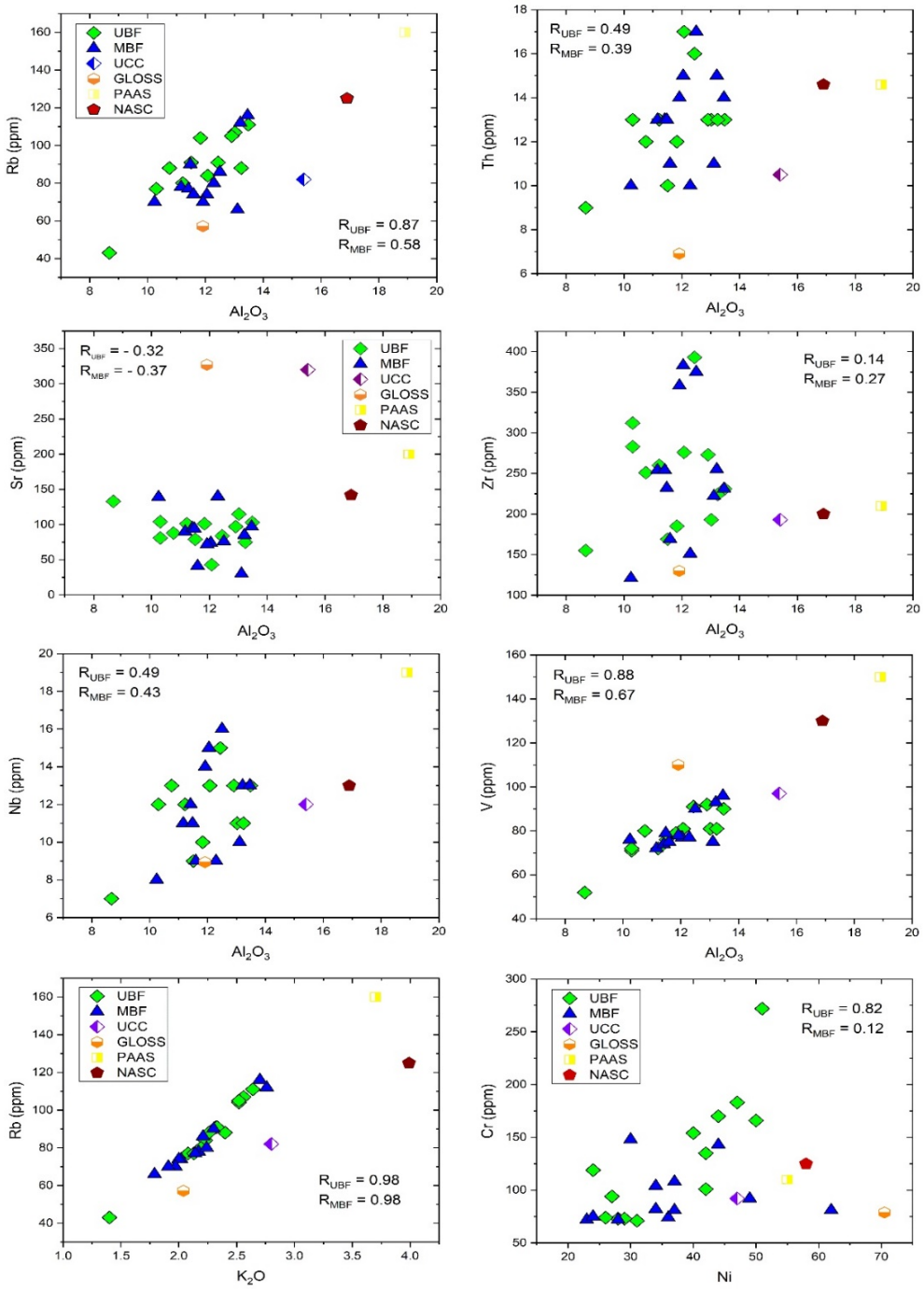

Figure 6.2 (C): Correlation between Al_2O_3 w.r.t. various Trace Elements of Bhuban sandstones, Lunglei town (Pearson, 1895).

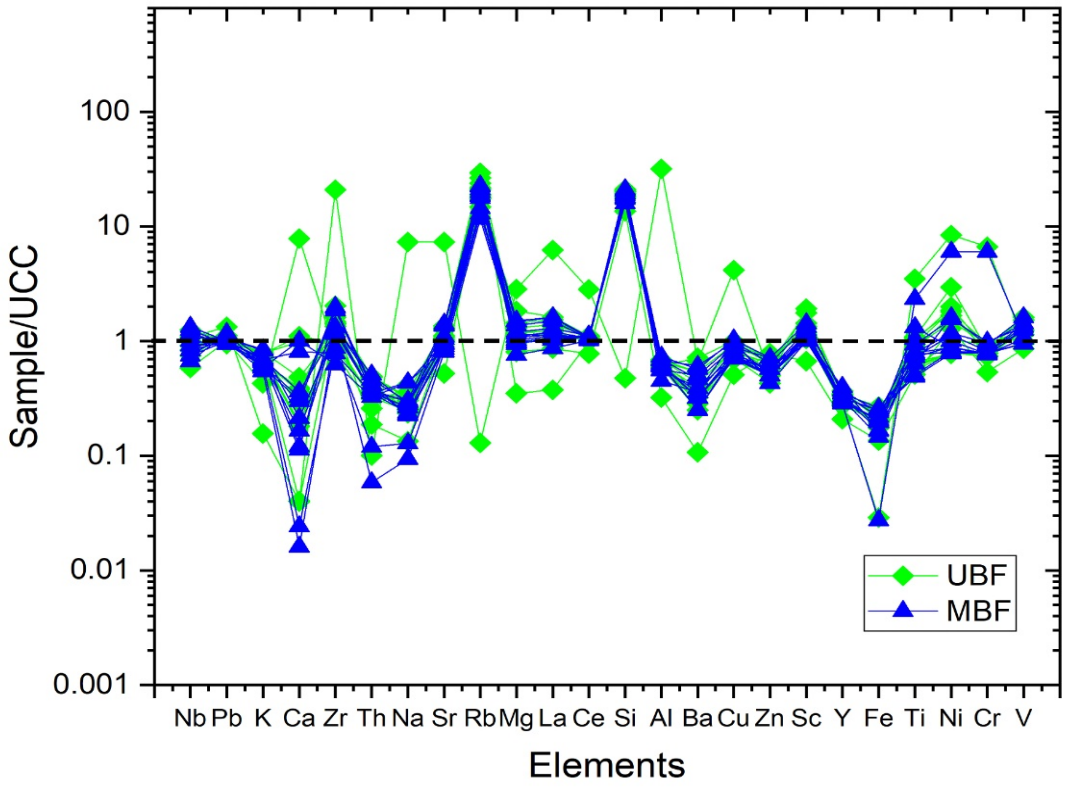

Figure 6.2 (D): UCC normalized the elemental pattern of Bhuban sandstones, Lunglei town.

6.2.3 Rare Earth Elements (REE)

The characteristics of rare earth elements are not greatly affected by sedimentary processes such as transportation, deposition, diagenesis, and weathering. Hence, they can be utilized effectively to determine the source rock characteristics and their tectonic setting as these elements are usually well preserved in the sediments. (Taylor and McLennan, 1985; Fu *et al.*, 2010, 2011; Bhatia, 1985; Bhatia and Crook, 1986). The rare earth elemental concentrations in the Bhuban sandstone of the study area are represented in Table 6.3. The Chondrite normalized REE pattern of the Bhuban samples {Figure 6.2 (E)} shows enrichment of LREE (La-Gd) and depletion of HREE (Tb-Lu) with negative Eu anomaly (average UBF = 0.62%, MBF = 0.61%). The REE pattern of Bhuban sandstones of Lunglei is nearly identical to the UCC patterns. The extremely uniform REE pattern of the samples may suggest that the derivation of sediments has a certain homogeneity. The typical characteristics of sedimentary rocks are also reflected by their negative Eu anomaly

(Ma *et al.*, 2021). Furthermore, the ratios of Eu/Eu* = (UBF ranging from 0.58 - 0.66, avg. 0.62; MBF ranging from 0.57 - 0.66, avg. 0.61), (La/Sm)N = (UBF ranging from 3.27 - 3.67, avg. 3.43; MBF ranging from 2.91 - 4.16, avg. 3.42), and (Gd/Yb)N= (UBF ranging from 2.12 - 2.48, avg. 2.25; MBF ranging from 2.10 - 2.70, avg. 2.34) nearly match the specifications of UCC when compared with the other standards. The fractionation of LREE is further demonstrated by $(La/Sm)_N$ = (UBF ranging from 3.27 - 3.67; avg. 3.43, MBF ranging from 2.91 - 4.16; avg. 3.42. The fractionation of HREE is demonstrated by the ratio of LREE/HREE, i.e., $(La/Lu)_N$ = (UBF ranging from 11.31 – 14.27, avg. 12.94; MBF ranging from 11.28 – 17.22, avg. 13.91). Also, the high $(Gd/Yb)_N$ ratio (avg. 2.34) indicates a trend of HREE depletion. Based on the REE pattern, and the ratios of LREE and HREE, along with the total REEs, the properties of the source rock can be identified (Allègre *et al.*, 1978). Hence, fractionated felsic to intermediate source rocks, such as granitoids are likely the main source of the studied Bhuban sandstone.

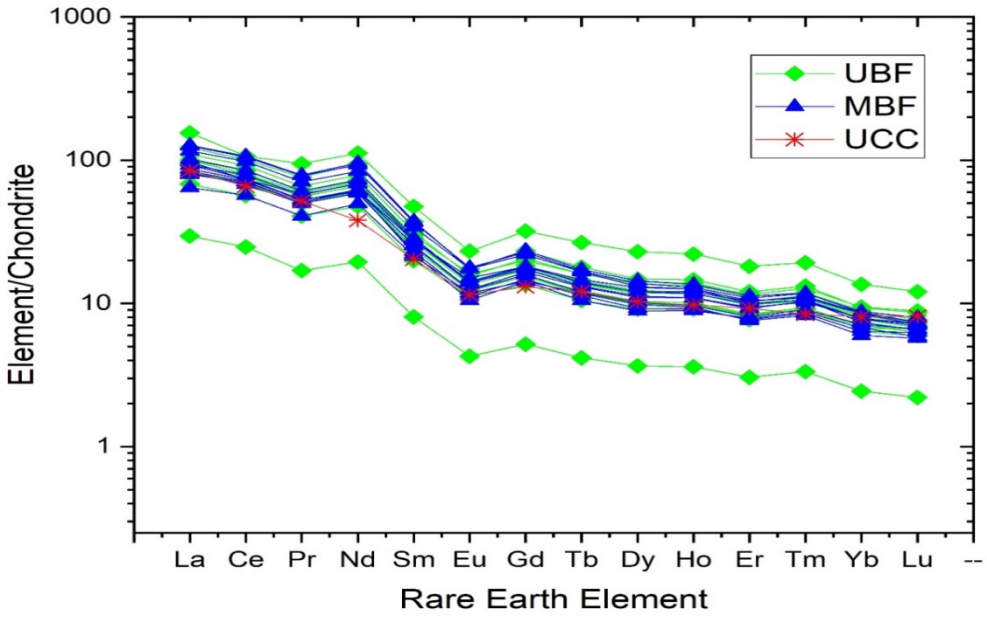

Figure 6.2 (E): Chondrite-normalized REE distribution pattern of Bhuban sandstones, Lunglei town (after Taylor and McLennan, 1985)

Table 6.1: Major element concentration in weight (wt %) for Bhuban sandstones in and around Lunglei Town [Standard concentration of major oxides- UCC (after Rudnick and Gao, 2003 & 2005); GLOSS after Plank and Langmuir, 1998); PAAS (after Taylor and McLennan, 1985); NASC (after Gromet *et al.*, 1984) are also highlighted in the table].

Litho Unit	Sample Nos.	SiO_2	TiO_2	Al_2O_3	Fe_2O_3	MnO	MgO	CaO	Na_2O	K_2O	P_2O_5	SiO_2/Al_2O_3	Al_2O_3/TiO_2	K_2O/Al_2O_3	K_2O/Na_2O
Upper Bhuban Formation	LS-6	65.51	0.50	13.02	5.07	0.05	2.65	2.44	1.14	2.56	0.16	5.03	26.04	0.20	2.25
	LS-7	73.61	0.62	12.08	4.81	0.03	1.48	0.10	0.67	2.23	0.08	6.09	19.48	0.18	3.33
	LS-9	68.68	0.54	11.83	4.17	0.09	2.38	2.74	1.13	2.52	0.11	5.81	21.91	0.21	2.23
	LS-10	69.84	0.65	12.91	4.70	0.04	2.09	0.45	1.24	2.52	0.12	5.41	19.86	0.20	2.03
	LS-18	74.32	0.56	10.30	3.77	0.05	1.74	0.94	1.77	2.08	0.09	7.22	18.39	0.20	1.18
	LS-19	73.03	0.56	11.22	3.87	0.05	1.86	0.89	1.75	2.19	0.10	6.51	20.04	0.20	1.25
	LS-26	67.10	0.60	13.48	5.10	0.05	2.93	1.20	1.26	2.64	0.12	4.98	22.47	0.20	2.10
	LS-27	51.77	0.38	8.68	2.88	0.38	1.76	19.41	0.93	1.40	0.13	5.96	22.84	0.16	1.51
	LS-28	69.37	0.58	13.24	5.08	0.04	2.17	0.48	1.51	2.40	0.13	5.24	22.83	0.18	1.59
	LS-29	70.82	0.75	12.44	4.76	0.05	2.16	0.72	1.32	2.32	0.11	5.69	16.59	0.19	1.76
	LS-30	74.01	0.57	10.30	4.02	0.05	1.80	0.97	1.48	2.13	0.10	7.19	18.07	0.21	1.44
	LS-33	72.42	0.49	11.51	4.60	0.05	1.91	0.45	1.16	2.33	0.08	6.29	23.49	0.20	2.01
	LS-34	72.56	0.58	10.76	4.32	0.05	2.58	0.67	1.62	2.26	0.09	6.74	18.55	0.21	1.40

Litho Unit	Sample Nos.	SiO_2	TiO_2	Al_2O_3	Fe_2O_3	MnO	MgO	CaO	Na_2O	K_2O	P_2O_5	SiO_2/Al_2O_3	Al_2O_3/TiO_2	K_2O/Al_2O_3	K_2O/Na_2O
Middle Bhuban Formation	LS-12	72.39	0.55	13.11	4.47	0.04	1.17	0.04	0.21	1.79	0.06	5.52	23.84	0.14	8.52
	LS-13	74.17	0.55	11.16	3.96	0.03	1.83	0.41	1.83	2.17	0.10	6.65	20.29	0.19	1.19
	LS-14	73.73	0.57	11.41	4.08	0.04	1.45	0.41	1.65	2.14	0.10	6.46	20.02	0.19	1.30
	LS-16	73.43	0.47	11.59	4.51	0.04	1.30	0.06	0.43	2.02	0.06	6.34	24.66	0.17	4.70
	LS-20	70.14	0.61	13.21	4.89	0.03	2.11	0.30	1.27	2.76	0.11	5.31	21.66	0.21	2.17
	LS-21	70.90	0.73	12.50	4.84	0.04	1.88	0.28	1.26	2.21	0.13	5.67	17.12	0.18	1.75
	LS-22	72.56	0.69	12.05	4.46	0.05	1.99	0.81	1.41	2.00	0.11	6.02	17.46	0.17	1.42
	LS-23	72.72	0.70	11.92	4.40	0.05	1.87	0.74	1.52	1.97	0.10	6.10	17.03	0.17	1.30
	LS-24	67.52	0.46	12.29	5.53	0.18	2.26	2.00	1.26	2.24	0.08	5.49	26.72	0.18	1.78
	LS-31	72.94	0.58	11.48	4.17	0.05	2.22	0.90	1.34	2.30	0.09	6.35	19.79	0.20	1.72
	LS-35	71.94	0.41	10.24	4.33	0.22	1.76	2.50	1.17	1.91	0.12	7.03	24.98	0.19	1.63
	LS-37	70.18	0.67	13.46	5.14	0.05	2.27	0.53	1.27	2.70	0.10	5.21	20.09	0.20	2.13

Standards	SiO_2	TiO_2	Al_2O_3	Fe_2O_3	MnO	MgO	CaO	Na_2O	K_2O	P_2O_5	SiO_2/Al_2O_3	Al_2O_3/TiO_2	K_2O/Al_2O_3	K_2O/Na_2O
UCC	66.6	0.64	15.4	5.04	0.1	2.48	3.59	3.27	2.8	0.15	4.32	24.06	0.18	0.86
GLOSS	58.57	0.62	11.91	5.21	0.32	2.48	5.95	2.43	2.04	0.19	4.92	19.21	0.17	0.84
PAAS	62.8	1	18.9	7.22	0.11	2.2	1.3	1.2	3.7	0.16	3.32	18.9	0.2	3.08
NASC	64.8	0.78	16.9	6.33	0.06	2.85	3.56	1.15	3.99	0.11	3.83	21.67	0.24	3.47

Table 6.2: Trace element concentration (in ppm) for Bhuban sandstones of Lunglei [Standard concentration of trace element - UCC (after Rudnick and Gao, 2003 & 2005); GLOSS (after Plank and Langmuir, 1998); PAAS (after Taylor and McLennan, 1985); NASC (after Gromet *et al.*, 1984) are also highlighted in the table].

Oxides/	UPPER BHUBAN FORMATION													Standards			
Elements	LS-6	LS-7	LS-9	LS-10	LS-18	LS-19	LS-26	LS-27	LS-28	LS-29	LS-30	LS-33	LS-34	UCC	GLOSS	PAAS	NASC
Sc	10.0	9.0	10.0	9.0	6.0	7.0	10.0	11.0	8.0	9.0	8.0	7.0	6.0	14.0	13.1	16.0	14.9
V	81.0	81.0	79.0	92.0	71.0	72.0	90.0	52.0	81.0	91.0	72.0	76.0	80.0	97.0	110.0	150.0	130.0
Cr	183.0	272.0	154.0	135.0	73.0	73.0	170.0	119.0	71.0	94.0	74.0	166.0	101.0	92.0	78.9	110.0	125.0
Co	57.0	44.0	41.0	48.0	47.0	46.0	51.0	40.0	73.0	93.0	60.0	39.0	53.0	17.3	21.9	23.0	25.7
Ni	47.0	51.0	40.0	42.0	28.0	29.0	44.0	24.0	31.0	27.0	26.0	50.0	42.0	47.0	70.5	55.0	58.0
Cu	20.0	8.0	12.0	15.0	7.0	9.0	15.0	3.0	11.0	10.0	8.0	7.0	8.0	28.0	75.0	50.0	-
Zn	67.0	53.0	57.0	63.0	48.0	46.0	63.0	34.0	57.0	54.0	46.0	48.0	50.0	67.0	86.4	85.0	-
Ga	15.0	11.0	13.0	13.0	13.0	12.0	15.0	5.0	14.0	13.0	12.0	14.0	13.0	-	-	-	-
Rb	107.0	84.0	104.0	105.0	77.0	80.0	111.0	43.0	88.0	91.0	77.0	91.0	88.0	82.0	57.2	160.0	125.0
Sr	115.0	43.0	101.0	97.0	104.0	101.0	103.0	133.0	75.0	84.0	81.0	79.0	88.0	320.0	327.0	200.0	142.0
Y	27.0	37.0	25.0	30.0	23.0	23.0	27.0	14.0	24.0	28.0	24.0	22.0	23.0	21.0	29.8	27.0	35.0
Zr	193.0	276.0	185.0	273.0	312.0	260.0	231.0	155.0	224.0	393.0	283.0	169.0	251.0	193.0	130.0	210.0	200.0
Nb	11.0	13.0	10.0	13.0	12.0	12.0	13.0	7.0	11.0	15.0	12.0	9.0	13.0	12.0	8.9	19.0	13.0
Ba	383.0	429.0	433.0	432.0	410.0	417.0	416.0	202.0	398.0	423.0	390.0	369.0	381.0	628.0	776.0	650.0	636.0
Pb	18.0	17.0	17.0	17.0	16.0	16.0	17.0	17.0	19.0	17.0	16.0	19.0	16.0	17.0	19.9	20.0	-
Th	13.0	17.0	12.0	13.0	13.0	13.0	13.0	9.0	13.0	16.0	13.0	10.0	12.0	10.5	6.9	14.6	12.0
U	3.8	3.9	0.0	2.9	1.0	3.2	0.0	0.0	0.0	2.2	2.6	0.0	0.0	2.7	1.7	3.1	2.7

Oxides/	UPPER BHUBAN FORMATION													Standards			
Elements	LS-6	LS-7	LS-9	LS-10	LS-18	LS-19	LS-26	LS-27	LS-28	LS-29	LS-30	LS-33	LS-34	UCC	GLOSS	PAAS	NASC
Rb/Sr	0.93	1.95	1.03	1.08	0.74	0.79	1.08	0.32	1.17	1.08	0.95	1.15	1.00	0.26	0.17	0.80	0.88
Y/Ni	0.57	0.73	0.63	0.71	0.82	0.79	0.61	0.58	0.77	1.04	0.92	0.44	0.55	0.45	0.42	0.49	0.60
Co/Th	4.38	2.59	3.42	3.69	3.62	3.54	3.92	4.44	5.62	5.81	4.62	3.90	4.42	1.65	3.17	1.58	2.14
Th/Co	0.23	0.39	0.29	0.27	0.28	0.28	0.25	0.23	0.18	0.17	0.22	0.26	0.23	0.61	0.32	0.63	0.47
Cr/Th	14.08	16.00	12.83	10.38	5.62	5.62	13.08	13.22	5.46	5.88	5.69	16.60	8.42	8.76	11.42	7.53	10.42
Cr/Ni	3.89	5.33	3.85	3.21	2.61	2.52	3.86	4.96	2.29	3.48	2.85	3.32	2.40	1.96	1.12	2.00	2.16
Th/Cr	0.07	0.06	0.08	0.10	0.18	0.18	0.08	0.08	0.18	0.17	0.18	0.06	0.12	0.11	0.09	0.13	0.10
Zr/Cr	1.05	1.01	1.20	2.02	4.27	3.56	1.36	1.30	3.15	4.18	3.82	1.02	2.49	2.10	1.65	1.91	1.60
Th/Sc	1.30	1.89	1.20	1.44	2.17	1.86	1.30	0.82	1.63	1.78	1.63	1.43	2.00	0.75	0.53	0.91	0.81
Zr/Sc	19.30	30.67	18.50	30.33	52.00	37.14	23.10	14.09	28.00	43.67	35.38	24.14	41.83	13.79	9.92	13.13	13.42
Cr/V	2.26	3.36	1.95	1.47	1.03	1.01	1.89	2.29	0.88	1.03	1.03	2.18	1.26	0.95	0.72	0.73	0.96
Cr/Zr	0.95	0.99	0.83	0.49	0.23	0.28	0.74	0.77	0.32	0.24	0.26	0.98	0.40	0.48	0.61	0.52	0.63
Th/U	3.42	4.36	0.00	4.48	13.00	4.06	0.00	0.00	0.00	7.27	5.00	0.00	0.00	3.89	4.11	4.71	4.51

Oxides/	MIDDLE BHUBAN FORMATION												Standards			
Elements	LS-12	LS-13	LS-14	LS-16	LS-20	LS-21	LS-22	LS-23	LS-24	LS-31	LS-35	LS-37	UCC	GLOSS	PAAS	NASC
Sc	6.00	7.00	8.00	7.00	10.00	10.00	8.00	7.00	7.00	8.00	7.00	9.00	14.0	13.1	16.0	14.9
V	75.00	72.00	74.00	75.00	93.00	90.00	77.00	78.00	77.00	79.00	76.00	96.00	97.0	110.0	150.0	130.0
Cr	81.00	72.00	82.00	92.00	108.00	148.00	72.00	75.00	74.00	104.00	81.00	143.00	92.0	78.9	110.0	125.0
Co	41.00	86.00	64.00	67.00	79.00	57.00	81.00	67.00	88.00	88.00	71.00	52.00	17.3	21.9	23.0	25.7
Ni	62.00	28.00	34.00	49.00	37.00	30.00	23.00	24.00	36.00	34.00	37.00	44.00	47.0	70.5	55.0	58.0
Cu	10.00	9.00	7.00	10.00	16.00	13.00	9.00	7.00	14.00	9.00	11.00	17.00	28.0	75.0	50.0	-
Zn	68.00	47.00	48.00	55.00	69.00	59.00	49.00	50.00	63.00	52.00	49.00	66.00	67.0	86.4	85.0	-
Ga	12.00	13.00	12.00	13.00	16.00	14.00	12.00	13.00	12.00	13.00	12.00	16.00	-	-	-	-
Rb	66.00	78.00	77.00	74.00	112.00	86.00	74.00	70.00	80.00	90.00	70.00	116.00	82.0	57.2	160.0	125.0
Sr	30.00	90.00	95.00	41.00	85.00	76.00	74.00	72.00	140.00	94.00	139.00	97.00	320.0	327.0	200.0	142.0
Y	21.00	23.00	22.00	24.00	30.00	30.00	26.00	25.00	22.00	24.00	21.00	28.00	21.0	29.8	27.0	35.0
Zr	222.00	254.00	254.00	169.00	255.00	375.00	383.00	358.00	151.00	232.00	121.00	231.00	193.0	130.0	210.0	200.0
Nb	10.00	11.00	12.00	9.00	13.00	16.00	15.00	14.00	9.00	11.00	8.00	13.00	12.0	8.9	19.0	13.0
Ba	282.00	401.00	391.00	376.00	458.00	436.00	389.00	381.00	353.00	382.00	347.00	426.00	628.0	776.0	650.0	636.0
Pb	17.00	16.00	16.00	17.00	18.00	17.00	16.00	16.00	20.00	17.00	20.00	18.00	17.0	19.9	20.0	-
Th	11.00	13.00	13.00	11.00	15.00	17.00	15.00	14.00	10.00	13.00	10.00	14.00	10.5	6.9	14.6	12.0
U	2.40	0.00	0.00	2.20	1.00	1.80	1.60	2.20	0.00	1.00	1.00	0.00	2.7	1.7	3.1	2.7

Oxides/	MIDDLE BHUBAN FORMATION												Standards			
Elements	LS-12	LS-13	LS-14	LS-16	LS-20	LS-21	LS-22	LS-23	LS-24	LS-31	LS-35	LS-37	UCC	GLOSS	PAAS	NASC
Rb/Sr	2.20	0.87	0.81	1.80	1.32	1.13	1.00	0.97	0.57	0.96	0.50	1.20	0.26	0.17	0.80	0.88
Y/Ni	0.34	0.82	0.65	0.49	0.81	1.00	1.13	1.04	0.61	0.71	0.57	0.64	0.45	0.42	0.49	0.60
Co/Th	3.73	6.62	4.92	6.09	5.27	3.35	5.40	4.79	8.80	6.77	7.10	3.71	1.65	3.17	1.58	2.14
Th/Co	0.27	0.15	0.20	0.16	0.19	0.30	0.19	0.21	0.11	0.15	0.14	0.27	0.61	0.32	0.63	0.47
Cr/Th	7.36	5.54	6.31	8.36	7.20	8.71	4.80	5.36	7.40	8.00	8.10	10.21	8.76	11.42	7.53	10.42
Cr/Ni	1.31	2.57	2.41	1.88	2.92	4.93	3.13	3.13	2.06	3.06	2.19	3.25	1.96	1.12	2.00	2.16
Th/Cr	0.14	0.18	0.16	0.12	0.14	0.11	0.21	0.19	0.14	0.13	0.12	0.10	0.11	0.09	0.13	0.10
Zr/Cr	2.74	3.53	3.10	1.84	2.36	2.53	5.32	4.77	2.04	2.23	1.49	1.62	2.10	1.65	1.91	1.60
Th/Sc	1.83	1.86	1.63	1.57	1.50	1.70	1.88	2.00	1.43	1.63	1.43	1.56	0.75	0.53	0.91	0.81
Zr/Sc	37.00	36.29	31.75	24.14	25.50	37.50	47.88	51.14	21.57	29.00	17.29	25.67	13.79	9.92	13.13	13.42
Cr/V	1.08	1.00	1.11	1.23	1.16	1.64	0.94	0.96	0.96	1.32	1.07	1.49	0.95	0.72	0.73	0.96
Cr/Zr	0.36	0.28	0.32	0.54	0.42	0.39	0.19	0.21	0.49	0.45	0.67	0.62	0.48	0.61	0.52	0.63
Th/U	4.58	0.00	0.00	5.00	15.00	9.44	9.38	6.36	0.00	13.00	10.00	0.00	3.89	4.11	4.71	4.51

Table 6.3: Concentration of Rare Earth Elements in Bhuban Sandstone of Lunglei (in ppm) [Standard REE concentration - UCC (after Rudnick and Gao, 2003 & 2005); GLOSS after Plank and Langmuir, 1998); PAAS (after Taylor and McLennan, 1985); NASC (after Gromet *et al.*, 1984) are also highlighted in the table].

Oxides/ Elements	Upper Bhuban Formation						
	LS-06	LS-07	LS-09	LS-10	LS-18	LS-19	LS-26
La	10.84	56.94	34.73	36.73	36.83	30.02	34.80
Ce	23.71	102.28	73.69	76.26	80.69	66.45	73.78
Pr	2.32	12.96	7.62	8.22	8.35	6.86	7.83
Nd	13.84	79.53	47.31	50.54	51.27	41.98	49.57
Sm	1.86	10.96	6.15	6.88	6.57	5.56	6.46
Eu	0.37	2.01	1.24	1.40	1.23	1.06	1.24
Gd	1.59	9.78	5.36	6.10	5.62	4.73	5.62
Tb	0.24	1.54	0.79	0.93	0.84	0.69	0.82
Dy	1.40	8.75	4.48	5.38	4.69	3.80	4.49
Ho	0.31	1.88	1.04	1.18	1.02	0.84	1.00
Er	0.76	4.52	2.44	2.87	2.56	2.08	2.42
Tm	0.12	0.69	0.37	0.45	0.40	0.32	0.40
Yb	0.61	3.36	1.92	2.33	2.03	1.65	2.02
Lu	0.08	0.46	0.26	0.34	0.28	0.26	0.29
(La/Yb)N	12.08	11.44	12.26	10.63	12.27	12.28	11.64
(La/Sm)N	3.67	3.27	3.56	3.36	3.53	3.4	3.39
(Gd/Yb)N	2.13	2.36	2.27	2.12	2.25	2.32	2.25
Eu/Eu*	0.65	0.58	0.64	0.65	0.6	0.62	0.61
(La/Lu)N	13.39	12.85	13.97	11.31	13.70	12.22	12.54

Oxides/ Elements	Upper Bhuban Formation					
	LS-27	LS-28	LS-29	LS-30	LS-33	LS-34
La	25.00	30.23	44.91	40.26	30.36	34.17
Ce	54.12	66.67	96.72	87.72	66.13	74.89
Pr	5.57	6.91	10.45	9.01	6.82	7.67
Nd	33.88	42.68	66.68	56.04	41.96	46.85
Sm	4.60	5.62	8.58	7.29	5.57	6.21
Eu	0.96	1.07	1.51	1.35	1.09	1.18
Gd	4.13	4.72	7.09	6.28	4.70	5.25
Tb	0.61	0.68	1.04	0.93	0.71	0.80
Dy	3.48	3.75	5.63	5.20	3.94	4.53
Ho	0.78	0.82	1.25	1.13	0.86	0.99
Er	1.91	2.05	3.00	2.80	2.10	2.47
Tm	0.30	0.32	0.47	0.42	0.33	0.39
Yb	1.58	1.72	2.32	2.21	1.74	1.95
Lu	0.23	0.26	0.33	0.29	0.24	0.28
(La/Yb)N	10.72	11.88	13.1	12.34	11.82	11.87
(La/Sm)N	3.42	3.39	3.29	3.48	3.43	3.46
(Gd/Yb)N	2.12	2.22	2.48	2.31	2.19	2.19
Eu/Eu*	0.66	0.62	0.58	0.6	0.63	0.61
(La/Lu)N	11.43	12.31	14.21	14.27	13.13	12.85

Oxides/ Elements	Middle Bhuban Formation							
	LS-12	LS-13	LS-14	LS-16	LS-20	LS-21	LS-22	LS-23
La	33.86	37.31	31.83	35.88	42.63	46.10	46.62	29.79
Ce	70.65	81.49	69.83	70.00	93.88	100.87	101.94	64.73
Pr	7.28	8.35	7.21	7.93	9.67	10.65	10.77	6.82
Nd	42.88	51.91	44.31	48.59	59.52	65.97	67.99	41.71
Sm	5.13	6.60	5.82	6.34	7.86	8.51	8.66	5.35
Eu	0.92	1.23	1.08	1.23	1.51	1.54	1.51	0.98
Gd	4.36	5.58	4.86	5.48	6.71	6.98	7.16	4.50
Tb	0.61	0.81	0.69	0.82	0.96	0.97	1.00	0.66
Dy	3.38	4.60	3.87	4.58	4.98	5.26	5.48	3.52
Ho	0.76	1.02	0.82	1.00	1.07	1.10	1.15	0.78
Er	1.96	2.57	2.01	2.46	2.60	2.72	2.80	1.93
Tm	0.31	0.40	0.32	0.38	0.39	0.42	0.42	0.30
Yb	1.67	2.12	1.77	1.94	2.10	2.17	2.15	1.58
Lu	0.22	0.28	0.25	0.27	0.27	0.30	0.28	0.24
(La/Yb)N	13.69	11.88	12.15	12.5	13.7	14.36	14.64	12.74
(La/Sm)N	4.16	3.56	3.44	3.56	3.41	3.41	3.39	3.51
(Gd/Yb)N	2.11	2.13	2.22	2.29	2.58	2.61	2.7	2.31
Eu/Eu*	0.58	0.61	0.6	0.62	0.62	0.6	0.57	0.6
(La/Lu)N	15.69	13.83	13.11	14.00	16.39	15.74	17.22	12.94

Oxides/ Elements	Middle Bhuban Formation				Standards			
	LS-24	LS-31	LS-35	LS-37	UCC	GLOSS	PAAS	NASC
La	23.58	30.70	29.17	34.04	31	28.8	38.2	31.1
Ce	54.36	67.85	67.14	75.75	63	57.3	79.6	67.03
Pr	5.60	7.00	6.99	7.85	7.1	-	8.83	-
Nd	35.24	43.30	43.79	48.78	27	27	33.9	30.4
Sm	4.95	5.89	6.31	6.37	4.7	5.78	5.55	5.98
Eu	1.03	1.09	1.31	1.22	1	1.31	1.08	1.25
Gd	4.38	5.06	5.53	5.31	4	5.26	4.66	5.5
Tb	0.68	0.75	0.85	0.77	0.7	-	0.77	0.85
Dy	3.75	4.19	4.91	4.30	3.9	4.99	4.68	5.54
Ho	0.80	0.93	1.07	0.93	0.83	-	0.99	-
Er	1.89	2.34	2.49	2.29	2.3	2.92	2.85	3.28
Tm	0.29	0.36	0.38	0.37	0.3	-	0.41	-
Yb	1.48	1.95	1.83	1.95	2	2.76	2.82	3.11
Lu	0.22	0.27	0.25	0.28	0.31	0.413	0.43	0.46
(La/Yb)N	10.77	10.63	10.76	11.81	10.47	7.05	9.15	6.75
(La/Sm)N	3	3.28	2.91	3.37	4.15	3.14	4.33	3.27
(Gd/Yb)N	2.4	2.1	2.45	2.21	1.62	1.54	1.34	1.43
Eu/Eu*	0.66	0.59	0.66	0.62	0.69	0.71	0.63	0.66
(La/Lu)N	11.28	11.63	12.21	12.80	10.38	7.24	9.22	7.08

CHAPTER 7

DISCUSSION

7.1 PROVENANCE

Provenance is the source rock from which the sediments are derived prior to the reworking process. Clastic sedimentary rocks, such as sandstone, siltstone, and shale, are composed of igneous, metamorphic, and other sedimentary rock fragments. Because the transportation mechanism cannot reveal much about the character of the parent rocks, it is crucial to ascertain the source of the sediments. The petrography of sandstones – more specifically, the petrographic modal data has long been successfully employed for the provenance determination of clastic sedimentary rocks. Furthermore, the geochemical characteristics of clastic sediments are becoming a reliable tool for provenance analysis.

7.1.1 Petrographic Provenance

To determine the provenance characteristics and the paleo-climatic conditions that prevail at the time of deposition, different varieties of quartz like monocrystalline quartz (both undulose and non-undulose) and polycrystalline quartz (2-3 grains and >3 grains per quartz) are utilized. Data obtained after thin section analysis revealed that the most common type of quartz is non-undulose monocrystalline (Q_{Mnu}: UBF: 52.08 – 66.61%, MBF: 50.21 – 66.11%) followed by monocrystalline undulose quartz (Q_{Mu} : UBF: 2.10 – 15.40%, MBF: 1.40 - 11.50 %), polycrystalline 2-3 grain per quartz (Q_{P2-3} : UBF: 0.20 – 3.70%, MBF: 0.50 – 3.20%) and polycrystalline >3 grain per quartz (QP>3 : UBF: 0.00 – 5.10%, UBF: 0.00 – 2.30%).

Basu *et al.* (1975) proposed a diamond plot by using the relative abundance of monocrystalline and polycrystalline quartz to classify the origin of the sediments into plutonic, middle and upper-rank metamorphic and low-rank metamorphic types. In the diamond plot {Figure 7.1 (A)}, the recalculated value of the different quartz varieties of Bhuban sandstones in the study area are plotted and it has been noticed that most of the sandstone samples fall within plutonic rocks and only a few

sandstones fall within middle and upper-rank metamorphic rocks. This indicates that most of the quartz grains are derived from plutonic rocks and only a few quartz grains are originated from metamorphic terrain. In some undulose quartz grains, the strain effects can be observed which indicates that the source rock might have undergone deformation due to compression.

Keeping the same variables of quartz varieties and introducing certain new fields of source rocks, another diamond diagram was suggested by Tortosa *et al.* (1991) which is the modified version of Basu *et al.* (1975). According to this diamond plot, most of the studied sandstone samples were assembled in the field of extreme left central position indicating their derivation from granitic rocks and middle and upper-rank metamorphic rocks {(Figure 7.1 (B)}. Therefore, based on these two provenance discrimination plots. it can be inferred that the sediments under study are derived from granitic rocks and middle to upper-rank metamorphic rocks Furthermore, the modal analysis of thin sections showing a low abundance of feldspars (with an average of UBF: 2.10%, MBF: 1.65%) suggested that the sediments are transported for a moderate distance or reworking of sediments. To establish the extent of maturity of clastic sediments during transportation, a ternary plot of Qm-P-K proposed by Dickinson (1985) was employed. Accordingly, due to their moderate distance of transport, the present studied Bhuban sandstone shows that the sediments are immature which are derived from the continental block provenance {Figure 7.1 (C)}.

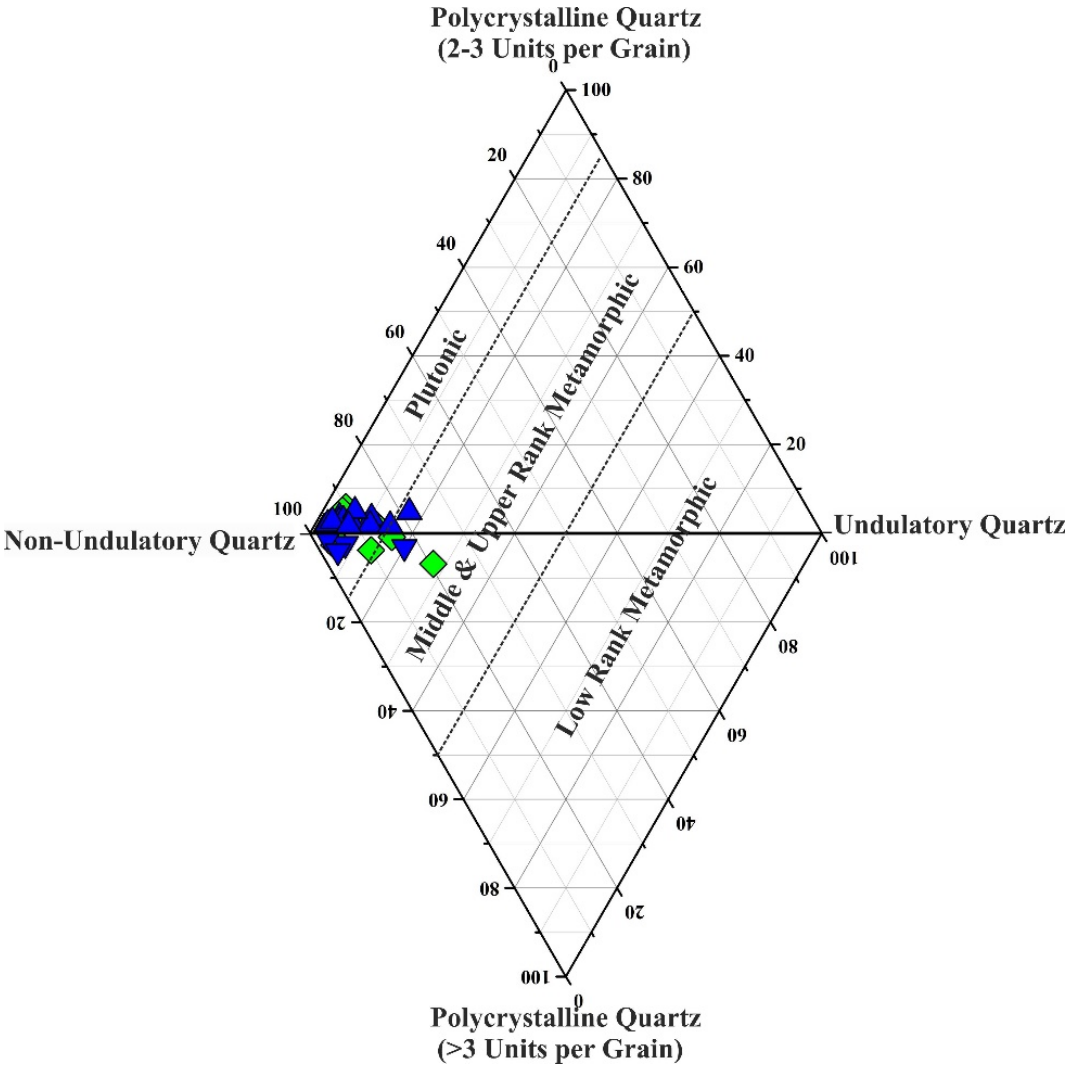

Figure 7.1 (A): Provenance plot for Bhuban sandstones, Lunglei town (after Basu *et al.*, 1975).

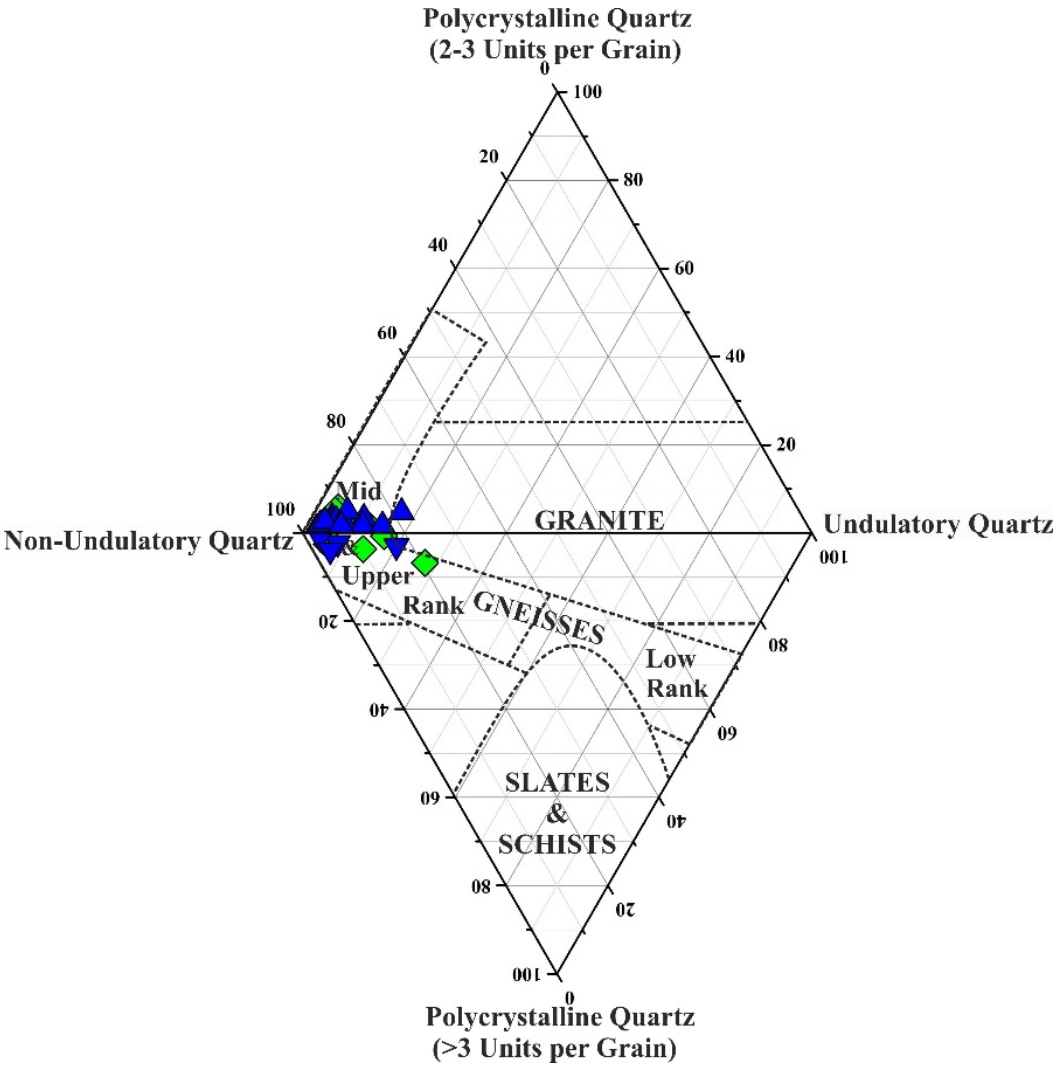

Figure 7.1 (B): Diamond plot for determining the provenance of Bhuban sandstones, Lunglei town (after Tortosa *et al.*, 1991).

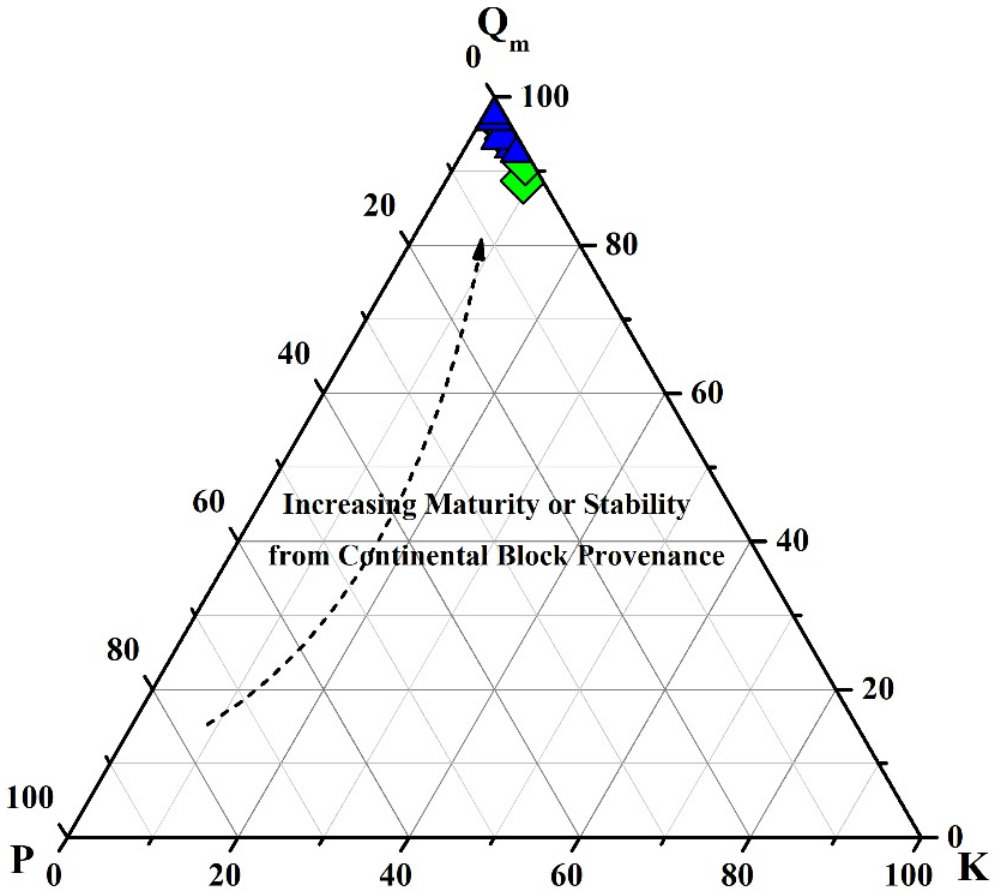

Figure 7.1 (C): Triangular Q_mPK plot for Bhuban sandstones, Lunglei town (after Dickinson, 1985).

7.1.2 Geochemical Provenance

According to Dickinson and Suczek (1979), the composition of clastic sedimentary rocks was primarily determined by the composition of the source rock and the nature and type of the dispersal pattern within the depositional basin. Geochemistry is a commonly used and very precise method for determining the nature and kind of source rock. Since trace elements are better able to distinguish between different petrological processes than major elements, which are also crucial for determining the provenance of clastic rocks, the study of trace elements has grown in importance in modern petrology. The properties of certain trace elements including Chromium (Cr), Cobalt (Co), Thorium (Th), Scandium (Sc), Zircon (Zr), and Rare Earth elements (REE) are not much affected by the processes of

sedimentation such as transportation, weathering, diagenesis, and lithification process (Taylor and McLennan, 1985; Bhatia and Crook, 1986; McLennan *et al.*, 1993). According to evidence from permeable clastic rocks of river and aeolian origin, some trace elements including Zr, Nb, and Y, along with REE, were admittedly immobile but unusually present throughout the last stage of diagenesis. Geochemical plots developed by Bhatia (1983), Bracciali *et al.* (2007), Floyd *et al.* (1989), Hayashi *et al.* (1997), Jinliang and Xin (2008), Schoenborn and Fedo (2011), Mongelli *et al.* (2006), and Mc Lennan *et al.* (1993) are all employed in the current work.

The derivation of sediments from multiple sources is once again successfully portrayed by Bhatia (1983) by employing the weight percentages of the principal oxides CaO, Na_2O, and K_2O in ternary plots, where the source fields are represented by the standard average values of andesite, dacite, granodiorite, and granite after Le Maitre (1976). The preponderance of the Bhuban sandstones {Figure 7.1 (D)} indicates that the sediments came from granitic terrain.

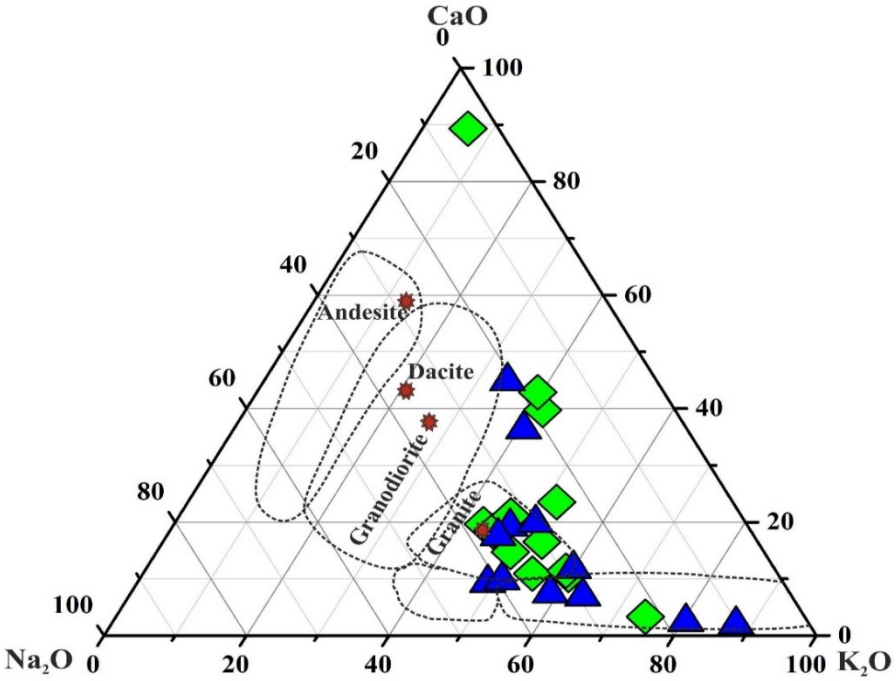

Figure 7.1 (D): Triangular provenance plot for Bhuban Sandstones, Lunglei town (after Bhatia, 1983).

Bracciali *et al.* (2007) proposed a triangular diagram (V-Ni-Th x10) for the determination of the source rock characteristics based on their immobile natures during the sedimentation process. Certain elements like Thorium are usually concentrated in felsic rocks while some elements including V and Ni are more dominant in mafic and ultramafic rocks. The Bhuban sandstones are rich in Th but depleted in V and Ni, as seen in the plot {Figure 7.1 (E)} following Bracciali *et al.* (2007). As a result, the majority of the samples are restricted to an area close to the felsic field.

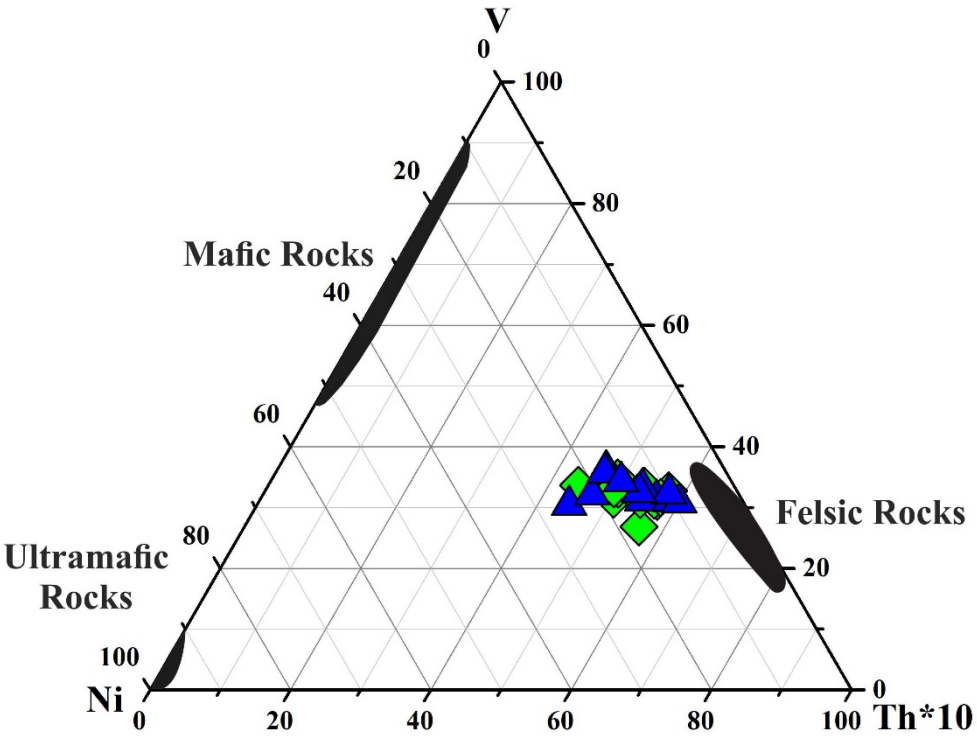

Figure 7.1 (E): V-Ni-Th x10 provenance ternary plot for Bhuban Sandstones, Lunglei town (after Bracciali *et al.*, 2007).

The bivariate TiO_2 vs Ni plot from Floyd *et al.*, (1989) is also commonly used provenance determination of sediments. This plot suggested that the Bhuban sandstone of the study area is an acidic rock derivation {Figure 7.1 (F)}. According to Hayashi *et al.* (1997), as SiO_2 concentration rises, the ratio of TiO_2/Zr falls. Based on these relations, he suggests that the TiO_2/Zr ratio in clastic deposits should be greater than 200 for mafic source rock, 195–55 for intermediate source rock, and 55

for felsic source rock. The ratios of TiO_2/Zr for the Bhuban sandstone of Lunglei are all less than 55 indicating the felsic source rocks {Figure 7.1 (G)}.

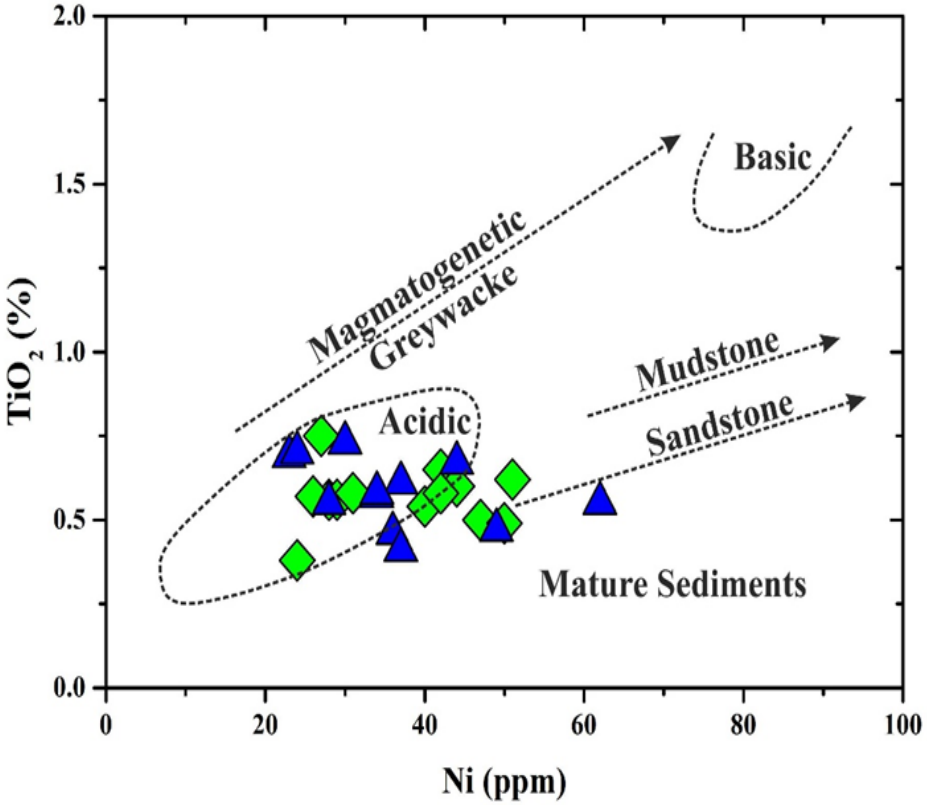

Figure 7.1 (F): Ni vs TiO_2 bivariate provenance diagram of Bhuban Sandstones, Lunglei town (after Floyd *et al.*, 1989).

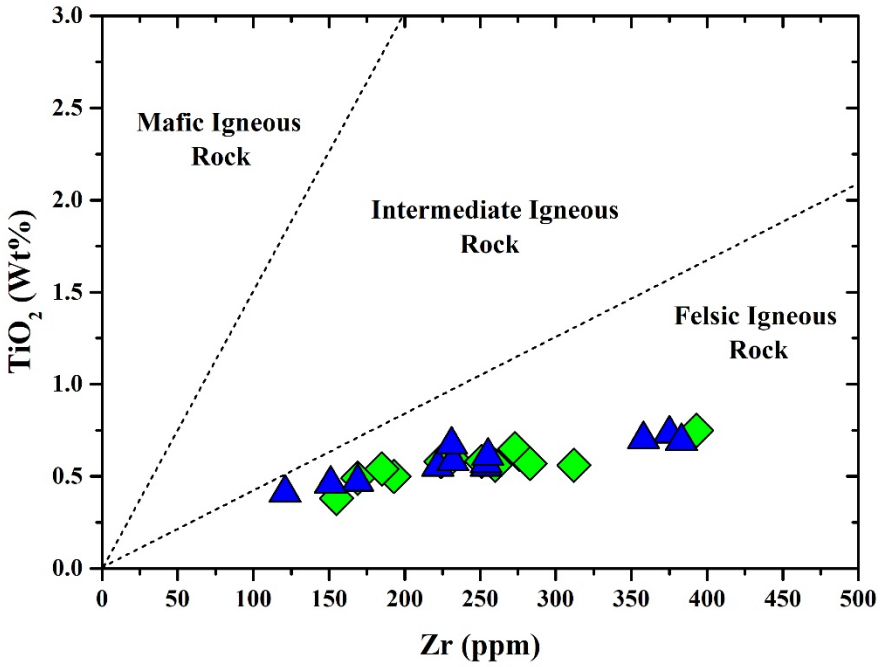

Figure 7.1 (G): Zr vs TiO_2 binary plot for Bhuban Sandstones, Lunglei town (after Hayashi *et al.*, 1997).

Additionally, Jinliang and Xin (2008) developed the La-Th-Sc ternary plot to indicate the origin of source sediments, mostly for sandstones, from the intermixing of granite (with Eu/Eu*: 0.5 and Th/Sc: 1.18) and granodiorite (with Eu/Eu*: 0.7 and Th/Sc: 0.5). Plotting of the Bhuban sandstones (average Eu/Eu*: UBF = 0.62, MBF = 0.62 and average Th/Sc: UBF = 1.57, MBF = 1.67), majority of the samples clustered close to the granitic region and few samples clustered towards granodiorite region as shown in {Figure 7.1 (H)} due to La enrichment. This diagram illustrates how sediments from the mixing of granite and granodioritic source rocks contributed to the formation of the Bhuban Formation.

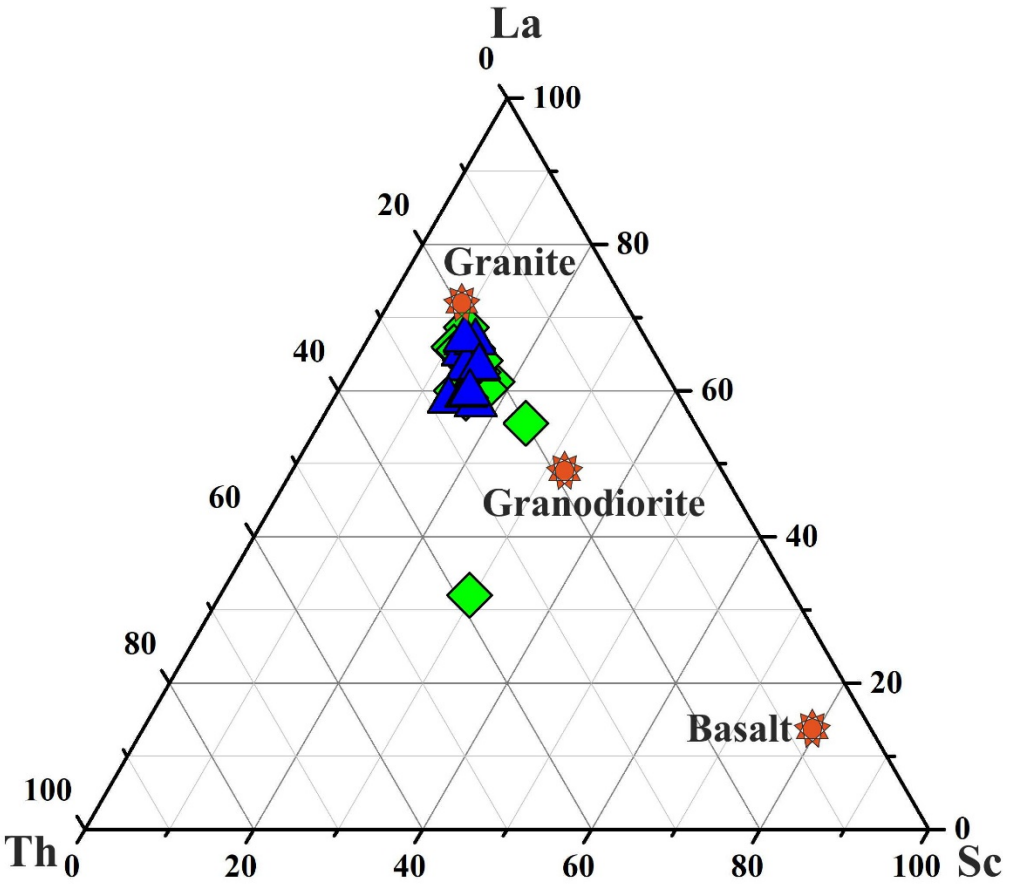

Figure 7.1 (H): Ternary provenance plot of La-Th-Sc depicting the mixing of different source sediments for Bhuban Sandstones, Lunglei town (after Jinliang and Xin, 2008).

For the analyses of the source rock for Bhuban sandstones in the study area, a ratio of Sc vs Th/Sc is plotted in a binary diagram (after Schoenborn and Fedo, 2011). The average ratio of Th/Sc for the Bhuban sandstones of the study area is 1.7 which is close to the intermixing model of Schoenborn and Fedo (2011) (Th/Sc=1.1.15) suggesting the input of intermixing of granodioritic and granitic source rocks {Figure 7.1 (I)}.

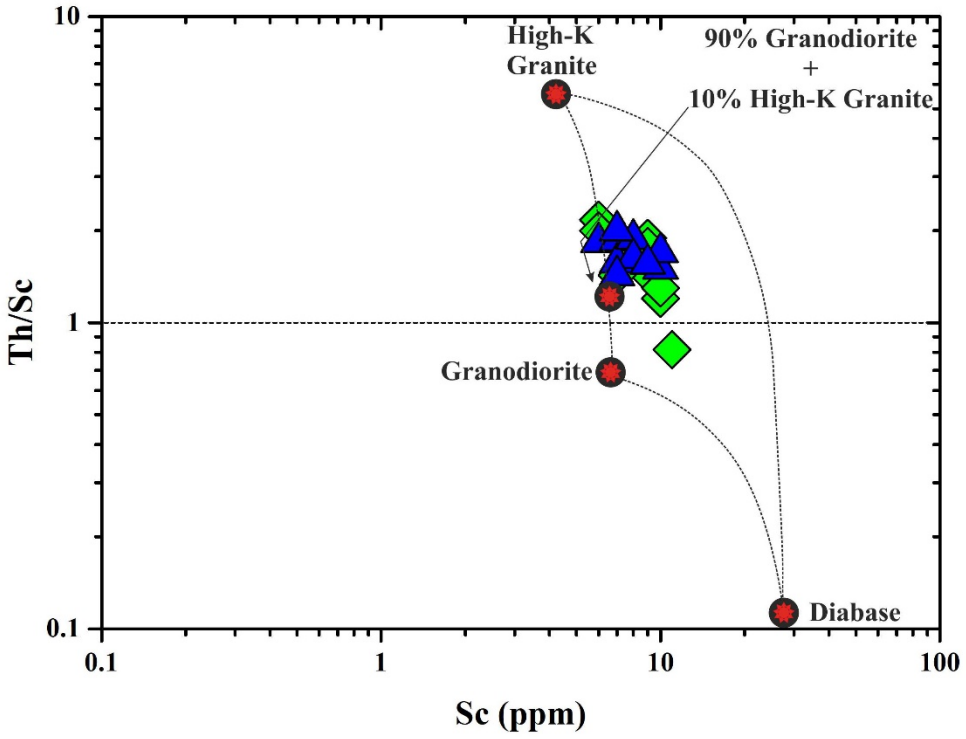

Figure 7. (I): A binary plot of Sc vs Th/Sc for Bhuban Sandstones, Lunglei town (after Schoenborn & Fedo, 2011).

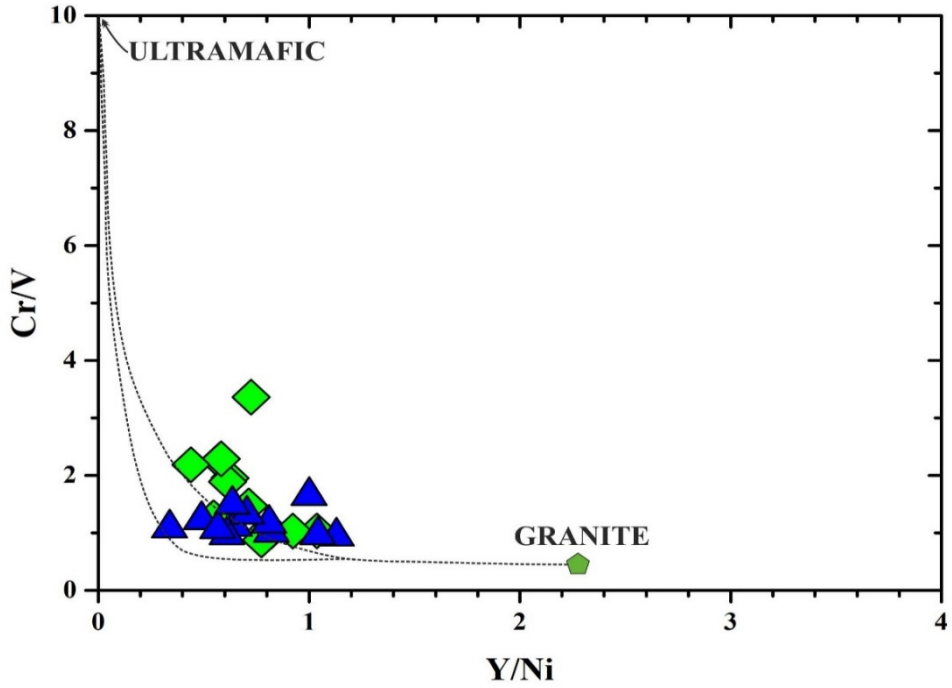

Figure 7.1 (J): Binary plot of Y/Ni vs Cr/V for Granite-Ultramafic end member mixing of Bhuban Sandstones, Lunglei town (after Mongelli *et al.,* 2006)

The ratios of Y/Ni vs Cr/V, which are frequently employed to depict a mixing of source rocks, were also used by Mongelli *et al.* (2006) to propose a curve binary mixing of Bhuban Sandstones, Lunglei town (after Mongelli *et al.,* 2006). mixing model between granite and ultramafic end-members. A small amount of input from ultramafic sources can also be taken into account. The lower to moderate ratio of Cr/V (avg. UBF: 1.66, MBF: 1.16) suggests that the sediments are likely derived from source rocks that were formed in granitic terrain. The Middle Bhuban sandstones are projected more towards the granitic field because they reflect a lower Cr/V ratio than the Upper Bhuban sandstones {Figure **7**.1 (J)}.

To illustrate the trends of the composition and the impact of the sedimentation process on the source rock, McLennan *et al.* (1993) proposed the bivariate plot utilizing the ratios of the trace elements Zr/Sc vs Th/Sc. The original composition of the source rock is indicated by a linear trend in the bivariate plot of McLennan *et al.* (1993), while the diverging trend in the graph suggests sedimentary recycling due to sedimentation processes. When the Bhuban sandstone samples are plotted in the bivariate diagram {Figure 7.1 (K)}, the majority of the samples fall

along the linear trend while few samples are plotted in the diverging trend. Therefore, it can be inferred that most of the Bhuban sandstones retained their original composition while some samples are sourced from recycled sediments. During the transit of sediments, some alkali elements become leached due to their mobility resulting in the enrichment of immobile elements such as Zr which causes the changing of the source composition. The association of detrital zircon and/or association of heavy minerals during sedimentation processes is the cause of the higher value of Zr in sandstone.

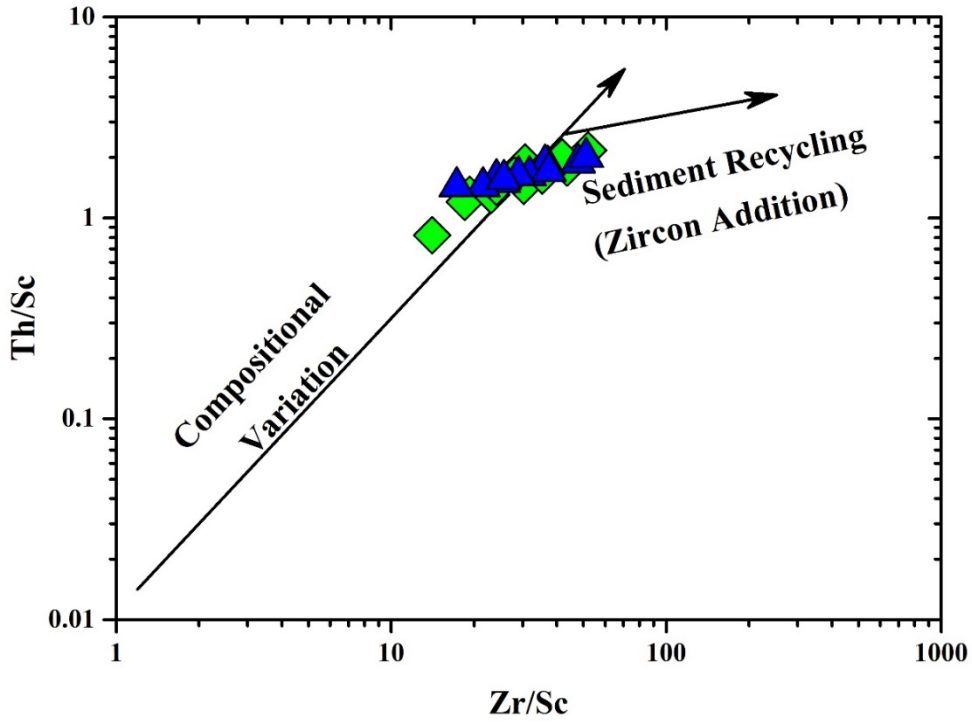

Figure 7.1 (K): Zr/Sc vs Th/Sc plot for Bhuban sandstone of Lunglei (after McLennan *et al.*, 1993).

The characteristics of certain trace elements and rare earth elements are not much affected by the sedimentary processes. Hence, the ratios of some trace elements vs REE can be useful tools for the analysis of the provenance of clastic sedimentary rocks. Cullers (1994, 2000) and Cullers and Podkovyrov (2002) suggested standard values for specific elemental ratios of trace and rare earth elements versus various sources, which are shown in Table 7.1. The ranges for some elemental ratios in the Bhuban sandstones (La/Sc = UBF: 1.08 - 6.33, MBF: 3.37 –

5.83; La/Co = UBF: 0.19 - 1.29, MBF: 0.27 – 0.83; Th/Sc = UBF: 1.20 - 2.17, MBF: 1.43 – 2.00 and Cr/Th = UBF: 5.46 – 16.60, MBF: 4.80 – 10.21), demonstrates the contribution of sediments primarily from felsic source rocks. In addition, a low to moderate concentration of some incompatible elements including Ni, Cr, V, and Sc, indicate the felsic source for the Bhuban sandstones of Lunglei.

Table 7.1: Trace element vs REE ratios for Bhuban sandstones of Lunglei. Where the felsic and mafic sources are from Cullers (1994, 2000) and Cullers & Podkovyrov (2000).

Element ratios	Range of ratios		Felsic Sources	Mafic Sources
	UBF	MBF		
Eu/Eu*	0.58-0.65	0.57-0.66	0.32-0.83	0.70-1.02
La/Lu	11.31-14.27	11.28-17.22	3.00-27.0	1.10-7.00
La/Sc	1.08-6.33	3.37-5.83	0.70-27.7	0.40-1.1
La/Co	0.19-1.29	0.27-0.83	1.4-22.4	0.14-0.38
Th/Sc	1.20-2.17	1.43-2.00	0.64-18.1	0.05-0.4
Th/Co	0.17-0.39	0.11-0.30	0.30-7.5	0.04-1.40
Cr/Th	5.46-16.60	4.80-10.21	4.00-15.0	25-500
Th/Cr	0.06-0.20	0.10-0.21	0.06-4.0	0.002-0.045

The nature and kinds of source rock can be inferred from chondrite-normalized REE patterns and Eu anomaly, which provide more information (Basu *et al.*, 1975; Armstrong-Altrin, 2009). Felsic rocks exhibit higher LREE/HREE ratios with negative Eu anomalies, whereas mafic rocks display lower LREE/HREE ratios (Cullers, 1994, 2000). According to a plot of Chondrite-normalized REE {Figure 6.2(F)}, the concentration of LREE is significantly greater than that of HREE. Therefore, the greater ratio of LREE/HREE reveals that Bhuban sandstones originated from granitoids. The ratio of $(La/Lu)_N$: 11.31–14.27 (UBF) and 11.28-17.22 (MBF) shows that the source rock has been fractionated, leading to a greater K content. The enrichment of potassium supports the delineation of a post-Archean source by negative Eu anomaly. The negative Eu anomaly in the studied sandstone is

also supported by the low concentration of Sr (average. UBF: 92.62 ppm, MBF: 86.08 ppm) which may be due to calcium-rich plagioclase fractionation in the source rock.

7.2 CLASSIFICATION OF SANDSTONE

7.2.1 Petrographic Sandstone Classification: The most commonly used scheme for the classification of sandstone using petrography is quantitative modal analysis (Pettijohn, 1972; Folk, 1980). The ternary plot of Pettijohn (1975) and the Q-F-R plot after Folk (1980) are used for the classification of the present studied Bhuban sandstone. In the present study, quartz is the most common mineral (UBF: 57.65 – 77%, MBF: 59.67 – 71.82%) followed by rock fragments (UBF: 1.50 – 12.60%, MBF: 3.30 – 13.50%) and feldspars (UBF: 0.00 – 8.10%, MBF: 0.00 – 4.80%). Modal count petrographic data and framework grains recalculated percentile values are displayed in Table 5.1. When plotting these data in the Q-F-L ternary diagram after Pettijohn (1972) and the ternary plot of Q-F-R after Folk (1980), most of the representative Bhuban sandstone are assembled in the field of sublitharenite while few are assembled in the area of subarkose as shown in Figure 7.2 (A). According to the Folk (1980) classification of sandstone, most of the representative Bhuban sandstones are sublitharenite with few subarkose as shown in Figure 7.2 (B).

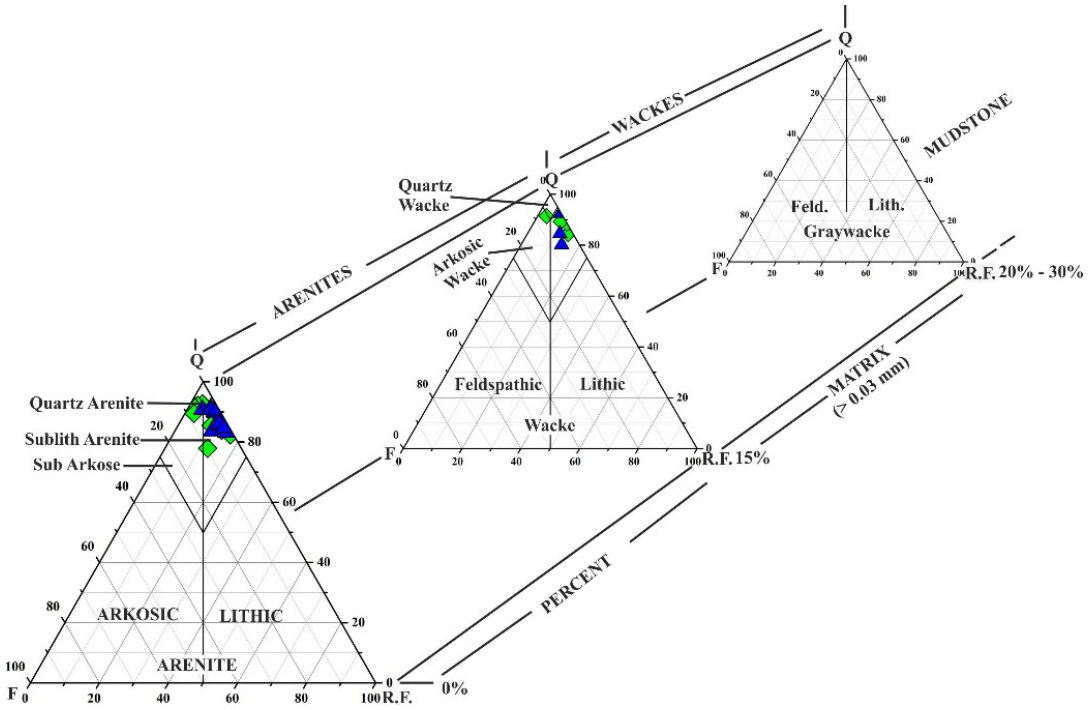

Figure 7.2 (A): Petrographic Classification of Bhuban Sandstones, Lunglei town (after Pettijohn, 1972).

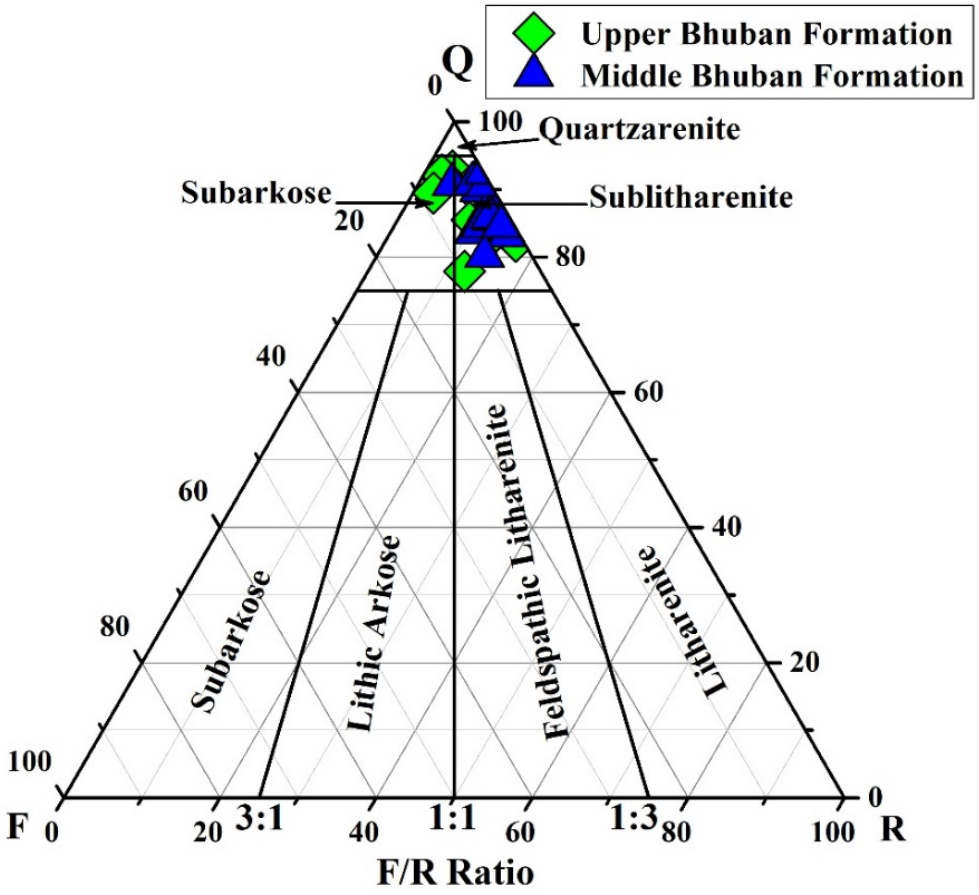

Figure 7.2 (B): Petrographic classification of Bhuban Sandstones, Lunglei town (after Folk, 1980).

7.2.2 Geochemical Sandstone Classification: Geochemistry is frequently useful for categorizing the various types of sandstones based on major oxides. Numerous researchers have proposed a geochemical classification of terrigenous sedimentary rocks using this significant elemental data, including Blatt *et al.* (1980), Pettijohn *et al.* (1972), and Herron (1988). By comparing the logarithmic values of the ratios of SiO_2/Al_2O_3 and Na_2O/K_2O, Pettijohn *et al.* (1972) proposed a method for classifying sandstone, where the majority of samples fell into the litharenite category and a small number of samples fall into the arkose category {Figure 7.2 (C)}. Herron (1988) modified the Pettijohn *et al.* (1972) diagram by using the log ratio of SiO_2/Al_2O_3 in the x-axis vs. the log ratio of Fe_2O_3/K_2O in the y-axis instead of the log ratio of Na_2O/K_2O to divide sandstones into two categories: Fe rich (Fe-shale) and other in

addition to Fe-sandstone and Fe-poor (shale, wacke, litharenite, sublitharenite, arkose, and sub- arkose) sandstone.

The majority of the Bhuban Formation samples are assembled in the Wacke field, while only a small number of samples fall in the litharenite fields of Herron (1988) {Figure 7.2 (D)}. Based on major element geochemistry, it can be inferred that the examined samples of the Upper and Middle Bhuban Formation are composed of litharenite and greywacke.

Blatt *et al.* (1980) classified the sandstone into Greywacke, Arkose, and Lithic sandstone using the values of Na_2O, (Fe_2O_3+MgO), and K_2O using a ternary plot. Based on this plot, all the samples of Bhuban sandstones are classed under lithic sandstones {Figure 7.2 (E)}.

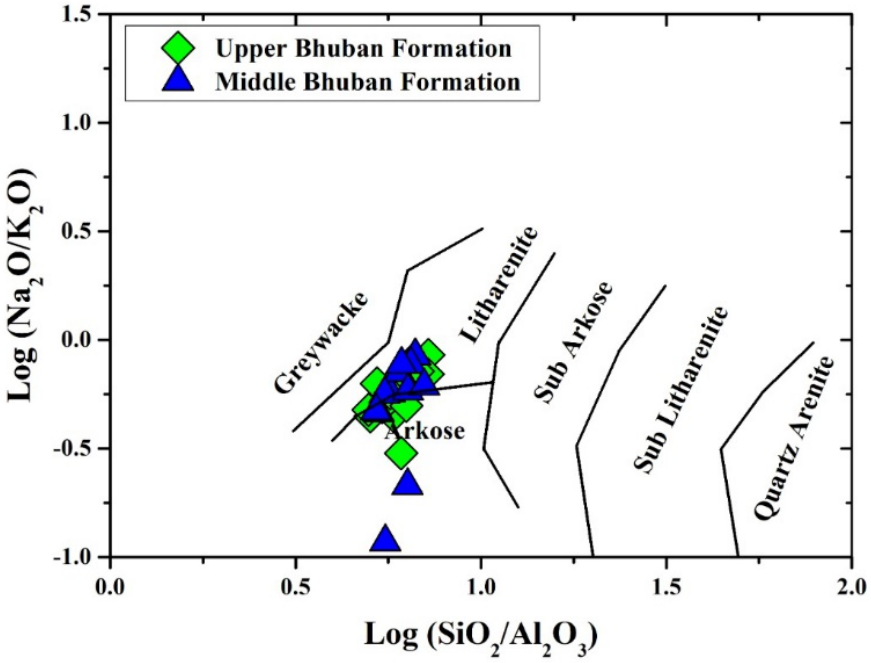

Figure 7.2 (C): Log(SiO_2/Al_2O_3) vs Log(Na_2O/K_2O) bivariate plot for Bhuban Sandstones, Lunglei town (after Pettijohn *et al.*, 1972).

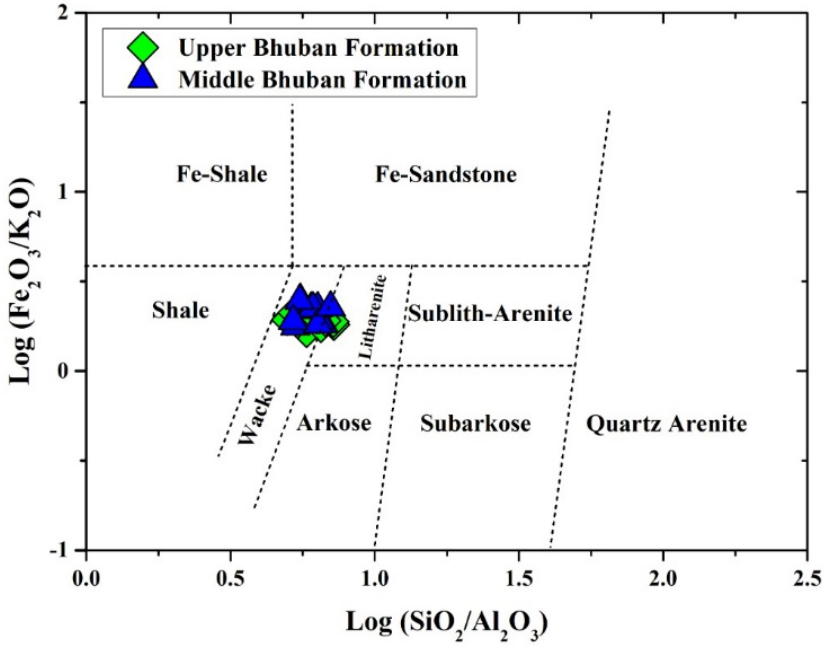

Figure 7.2 (D): $Log(SiO_2/Al_2O_3)$ vs $Log(Fe_2O_3/K_2O)$ classification scheme of Bhuban Sandstones, Lunglei town (after Herron, 1988).

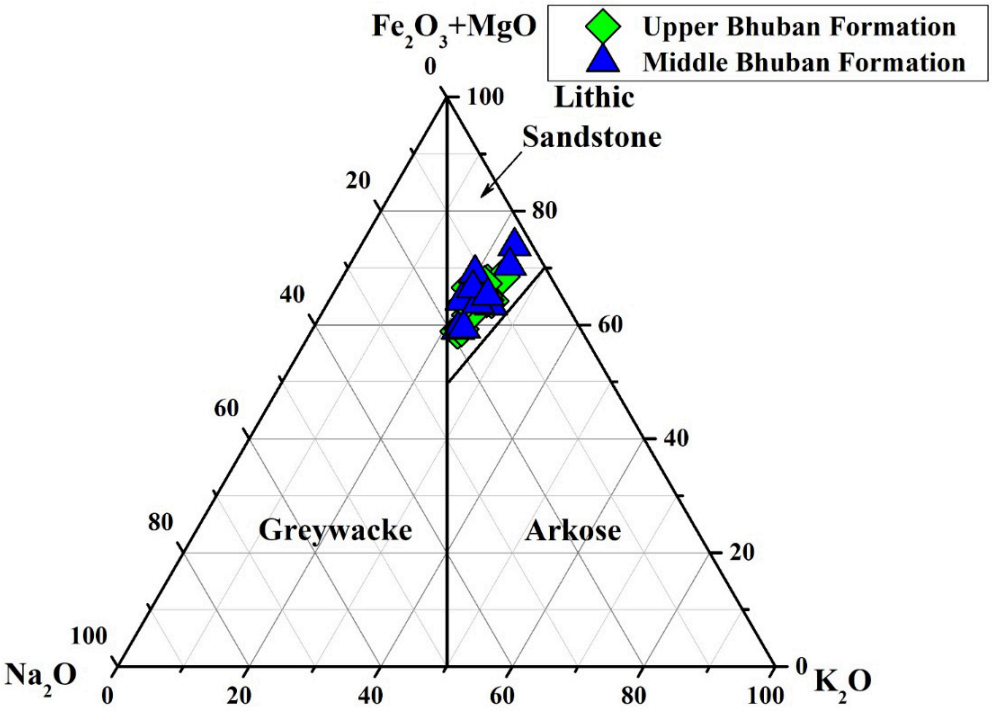

Figure 7.2 (E): Na_2O-(Fe_2O_3+MgO)-K_2O ternary plot for classification of Bhuban sandstones, Lunglei town (after Blatt *et al.*, 1980).

7.3 PALEOCLIMATIC CONDITIONS

Important clues to predict the type of climatic conditions that prevailed during the time of deposition of sediments can be obtained by the nature of framework grains and their abundance. The excessive abundance of quartz and relatively less amount of feldspar and rock fragments suggested that the sediments were derived from metamorphic sources under humid climatic conditions (Suttner *et al.,* 1981). When plotting the examined sandstone samples in a QFR ternary diagram of Suttner *et al.* (1981), all the samples are assembled in a metamorphic humid area, suggesting that the Bhuban sediments are derived from metamorphic terrain {Figure 7.3 (A)} and are deposited under the humid to semi-humid climatic conditions.

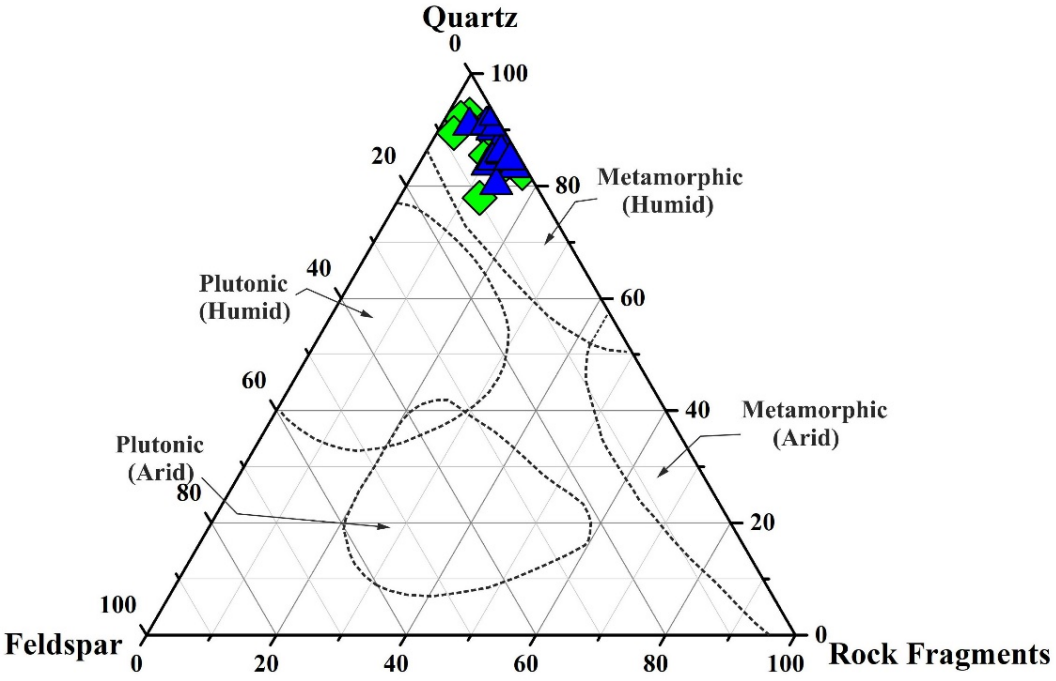

Figure 7.3 (A): Triangular QFR plot for climatic conditions of Bhuban sandstones, Lunglei town (after Suttner *et al.,* 1981) representing humid climatic conditions.

Besides the ternary plot, a bivariate plot of the semi-quantitative weathering index of ln(Q/R) vs ln(Q/F) (Weltje, 1994) and (Grantham and Velbel, 1988): WI = C x R (Where WI – Weathering index, C – Climate and R – Relief) also indicates similar nature of paleoclimatic conditions {Figure 7.3 (B)}. The semi-quantitative weathering index suggests that the sediments of Bhuban sandstones are derived from a metamorphic terrain, and the bulk of the samples fall within the area of weathering indices of 2 representing low relief areas (plains) with humid to semi-humid climates.

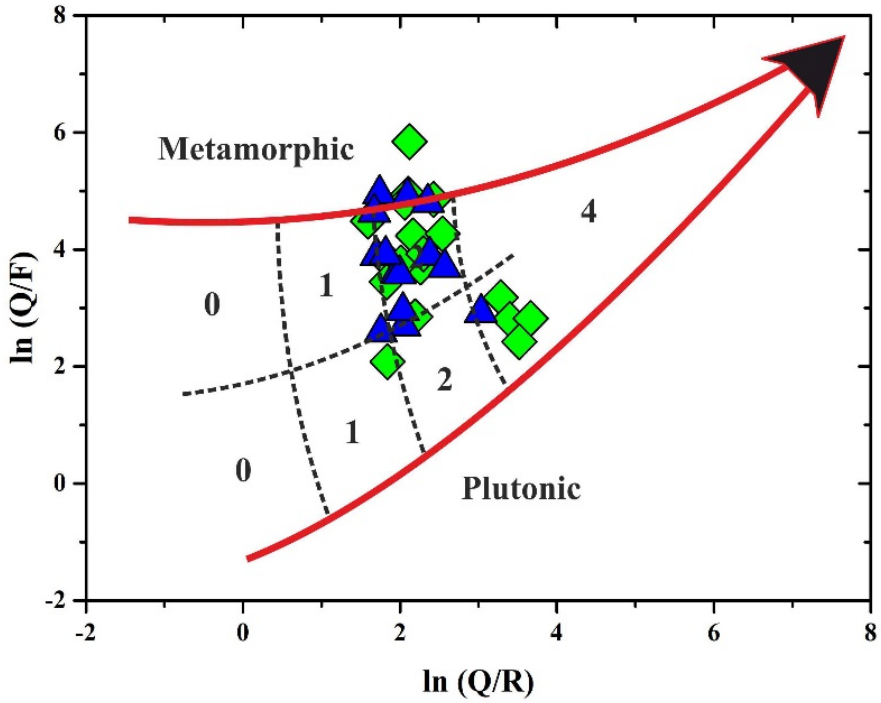

SEMI-QUANTITATIVE WEATHERING INDEX (Grantham and Velbel, 1988)			PHYSIOGRAPHY (Relief)		
			High (Mountain)	Moderate (Hills)	Low (Plains)
			0	1	2
CLIMATE (Precipitation)	(Semi-) Arid & Mediterranean	0	0	0	0
	Temperate Subhumid	1	0	1	2
	Tropical Humid	2	0	2	4

Figure 7.3 (B): ln(Q/R) vs ln(Q/F) plot (after Weltje, 1994) and the intensity of weathering for Bhuban sandstones, Lunglei town (after Grantham and Velbel, 1988).

Sedimentary rocks can preserve information about the extent of chemical weathering, making them an effective tool for assessing the state of source area weathering (Nesbitt and Young, 1982). The extent of weathering in the source area greatly affects the distribution of elements in the terrigenous rocks. When assessing the paleoclimatic conditions present at the time of sediment deposition, weathering indicators are particularly beneficial. In terms of the various geochemical weathering indices that have been proposed, the Weathering Index of Parker (WIP; Parker, 1970), Chemical Index of Alteration (CIA; Nesbitt and Young, 1982), Plagioclase Index of Alteration (PIA; Fedo *et al.,* 1995), Chemical Index of Weathering (CIW; Harnois, 1988), and Index of Chemical Variability (ICV; Cox *et al.,* 1995) are the most popular chemical indices that use major element concentrations. Following are the mathematical derivations of these parameters: (Where CaO* denotes the calcium integrated from the minerals that contain silicates; # denotes by using molecular proportions; and ^ denotes by using weight percentages).

$$WIP^{\#} = [\{2\frac{Na2O}{0.35}\} + \{\frac{MgO}{0.9}\} + \{2\frac{K2O}{0.25}\} + \{\frac{CaO*}{0.7}\}] \text{ x } 100$$

$$CIA^{\#} = [\frac{Al2O3}{Al2O + CaO* + Na2O + K2O}] \text{ x } 100$$

$$PIA^{\#} = [\frac{Al2O3 - K2O}{Al2O3 + CaO* + Na2O - K2O}] \text{ x } 100$$

$$CIW^{\#} = [\frac{Al2O3}{Al2O3 + CaO* + Na2O}] \text{ x } 100$$

$$ICV^{\wedge} = [\frac{Fe2O3 + K2O + Na2O + CaO* + MgO + MnO + TiO2}{Al2O3}] \text{ x } 100$$

Table 7.2: Weathering indices for Bhuban sandstones, Lunglei town.

Litho unit	Sample Number	Chemical Index of Alteration (CIA)	Plagioclase Index of Alteration (PIA)	Chemical Index of Weathering (CIW)	Weathering Index of Parker (WIP)	Index of Chemical Variability (ICV)
Upper Bhuban Formation	LS-6	58.91	61.89	67.35	45.77	1.11
	LS-7	76.56	88.27	90.39	29.45	0.82
	LS-9	55.29	57.09	63.36	45.36	1.15
	LS-10	69.80	78.08	81.87	39.74	0.91
	LS-18	59.98	63.53	69.03	41.18	1.06
	LS-19	62.03	66.31	71.39	42.13	1.00
	LS-26	65.46	71.40	76.01	45.17	1.02
	LS-27	18.46	16.29	19.08	74.76	3.13
	LS-28	68.98	76.02	79.77	41.51	0.93
	LS-29	67.49	74.04	78.14	39.66	0.97
	LS-30	61.30	65.57	71.04	39.17	1.07
	LS-33	68.68	76.73	80.85	36.89	0.95
	LS-34	68.68	76.73	80.85	36.89	0.95
	Average	61.66	67.07	71.47	42.90	1.16
Middle Bhuban Formation	LS-12	84.77	96.39	96.91	20.47	0.63
	LS-13	64.64	70.11	74.82	41.39	0.97
	LS-14	66.39	72.44	76.73	38.43	0.91
	LS-16	79.42	92.01	93.42	24.86	0.76
	LS-20	70.15	79.51	83.37	41.73	0.91
	LS-21	71.54	79.65	82.88	36.28	0.90
	LS-22	66.92	72.27	76.06	37.53	0.95
	LS-23	66.60	71.79	75.61	37.78	0.94
	LS-24	60.18	63.34	68.28	41.97	1.13
	LS-31	64.46	70.07	74.93	40.30	1.01
	LS-35	54.53	55.81	61.28	38.23	1.20
	LS-37	54.53	55.81	61.28	38.23	1.20
	Average	67.01	73.27	77.13	36.43	0.96
Standards	UCC	50.17	50.22	55.81	69.91	1.19
	GLOSS	41.16	39.57	44.56	61.72	1.6
	PAAS	69.38	77.45	81.33	51.86	0.89
	NASC	57.13	60.07	66.89	61.41	1.11

In Table 7.2, calculated values for various weathering indices from the current investigation are provided. In comparison to PAAS (69.38) and NASC (57.13), the average Chemical Index of Alteration values for the upper and middle Bhuban sandstones are moderate (UBF: 61.66, MBF: 67.01). The moderate value of the CIA typically denotes that the sediments are transported for a moderate distance

with little to no mechanical breakdown and just minor chemical modification. Additionally, modest CIA values and a negative Eu anomaly suggest that sediments from nearby sources may have contributed, though their mechanical weathering rates are higher and their amounts of alkali-bearing minerals are lower.

It was determined that for the Bengal basin, the sediments were obtained from Himalayan ranges and transported by paleo-Brahmaputra and its tributaries based on some outstanding contributions by Najman and Garzanti (2000), Bracciali *et al.* (2015) and Govind *et al.* (2018). We can also assume that the sediments in the current research region came from the Himalayan mountains, with some nearby sources that are most likely to have contributed, such as the Indo-Burmese Arc and the Naga Hills. Figure 7.3 (C) is the A-CN-K [Al_2O_3– (CaO + Na_2O) – K_2O] ternary plot of Nesbitt and Young (1982) for the Bhuban sandstone of the study area. In the ternary plot, the samples are trending almost parallel to the A-CN line and are closer to the feldspar join suggesting that the samples have undergone mild to moderate weathering. A few samples show intense weathering as they are plotted closer to the A-K line. Fedo *et al.* (1995) suggested that the near the feldspar join indicates the start of chemical weathering. Also, this indicates the weathering effect has not yet reached the removal stage of alkali and alkaline earth elements from clay minerals (Taylor and Mc Lennan, 1985) suggesting the breakdown of plagioclase. CaO and Na_2O leach at extreme weathering conditions, reversing the trend towards the A-K line and showing K enrichment. Under severe weathering, K will be completely removed, and the trend will change to Al_2O_3 at its peak. The concentration of K, which entails the elimination of K is also reflected in the metasomatism of K. Potassium may also be added concurrently via K-rich pore fluids. The trend will be driven towards the K apex by K-addition. Due to the enrichment of K caused by the metasomatism process, the conversion of plagioclase into K-feldspar or clay minerals may occasionally take place (Fedo *et al.,* 1995).

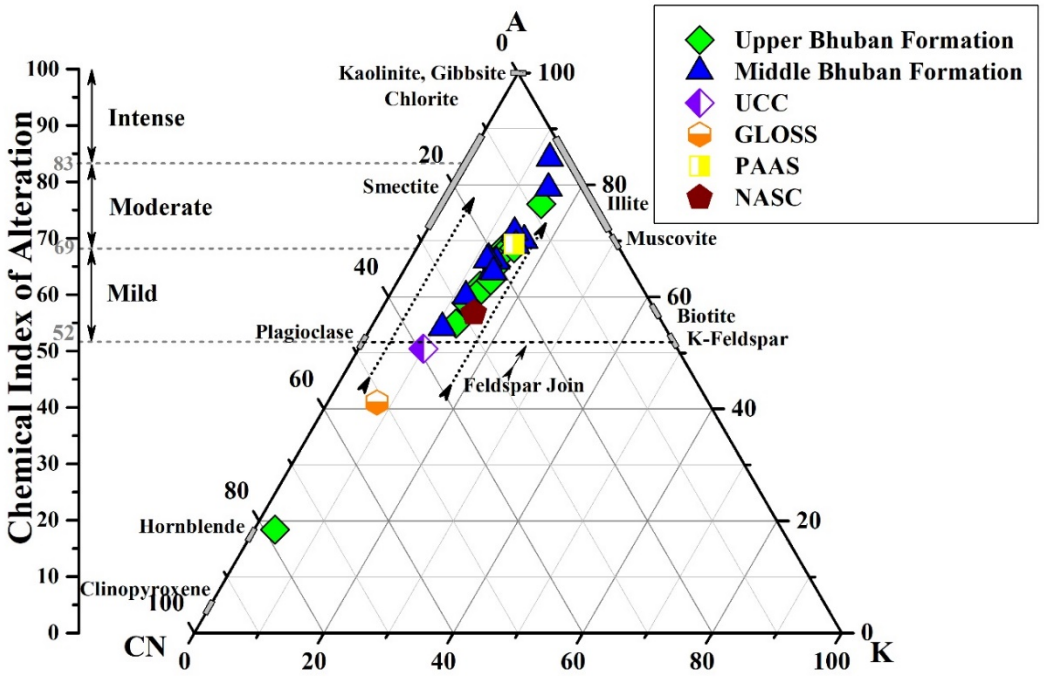

Figure 7.3 (C): A ternary A-CN-K plot of Bhuban Sandstones, Lunglei town indicating mild to moderate weathering of source rocks (after Nesbitt and Young, 1983).

Although K is remobilized during the sedimentation and metamorphic processes, CIA is still regarded as one of the essential indices for determining the degree of weathering. Chemical Index of Weathering (CIW; Harnois, 1988) is also commonly employed to analyze the degree of weathering. To avoid K-metasomatism, Harnois (1988) employs wt% of alkalis other than K_2O. K might be leached or it can accumulate in the weathering products during the sedimentation processes. The pore solution in which K-bearing minerals can develop is connected with the K^+ ion. It can tolerate clay minerals instead of Na^+ and Ca^+ due to its increased exchange capacity (Kroonenberg, 1992; Harnois, 1988). The CIW values of Bhuban Sandstones of Lunglei are well above the UCC (avg: 55.81) and slightly lower than PASS (avg: 81.33). Thus, it can be assumed that the sandstones of the study area are mild to moderately weathered.

Fedo *et al.* (1995) proposed the Plagioclase Index of Weathering (PIA), which uses the weight percentage of alkalis to determine the degree of source rock weathering. The highest PIA value, which is 100, denotes completely weathered materials such as kaolinite, gibbsite, etc., whereas the value for un-weathered plagioclase is 50. The Bhuban Sandstones have a moderate to high average PIA value (UBF: 67.07, MBF: 73.27) that is comparable to PAAS (77.45). This suggests that the source location provided nearly fresh feldspar debris {Figure 7.3 (D)}.

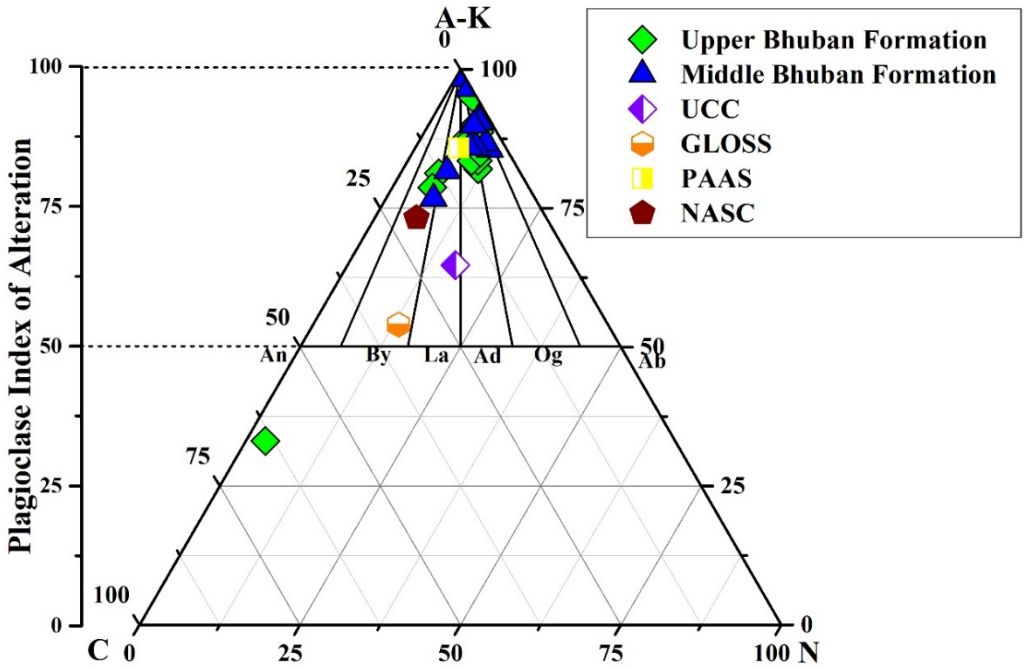

Figure 7.3 (D): AK-C-N ternary plot for the Bhuban Sandstones, Lunglei town (after Fedo *et al.,* 1995).

Parker (1970) created the first chemical weathering index employing alkali and alkaline elements, sometimes known as the Parker Index or Weathering Index of Parker (WIP). The amount of mobile alkali and alkaline earth elements in the rock determines the value of WIP. Since Ca, Mg, Na, and K are extremely mobile, they are removed in the process of hydrolysis. Although the silica contents in the rock are sometimes mobile, the amount that is leached or removed is much less in comparison to mobile alkali and alkaline earth elements. Parker (1970) therefore suggested the mobile elements Na, Mg, K, and Ca as the base for the weathering index. Indicating

less worn source rocks, the Bhuban sandstones exhibit a lower WIP value (UBF: 42.90, MBF: 36.43).

Indicator of Chemical Variability (ICV; Cox *et al.*, 1995) is a significant geochemical characteristic that is frequently used to distinguish between clay and non-clay minerals based on the fraction of Al_2O_3. With the other major cations, it quantifies the abundance of alumina. Hence, as the non-clay silicates have a lesser value of Al_2O_3, we can expect a higher value of ICV. According to Cox *et al.* (1995), feldspars, illite, and muscovite have an ICV range of 0.6 – 1.0 while clay minerals have a K_2O/Al_2O_3 range of 0 - 0.3 and feldspars have a range of 0.3 – 1.0. The average values for ICV = UBF: 1.16, MBF: 0.96, and K_2O/Al_2O_3 = UBF: 0.19, MBF: 0.18 are found in the Bhuban sandstones. Based on these observations, it may be suggested that feldspars and their equivalent weathered products make up a smaller portion of the Bhuban sandstones. Figure 7.3 (E) depicts the maturity and weathering nature of clastic sediments, which is another significant plot CIA vs. ICV that Long *et al.* (2012) provided. ICV values ~ 1 and the average CIA (UBF: 61.66, MBF: 67.01) are present for the majority of the samples in the plot. Thus, based on the different weathering parameters, the sediments for Bhuban sandstones of the study area are chemically immature to mature and mild to moderately weathered.

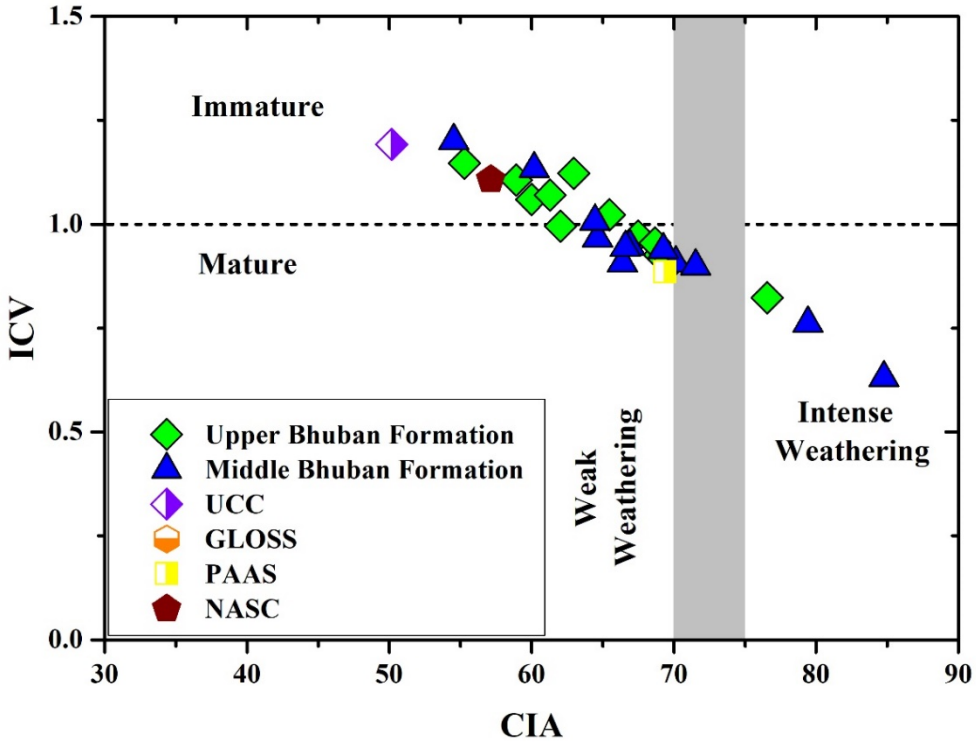

Figure 7.3 (E): Binary plot of CIA vs ICV for the Bhuban Sandstones, Lunglei town representing maturity and weathering nature (after Long *et al.*, 2012).

Additionally, the binary plot of Th vs. Th/U following McLennan *et al.* (1993), shown in Figure 7.3 (F) can be used to comment on the severity of the weathering behavior of the sediments. According to McLennan *et al.* (1993), the Th/U ratio in upper crustal rock ranges from 3.5 to 4.0; beyond this range indicates a weathering trend. The Bhuban sandstone samples display an average value of Th/U = UBF: 3.20, MBF: 6.06, which is similar to the upper crust's signature and indicates that weathering has taken place.

The ratio of Rb/Sr rises as a result of Sr leaching relatively more than Rb during various sedimentary processes like weathering and diagenesis. Consequently, a higher ratio denotes extensive weathering. The majority of the examined samples have moderate average Rb/Sr values (UBF: 1.02, MBF: 1.11), with similar weathering patterns for PAAS and NASC (Rb/Sr: 0.80 and 0.88, respectively). The ratios of (Th/U) and (Rb/Sr) show that the source rock has undergone only mild to moderate weathering.

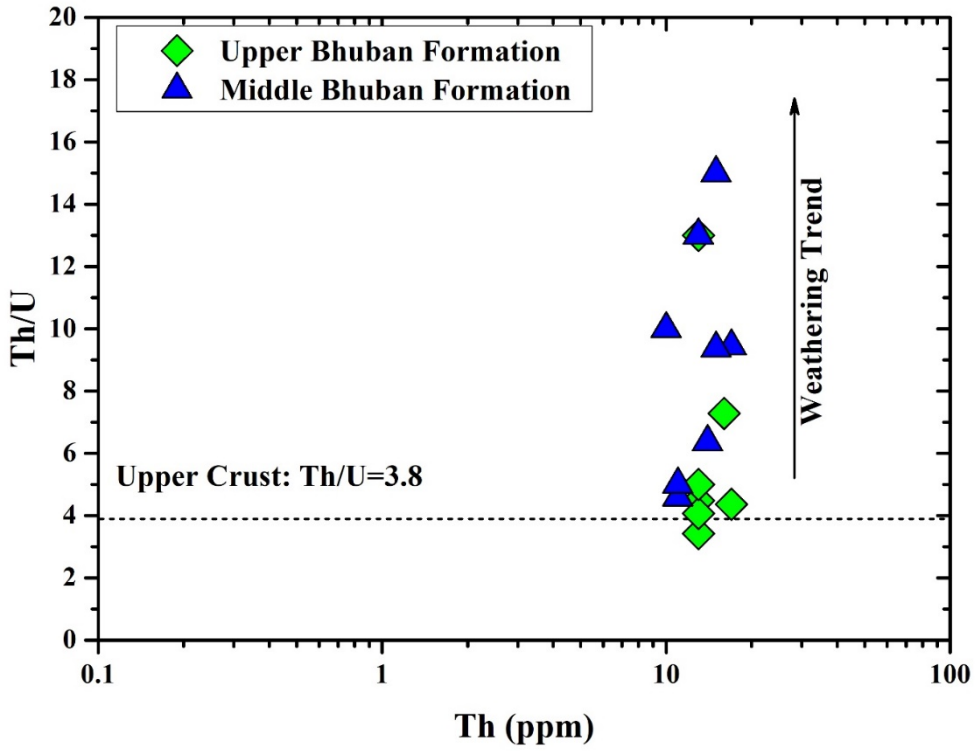

Figure 7.3 (F): Th vs Th/U binary plot of Bhuban Sandstones, Lunglei town representing the weathering trend (after McLennan *et al.,* 1993).

The geochemical data obtained from the Bhuban sandstones of Lunglei as well as the weathering indices shows the decrease of some major minerals CaO, Na_2O, MgO, and K_2O. This observation is supported by a sparse occurrence of feldspars in thin-section studies. The removal of alkali-bearing minerals has an impact on the weathering indices, reflecting the mild nature of source rock weathering. Certain elemental ratios, such as Th/U and Rb/Sr, can likewise be interpreted similarly. Because of this, it can be assumed that the source sediments underwent mild to moderate weathering before the occurrence of the deposition.

Again, when plotting the values of (Q_{Total}/ F+RF) vs (Q_P/F+RF) in a bivariate diagram based on Suttner and Dutta (1986), the majority of the samples are assembled within the area of humid to semi-humid regions {Figure 7.3 (G)}. Therefore, based on the two climatic condition diagrams, it can be observed that the Bhuban sandstones have a metamorphic origin and were deposited in a semi-humid to humid climate.

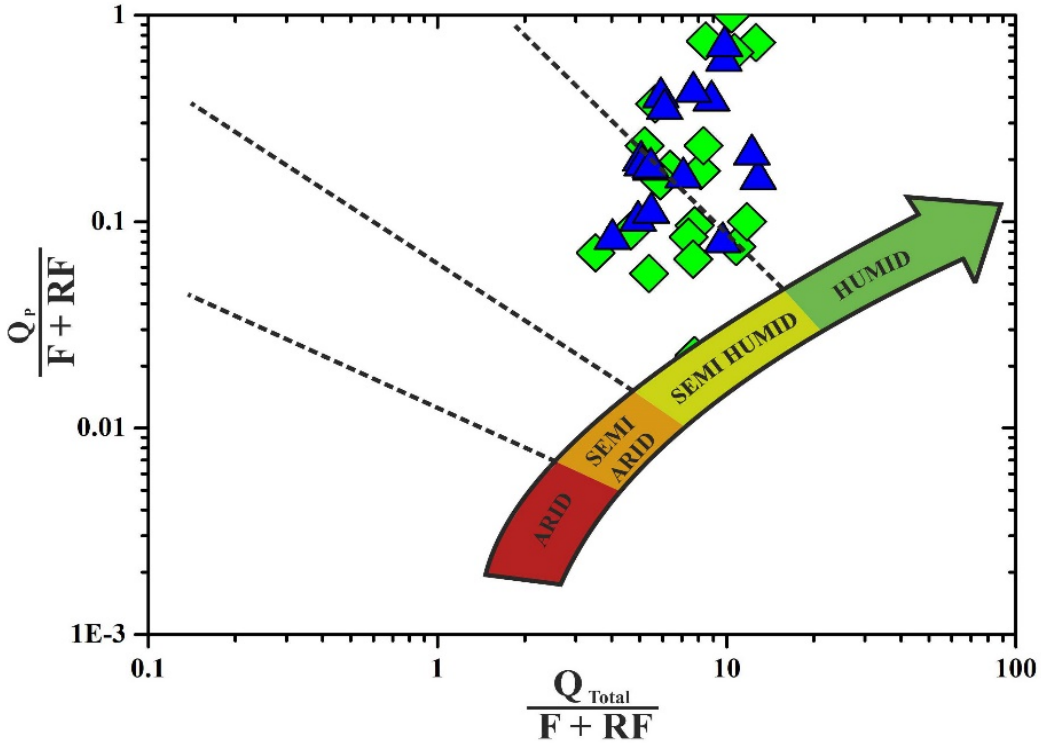

Figure 7.3 (G): Bivariate plot of modal data for climatic conditions of Bhuban sandstones, Lunglei town (after Suttner and Dutta, 1986) representing humid to semi-humid climatic conditions.

7.4 TECTONIC SETTINGS

The characteristics of the source area of sediments and their tectonic setting can be determined by using the relative abundance of primary framework grains. To represent the tectonic settings of source areas, Dickinson & Suczeck (1979) and Dickinson *et al.* (1983) formulated QFL and QmFLt compositional diagrams. When the studied samples are plotted in the QFL ternary diagram, the majority of the

samples fall within the area of the recycled orogen while a craton interior setting is indicated by only a few samples {Figure 7.4 (A)}. However, a QmFLt ternary plot suggested a quartzose recycle and craton interior {Figure 7.4 (B)}.

The metamorphic source is suggested by the presence of monocrystalline quartz with undulatory extinction whereas the occurrence of polycrystalline quartz (>3 crystal units per grain) with slightly curved inter-crystal boundaries and monocrystalline quartz with non-undulatory extinction supported the plutonic source. The presence of perthite is an obvious indicator of granite or pegmatite sources and rounded grains of quartz designate recycled origin. Texturally immature sediments are advocated by the abundance of rock fragments and angular to sub-angular detrital grains.

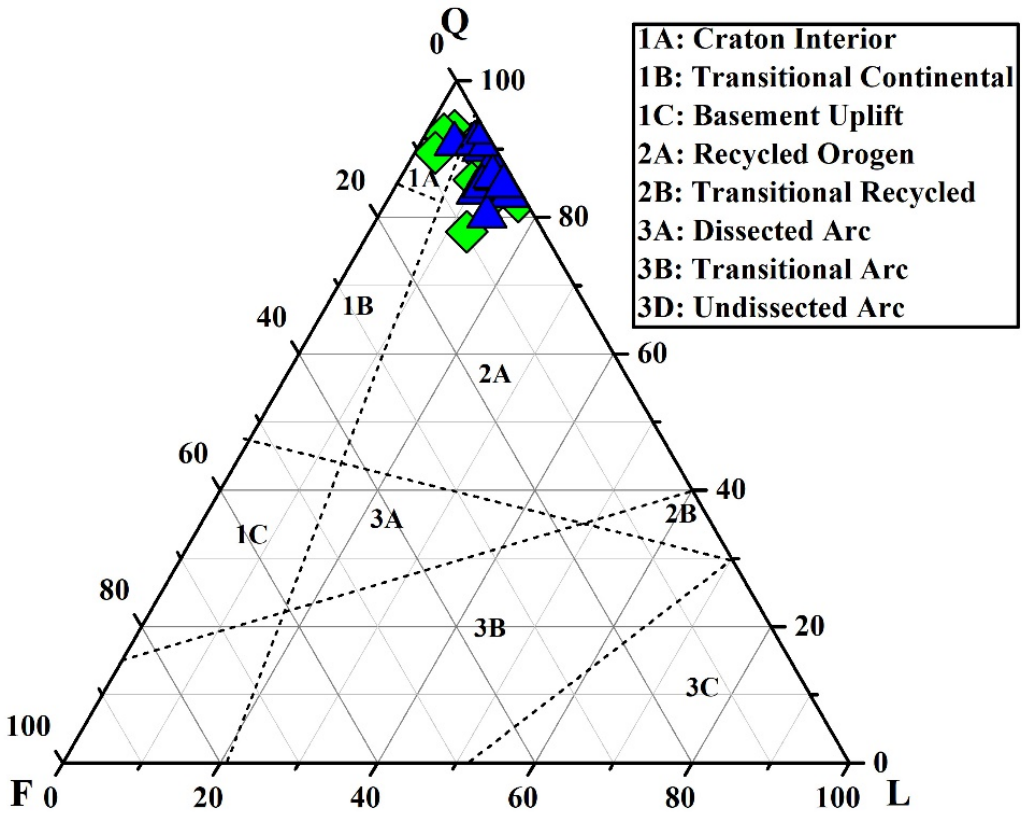

Figure 7.4 (A): Triangular QFL plot for Bhuban sandstones, Lunglei town (after Dickinson & Suczeck, 1979).

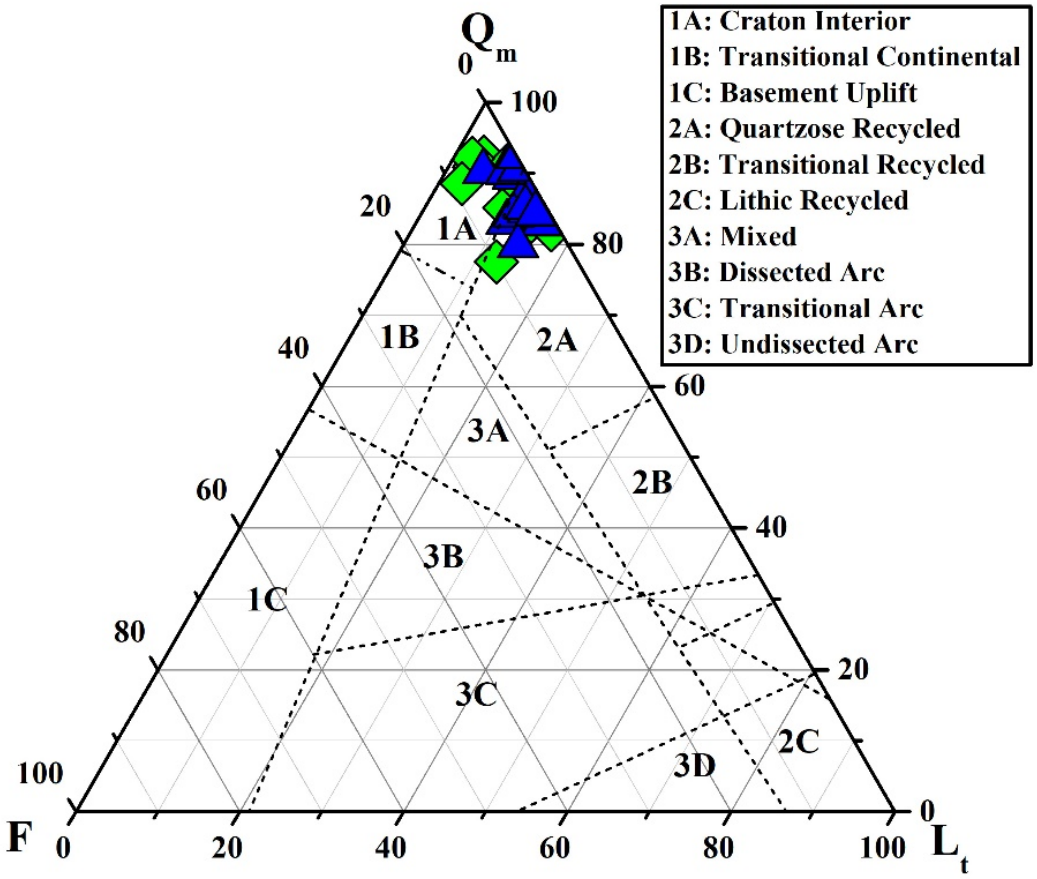

Figure 7.4 (B): Triangular QmFLt plot for Bhuban sandstones, Lunglei town (after Dickinson *et al.,* 1983).

Many researchers over the past few decades, including Bhatia (1983, 1985), Taylor and McLennan (1985), Bhatia and Crook (1986), McLennan *et al.* (1990), McLennan and Taylor (1991) and Roser and Korsch (1986) have put forth a variety of theories that are primarily based on the geochemical composition of clastic sediments to identify ancient tectonic settings. Frequently used major elemental discrimination plots used in the current investigation included viz. (Fe_2O_3+MgO) vs Al_2O_3/SiO_2 (Bhatia, 1983), (Fe_2O_3+MgO) vs K_2O/Na_2O (Bhatia, 1983), the bivariate plot of La/Sc vs Ti/Zr after Bhatia and Crook (1986), La-Th-Sc ternary plot after Bhatia and Crook (1986), and also binary plots of discriminant function after Bhatia (1983), where:

DF-1: (- 0.0447 x SiO_2) - (0.972 x TiO_2) + (0.008 x Al_2O_3) - (0.267 x Fe_2O_3) + (0.208 x FeO) – (3.082 x MnO) + (0.14 x MgO) + (0.195 x CaO) + (0.719 x Na_2O) - (0.032 x K_2O) + (7.51 x P_2O_5) + 0.303

DF-2: (- 0.421 x SiO_2) + (1.988 x TiO_2) - (0.526 x Al_2O_3) - (0.551 x Fe_2O_3) - (1.61 x FeO) +(2.72 x MnO) + (0.881 x MgO) - (0.907 x CaO) - (0.177 x Na_2O) -(1.84 x K_2O) + (7.244 x P_2O_5) + 43.57]

The tectonic setting for the Bhuban Sandstone as an active Continental Margin is successfully represented {Figure 7.4 (C)} by a bivariate plot of La/Sc vs Ti/Zr following Bhatia and Crook (1986). In addition, putting the studied samples in the binary discrimination function plot (Bhatia, 1983) reveals that the majority of the Bhuban sandstones fall in the active continental margin region {Figure 7.4 (D)}. According to Bhatia and Crook (1986), the ratio of La/Sc for sandstone deposited along the continental edge should be 4, allowing the samples to be plotted close to the La apex on the ternary plot of La-Th-Sc. The average La/Sc ratio of the investigated Bhuban sandstones is 4.23 UBF and 4.52 MBF, which is nearly identical to the La/Sc ratio proposed by Bhatia and Crook (1986) for samples of continental margins. The ternary plot of Bhatia (1980) (La-Th-Sc) indicated an active continental margin (ACM) and continental island arc (CIA) tectonic setting for the Bhuban sandstones of Lunglei {Figure 7.4 (E)}. He proposed lower values of Fe_2O_3+MgO (2-5 wt%), lower Al_2O_3/SiO_2 (0.1-0.2), and higher K_2O/Na_2O (≈1) for the sandstones deposited in an active continental edge where the sediments were primarily produced from felsic sources (granite, gneisses, etc.). The average values of Al_2O_3/SiO_2 (Avg. UBF: 0.17, MBF: 0.17), Fe_2O_3+MgO (Avg. UBF: 6.51, MBF: 6.41), and K_2O/Na_2O (Avg. UBF: 1.74, MBF: 1.79) found in Bhuban sandstones are almost identical to those proposed by Bhatia (1983). Binary discrimination diagrams of (Fe_2O_3+MgO) vs. Al_2O_3/SiO_2 (Bhatia, 1983) show that the bulk of the samples fell in the active continental margin {Figure 7.4 (F)}.

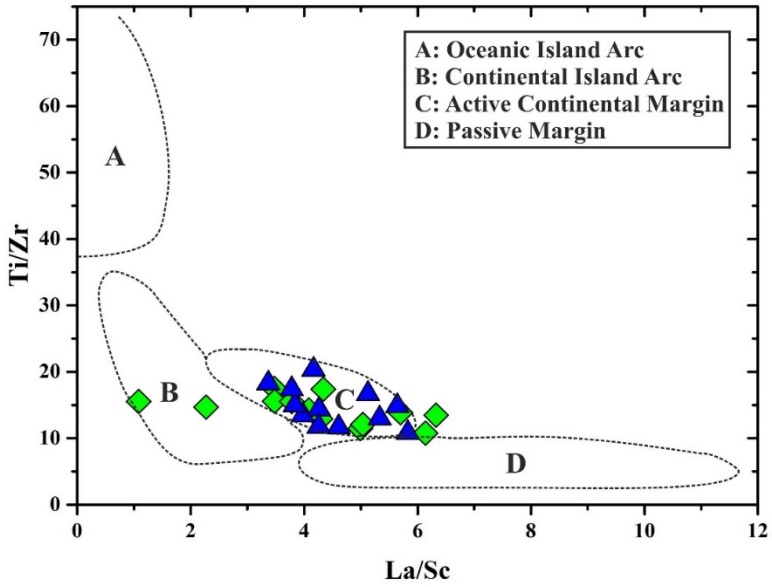

Figure 7.4 (C): A bivariate plot (La/Sc vs Ti/Zr) for the tectonic setting of Bhuban Sandstones, Lunglei town (after Bhatia and Crook, 1986).

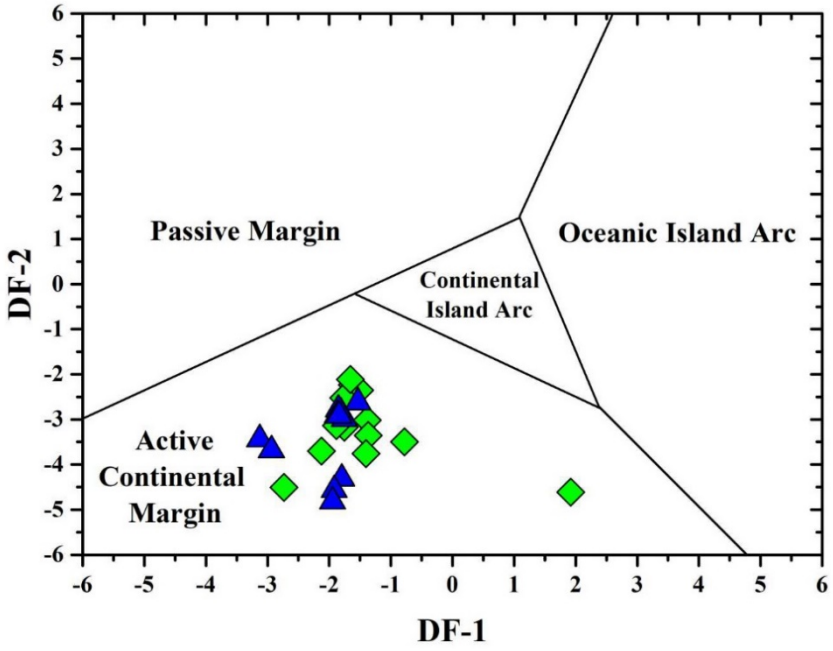

Figure 7.4 (D): Discrimination function plot of DF-1 against DF-2 for tectonic settings of Bhuban Sandstones, Lunglei town (after Bhatia, 1983).

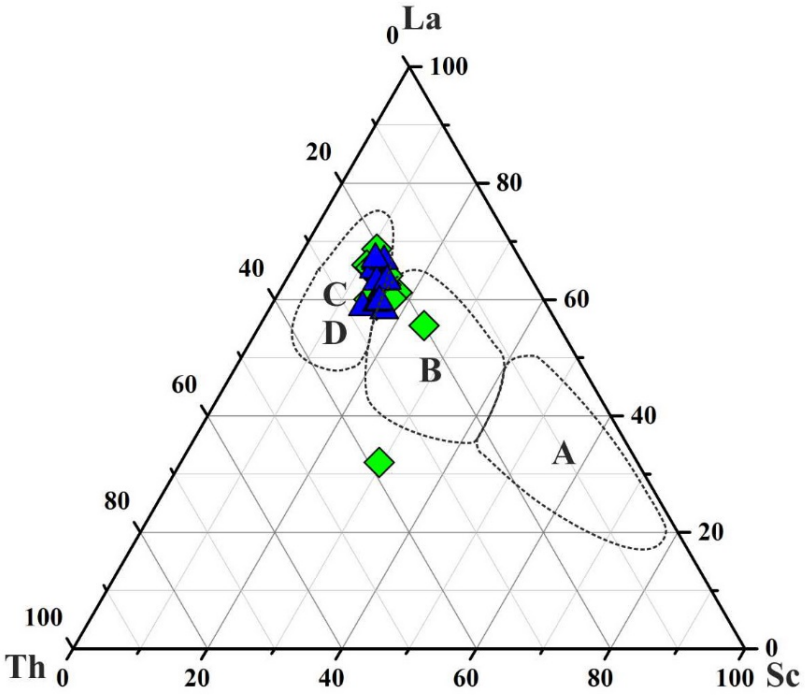

Figure 7.4 (E): Th-La-Sc ternary tectonic setting plot of Bhuban Sandstones, Lunglei town (after Bhatia, 1983).

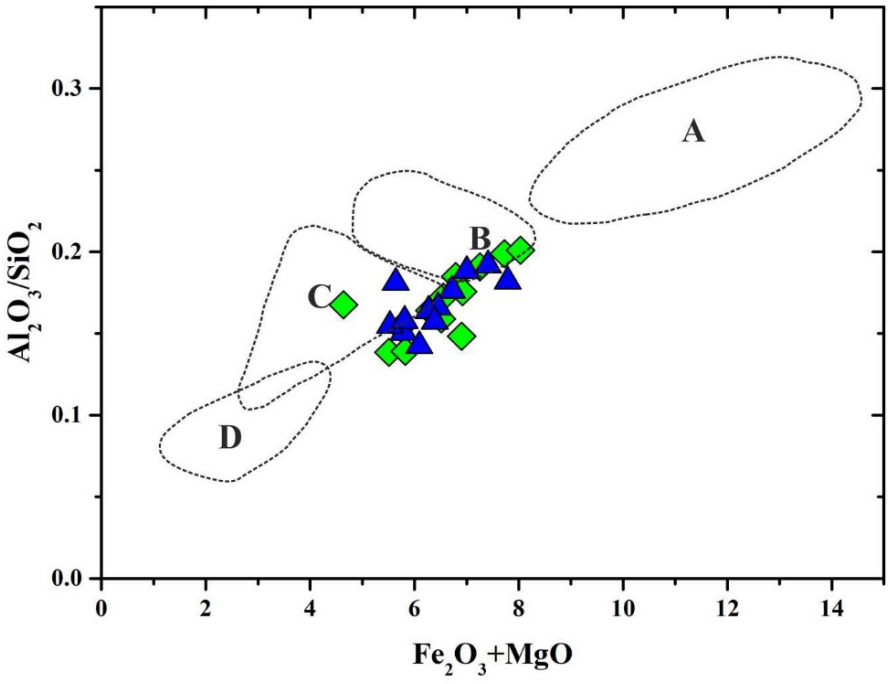

Figure 7.4 (F): Tectonic discrimination plot of (Fe_2O_3+MgO) vs Al_2O_3/SiO_2 for the Bhuban Sandstones (after Bhatia, 1983).

7.5 DIAGENESIS

The term ‘Diagenesis’ was first introduced by Von Gumbel in 1888 (Pettijohn, 1975). According to Pettijohn (1973), mineral reactions among themselves or with other minerals and the interstitial fluids are called diagenesis. Changes that were undergone by sediments after deposition, during and after lithification with regards to chemical, physical, and biological composition are called diagenesis (Dapples, 1962). Hence, the diagenetic process is drawn-out and highly complex where the newly deposited loose sediments undergo transformation and are converted into compact and indurated rocks. The effects of diagenesis include the replacement of biotite mineral by chlorite, authigenic growth and replacement of quartz grains, more silica and iron cementing materials, crenulation of grain boundary, and alteration of feldspar into clay minerals. The different factors that control the diagenesis of sandstones include sand shale ratio, pressure, temperature, influx of fluid, pore water chemistry, texture, mineralogy of the rock, and time (Blatt, 1980).

Compaction: In the current investigation, straight or long contact is frequently observed (Plate 5.1, 5.2 & 5.3). However, concavo-convex contact and suture contact are also observed at places {Plate 5.1 (D & E)}. In many thin sections, it has been observed that the mica grains and ductile clay minerals were driven into the nearby pore spaces as a result of the compaction process. In most of the samples of the present study, the micas flakes are orienting more or less in the same direction. At places, mechanical compaction is taken over by chemical compaction processes as suggested by suture contact between quartz grain which is observed locally {Plate 5.1 (E)}. Undulose quartz with concavo-convex contact is also occasionally observed, which may be attributed to external stresses rather than the optical characteristics retained from the source rock.

Cementation: Silica cement occurred as overgrowths in monocrystalline quartz in some samples of Bhuban sandstones from Lunglei {Plate 5.2 (B)}. Under a microscope, the quartz overgrowth can occasionally be difficult to recognize, and most sections lack the instantly noticeable "dust rims" that indicate the grain

boundary of the original detrital quartz crystal. Kaolinite is a common clay cement that is found intermixing with various clay minerals {Plate 5.1 (C)}. Kaolinite is likely related to the alteration of unstable feldspar because feldspar grain is frequently present in most of the section. The frequent presence of feldspar grain in the majority of the section suggests that kaolinite is connected to the alteration of unstable feldspar. Chlorite cement is also observed in some slides showing a greenish color under plane-polarized light {Plate 5.3 (D)}. It is common to identify carbonate cement as the main cementing material in the Bhuban sandstones of Lunglei and some sections show carbonate mud filling pore spaces {Plate 5.2 (C)}. There are also instances of poikilotopic calcite cement enclosing some detrital grains like quartz, feldspar, and other rock fragments.

Dissolution and Replacement: The dissolution of detrital K-feldspar and plagioclase are commonly seen in the Bhuban sandstones of Lunglei. Although the partial dissolution of microcline and plagioclase is frequently seen, complete dissolution is not common {Plate 5.1 (D)}. The subsequent precipitation of cement fills the pore space left by the dissolution. The majority of the observed alterations in the area under study are the partial replacement of the host grains, primarily plagioclase and K-feldspar grains by clay minerals.

Sengupta (1994) suggested three stages of diagenesis based on the depth of occurences namely telegenetic, eogenetic, and mesogenetic. The telegenetic stage occurs close to the surface of the earth, while the eogenetic stage takes place at a shallow depth, and the mesogenic stage occurs in a deeper environment. The examined Bhuban sandstones of Lunglei town have undergone all three stages of diagenesis in varying degrees. Mechanical compaction due to rearrangement of the framework grains forming point and long contact occurred during an early stage of diagenesis. The different features identified in the present study like bending of mica flakes, concavo-convex and sutured contacts, dissolution of feldspar grains by cementing materials, quartz overgrowth, different cementing types such as silica cement, carbonate cement, ferric oxides, and clay materials are all clear indicators of post-depositional tectonic disturbance of the sediments (Plates 5.1, 5.2 & 5.3).

According to Blatt (1980), the presence of concavo-convex contact, straight or long contact, and sutured grain contact suggested a moderate-pressure solution.

Hence, it can be inferred that the feldspar grain dissolution by cementing materials and quartz overgrowth designate an early stage of diagenesis (telegenetic). The oxidation of ferruginous sediments results in the formation of ferric oxides in hot and humid climates imparting red coloration to sediments at shallow depths. In Bhuban sandstones, the detrital quartz grains are coated by ferruginous cement and also occur as void filling which are likely developed due to weathering and leaching of ferromagnesian minerals which can be designated shallow depth of diagenesis (eogenetic). The presence of mica flakes enclosing quartz grains and fracturing quartz suggest diagenesis at a deeper level (mesogenetic).

CHAPTER 8

SUMMARY AND CONCLUSION

The Miocene succession of the Bhuban formations belonging to the Surma Group is well-exposed in Mizoram. The vast majority of the rocks of Bhuban formations are composed of sandstone, siltstone, mudstone, and their various combinations. The study area covers the whole of Lunglei town and its surrounding areas. It is covered within the Survey of India Toposheet Nos. 84B/9 and 84B/13 and falls within the coordinates of $22^{o}45'0"$ N latitudes to $23^{o}0'0"$ N and $92^{o}20'30"$ E to $92^{o}51'30"$ E longitudes.

In this present work, various methods and techniques of sedimentary analyses like petrography and geochemistry are used to decipher the mode of formation, provenance, depositional history, tectonic setting, paleoclimatic condition, and nature of weathering. The present research work aims to establish the petrochemical characteristics of the main litho-unit belonging to the Bhuban formation in and around Lunglei Town and to explore provenance characteristics, depositional environment, and tectonic settings. The current study also attempts to explore the burial history of rocks where detrital sedimentary materials resulting from the disintegration of pre-existing rocks consolidated or lithified into sedimentary rock.

The study area is constituted by a repeated succession of arenaceous and argillaceous in various proportions belonging to the Middle Bhuban and Upper Bhuban formations of the Surma group. With gradational and transitional contact the upper Bhuban formation is underlain by the middle Bhuban formation. Shale and siltstone are the important rocks in the middle Bhuban formation, whereas, the dominant rock type of the upper Bhuban formation is sandstone which is mostly encountered along the limbs of anticlines. Sandstones exposed in the study area vary from fine grey, fine to medium brown color alternated with various proportions of clay and silt size particles of shales. The southern part of the town and its adjoining areas are dominated by argillaceous rocks of the Middle Bhuban formation which is characterized by occasional sandstone beds with thick shale beds. Most of the shales are grey, olive green to yellowish brown in color and exhibit spheroidal pattern and

fissility. Frequent occurrences of silty shale beds and silty sandstone beds with thin lamination of sandstone beds are encountered throughout the middle Bhuban formation.

A total number of 37 (thirty-seven) samples of Bhuban sandstone from the study area are accounted for petrographic analysis. The framework grains are mainly quartz, feldspars, and rock fragments. Other detrital components include micas like muscovite and biotite.

Cementing materials identified are argillaceous, siliceous, calcite, and ferruginous cement. The petrographic study reveals that the framework grains are represented by moderately sorted, angular to sub-rounded, and medium to fine-grained textures. The most common type of detrital component is quartz, and non-undulose monocrystalline quartz is the most abundant type. Felspar grains in the studied sandstones are angular to sub-angular in which potash felspar dominates over plagioclase felspar. Both sedimentary and metamorphic rock fragments are identified in the studied samples where the former is identified by their sedimentary character and the latter is identified by preferred orientation and high-order interference color. Important rock fragments reported include chert, shale, slate, and schist.

Mica commonly occurs as elongated, slender, flaky minerals showing cleavages. Muscovite and biotite are the two important mica observed in the present study area. Muscovite being more resistant to chemical alteration is more common than biotite. Authigenic and detrital bended mica flakes are also commonly observed. The cementing materials frequently observed in the examined sandstones are mainly siliceous, calcareous, ferruginous, and argillaceous cement.

The concentration of major oxides in Bhuban sandstones of Lunglei roughly corresponds to the UCC except for depletion in Na_2O, CaO, and K_2O. The ratio of K_2O/Na_2O all greater than 1 (>1) is also consistent with the petrographic data. When correlating major oxides against Al_2O_3, Bhuban sandstones of Lunglei show a negative correlation with SiO_2 and a positive correlation with K_2O, Fe_2O_3, and TiO_2. X-ray diffraction analysis of shale samples shows an intense peak in Quartz,

cristobalite, and muscovite. Among the clay minerals, chlorite and illite are prominent although overshadowed by the intense peak of quartz.

The UCC normalized trace element pattern shows narrow compositional changes for Nb, Pb, Zr, Mg, La, Ce, Sc, Ni, and Cr. In comparison with UCC, the Bhuban sandstone samples are enriched in Si, and Rb, as well as depletion of Ca, Th, Na, Ba, and Fe. Among the High Field Strength elements (HFSE), the depletion of Th, Y, and Ti may be associated with the source rocks. The common occurrence of K-felspar, mica, and clay minerals may account for the high Rb level in the Bhuban sandstone.

The Chondrite normalized REE pattern of the Bhuban samples shows enrichment of LREE (La-Gd) and depletion of HREE (Tb-Lu) with negative Eu anomaly. The REE pattern of Bhuban sandstones of Lunglei is nearly identical to the UCC patterns. The extremely uniform REE pattern of the samples may suggest that the derivation of sediments has a certain homogeneity.

The provenance analysis for the Bhuban sandstones of Lunglei has been carried out using petrographic modal data and geochemistry. The different quartz varieties of Bhuban sandstones within the study area indicated their derivation from granitic rocks and middle to upper-rank metamorphic rocks. The modal analysis also suggested that the sediments are transported for a moderate distance or reworking of sediments. In addition, the sediments are immature and derived from the continental block provenance. However, the C-N-K ternary plots indicated the sediments came from granitic terrain. Based on the TiO_2 vs Ni bivariate plot and La-Th-Sc ternary plot, the Bhuban sandstone of the study area is an acidic rock derivation and intermixing of granite and granodioritic source rocks. When the Bhuban sandstone samples are plotted in the bivariate diagram of Zr/Sc vs Th/Sc, it can be inferred that most of the Bhuban sandstones retained their original composition, however, some samples are sourced from recycled sediments.

Different classification schemes are employed to classify the Bhuban sandstones within the study area. The Q-F-L and Q-F-R ternary plot demonstrates that most of the samples in the study area are sublitharenite, with few subarkose.

However, major element geochemistry suggested that the sandstones are litharenite, lithic sandstone, and greywacke.

To ascertain the depositional environment and the degree of weathering of the sediments for the Bhuban sandstones in the study area, a variety of ternary and bivariate plots are utilized. All the discrimination plots indicated that the Bhuban sandstones of Lunglei are deposited under humid to semi-humid climatic conditions in low-relief areas (plains). The degree of weathering for the sandstone of the study area is assessed using the ternary plot of Nesbitt and Young (1982) and different weathering parameters. Based on the analysis, the sediments are chemically immature to mature and have undergone mild to moderate weathering.

The tectonic setting of the Bhuban sandstones in the study area is represented using the petrographic modal data. All the analyzed samples showed a quartzose recycled and craton interior in the QFL and QmFLt ternary plots. Texturally immature sediments are also advocated by the abundance of rock fragments and angular to sub-angular detrital grains. However, the discrimination diagram using geochemical data indicated an active continental margin tectonic setting for the Bhuban sandstones of Lunglei.

CONCLUSION

1. The study area is constituted by a repeated succession of arenaceous and argillaceous in various proportions belonging to the Middle Bhuban and Upper Bhuban formations of the Surma group.
2. The petrographic analysis shows that the detrital components are mainly quartz, feldspars, and rock fragments including micas. Cementing materials are argillaceous, siliceous, calcite, and ferruginous cement. Important rock fragments include chert, shale, slate, and schist.
3. The petrographic study also reveals that the framework grains are represented by moderately sorted, angular to sub-rounded, and medium to fine-grained textures. X-ray diffraction analysis of shale samples shows an intense peak in Quartz, cristobalite, and muscovite. Among the clay minerals, chlorite and illite are prominent.
4. Based on the different provenance discrimination plots, it can be inferred that the sediments under study are derived from granitic rocks and middle to upper-rank metamorphic rocks. The sediments are transported at a moderate distance or undergo reworking. They are sourced from the continental block provenance and are immature to mature sediments. Texturally immature sediments are also advocated by the abundance of rock fragments and angular to sub-angular detrital grains.
5. Different classification schemes show that the sandstones in the study area are sublitharenite, lithic sandstone, and greywacke with few subarkose.
6. Various discrimination plot reveals that the Bhuban sandstones of Lunglei are deposited under humid to semi-humid climatic conditions in low-relief areas (plains). The sediments are chemically immature to mature and have undergone mild to moderate weathering.
7. The petrographical evidence showed the quartzose recycled and craton interior tectonic setting for the Bhuban sandstones in the study area. Further, the discrimination diagram using geochemical data indicated an active continental margin tectonic setting.

REFERENCES

Al-Juboury, A. (2012). A combined petrological-geochemical study of the Paleozoic successions of Iraq. *Petrology- New Perspectives and Application*. 169-198.

Allègre C.J, Minster J.F. (1978). Quantitative models of trace element behavior in magmatic processes. Earth Plan Sci Lett 38:1–25.

Alam, Mahmood & Curray, Joseph & Chowdhury, M. Lutfar & Gani, M. (2003). An overview of the sedimentary geology of the Bengal Basin in relation to the regional tectonic framework and basin-fill history. Sedimentary Geology. 155(3-4), 179-208.

Argast, S., Donnely, T.W. (1987). The Chemical Discrimination of Clastic Sedimentary Composition. J. Sediment. Petrol. 57, 813–823.

Armstrong-Altrin, J.S., (2009). Provenance of sands from Cazones, Acapulco, and Bahía Kino beaches, México. Rev. Mex. Ciencias Geol. 26, 764–782.

Armstrong-Altrin, J. S., Nagarajan, R., Lee, Y. I., Kasper-Zubillaga, J. J., and Cordoba Saldana, L. P. (2014). "Geochemistry of sands along the San Nicolas and San Carlos beaches, Gulf of California, Mexico: Implication for provenance". Turkish Journal of Earth Science. 23: 533–558.

Banerjee, S. P., Sarkar, K., Dasgupta, S. (1979). Geological Mapping in parts of Serchip-Thenzuwal area and Mineral Survey, Aizwal dist., Mizoram. Unpub. Prog. Report, Geol. Surv. India.

Basu, a, Young, S.W., Young, S.W., Suttner, L.J., Suttner, L.J., James, W.C., James, W.C., Mack, G.H., Mack, G.H. (1975). Re-evaluation of the use of undulatory extinction and polycrystallinity in detrital quartz for provenance interpretation. J. Sediment. Res. https://doi.org/10.1306/212F6E6F-2B24-11D7-8648000102C1865D

Bharali, B., Borgohain, P., Bezbaruah, D., Vanthangliana, V., Phukan, P. P., and Rakshit, R. (2017). "A geological study on Upper Bhuban Formation in parts of Surma Basin, Aizawl, Mizoram". Science Vision. 17(3): 128-147.

Bhatia, M. R. (1983). "Plate tectonics and geochemical composition of sandstones". Journal of Geology. 91: 611–627.

Bhatia, M.R. (1985). “Rare earth element geochemistry of Australian Paleozoic graywackes and mudrocks: provenance and tectonic control”. Sedimentary Geology. 45: 97–113.

Bhatia, M. R. and Crook, K. A. W. (1986). “Trace element characteristics of graywackes and tectonic setting discrimination of sedimentary basins”. Contributions to Mineralogy and Petrology. 92: 181-193.

Blatt, H. (1967). “Original characteristics of clastic quartz grains”. Jour. Sed. Petrol. 37: 401-424.

Blatt, H., Middleton, G., Murray, R. (1980). Origin of Sedimentary Rocks. Prentice Hall, New Jersey.

Borgohain, P., (2012). “Grain size distribution of Tipam sandstones in TipongPani river section, Assam”. Indian Journal of Research. 1(4): 4-6.

Bracciali, L., Marroni, M., Luca, P., Sergio, R., (2007). “Geochemistry and petrography of Western Tethys Cretaceous sedimentary covers (Corsica and Northern Apennines): From source areas to configuration of margins”. Geol. Soc. Am. Spec. Pap. 420: 73–93.

Bracciali, L., Najman, Y., Parrish, R.R., Akhter, S.H., Millar, I. (2015). The Brahmaputra tale of tectonics and erosion: Early Miocene river capture in the Eastern Himalaya. Earth Planet. Sci. Lett. 415, 25–37. https://doi.org/10.1016/j.epsl.2015.01.022

Chaudhuri, A., Banerjee, S. and Gaurav Chauhan, G. (2020). Compositional evolution of siliciclastic sediments recording the tectonic stability of apericratonic rift: Mesozoic Kutch Basin, western India. *Mar. Pet, Geol*. 111: 476-495.

Condie, K. C. (1993). “Chemical composition and evolution of upper continental crust: Contrast-ing results from surface samples and shales”. Chemical Geology. 104: 1– 37.

Conolly, J.R. (1965). The occurrence of polycrystallinity and undulatory extinction in quartz in sandstones. J. Sediment. Petrol. 35, 116–135.

Cox, R., Lowe, D.R., Cullers, R.L., 1995. The influence of sediment recycling and basement composition on the evolution of mudrock chemistry in the southwestern United States. Geochim. Cosmochim. Acta 59, 2919–2940. https://doi.org/10.1016/0016-7037(95)00185-9.

Crook, K. A. W. (1974). "Lithogenesis and geotectonics: The significance of compositional variation in flysch arenites (greywackes): in R.H. Dott., and R.H. Shavar (Eds.) Modern and ancient geosynclinals Sedimentation". Soc. Econ. Palaeonton. Mineral. Spec. Publ. 19: 304-310.

Cullers, R.L., 1994. The controls on the major and trace element variation of shales, siltstones, and sandstones of Pennsylvanian-Permian age from uplifted continental blocks in Colorado to platform sediment in Kansas, USA. Geochim. Cosmochim. Acta 58, 4955–4972. https://doi.org/10.1016/0016-7037(94)90224-0

Cullers, R.L., 2000. The geochemistry of shales, siltstones and sandstones of Pennsylvanian-Permian age, Colorado, USA: Implications for provenance and metamorphic studies. Lithos 51, 181–203. https://doi.org/10.1016/S0024-4937(99)00063-8

Cullers, R. L., Barrett, T., Carlson, T. and Robison, B., (1987). "Rare-earth element and mineralogical changes in Holocene soil and stream sediment: a case study in the Wet Mountains, Colorado, U.S.A.". Chem. Geol.63: 275-297.

Cullers, R. L. and Podkovyrov, V. N., (2000). "Geochemistry of the Mesoproterozoic Lakhanda shales in south-eastern Yakutia, Russia: Implications for mineralogical and provenance control, and recycling". Jour. Precambrian Res. 104: 77–93.

Cullers, R.L., Podkovyrov, V.N., 2002. The source and origin of terrigenous sedimentary rocks in the meso-proterozoic Ui group, south-eastern Russia.

Precambrian Res. 117, 157–183. https://doi.org/10.1016/S0301-9268(02)00079-7.

Curray, J.R. (1991). Geological history of the Bengal geosyncline. J. Assoc. Explor. Geophys. XII, 209–219.

Dapples, E. C. (1962). “Stages of Diagenesis in the development of sandstone”. Geol. Soc. Am. Bull. 73: 913-933.

Das Gupta, S. (1984). Tectonic trends in the Surma Basin and possible genesis of the folded belt. Rec. Geol. Surv. Ind., 113(IV): 58 - 61.

Dasgupta, S., Nandy, D. R. (1995). Geological framework of the Indo-Burmese convergent margin with special reference to ophiolitic emplacement. Indian J. Geol. 67(2), pp. 110–125.

Dickinson, W.R. (1983). Provenance of North American Phanerozoic sandstones in relation to tectonic settings. Geol. Soc. Am. Bull. https://doi.org/10.1130/0016-7606(1983)94<222:PONAPS>2.0.CO;2**.**

Dickinson, W. R. (1985). “Interpreting Provenance Relations from Detrital Modes of Sandstones, in Zuffa, G.G., ed”. Provenance of Arenites: Boston, D. Reidel: 333- 361.

Dickinson, W. R. and Suczek, C. (1979). “Plate tectonics and Sandstone Composition”. American Association of Petroleum Geologists Bulletin. 63: 2164-2182.

Dickinson, W. R., Bead, L. S., Brakenridge, G. R., Erjavec, J. L., Ferguson, R. C., Inman, K. F., Kenpp, R. A., Lindberg, F. A and Ryberg, P. T. (1983). “Provenance of North American Phanerozoic sandstones in relation to the tectonic setting”. Geol Soc Am Bull. 94: 222-235.

Duhawma, K and Shiva Kumar. (2014). Petrochemistry of Bhuban Formation rocks in and around Aizawl City, Mizoram, India. *Sci Vis.* 14 (2),74-83.

Dupre, B., Gaillardet, J., Rousseau, D., and Allegre, C. (1996). “Major and trace elements of river-borne material: the Congo Basin”. Geochim. Cosmochim. Acta. 60: 1301- l 321.

Evans, P., (1932). “Tertiary succession in Assam”. Trans. Min. Geol. Inst. India. 27: 155– 260.

Evans, P., (1964). “Tectonic Framework of Assam”. *Jour. Geol. Soc. India*. 5. 80-96.

Fedo, C.M., Nesbitt, H.W., Young, G.M., 1995. Unraveling the effects of potassium metasomatism in sedimentary rocks and paleosols, with implications for paleo weathering conditions and provenance. Geology. https://doi.org/10.1130/0091-7613(1995)0232.3.CO

Feng, R., and Kerrich, R. (1990). “Geochemistry of fine-grained clastic sediments in the Archean Abitibi greenstone belt, Canada: implications for provenance and tectonic setting”. Geochimica et Cosmochimica Acta. 54: 1061–1081.

Floyd, P.A., Winchester, J.A., Park, R.G., 1989. Geochemistry and tectonic setting of Lewisian clastic metasediments from the Early Proterozoic Loch Maree Group of Gairloch, NW Scotland. Precambrian Res. 45, 203–214. https://doi.org/10.1016/0301-9268(89)90040-5

Folk, R.L. (1980). Petrologie of sedimentary rocks, Hemphill Publishing Company, Austin. https://doi.org/10.1017/CBO9781107415324.004.

Fu X, Wang J, Zeng Y, Tan F, Feng X. (2010) REE geochemistry of marine oil shale from the Changshe Mountain area, northern Tibet. China Int J Coal Geol 81:191–199.

Fu X, Wang J, Zeng Y, Tan F, He J. (2011) Geochemistry and origin of rare earth elements (REEs) in the Shengli River oil shale, northern Tibet. China Chem Erde 71:21–30.

Fyffe, L. R. and Pickerill, R. K. (1993). Geochemistry of Upper Cambrian – Lower Ordovician black shale along a northeastern Appalachian transect. Bull. Geol. Soc. Am. 105: 897-910.

Ganguly, S. (1975). “Tectonic Evolution of Mizo Hills”. Bull. Geol. Min. Met. Soc. India.48: 28-40.

Ganju, J.L. (1975). Geology of Mizoram. Geol. Mineralogy Metall. Soc. India 17–26.

Gansser, A. (1964). Geology of the Himalayas, Interscience. *New York, 273*.

Gazzi-Dickinson (1966). Le arenarie del flysch sopracretaceo dell’ Appennino modenese; correlazioni con il flysch di Monghidoro. Mineral. e Petrogr. Acta 12, 69–97.

Goldstein, S. J., and Jacobsen, S. B. (1988). “Rare earth elements in river waters. Earth Planet”. Sci. Lett. 89: 35-47.

Govind, G., Najman, Y., Copley, A., Millar, I., van der Beek, P., Grujic, D., and Davenport, J. (2018). “Timing and mechanism of the rise of the Shillong Plateau in the Himalayan foreland”. Geology. 46: 279-282.

Grantham, J. J., and Velbel, M. A. (1998). “The influence of climate and topography on rock fragment abundance in modern fluvial sands of the southern Blue Ridge Mountains, North Carolina”. Jour. Sedimentary Petrology. 58: 219-227.

Gromet, L.P., Haskin, L.A., Korotev, R.L., Dymek, R.F. (1984). The “North American shale composite”: Its compilation, major and trace element characteristics. Geochim. Cosmochim. Acta 48, 2469–2482. https://doi.org/10.1016/0016- 7037(84)90298-9.

Harnois, L. (1988). The CIW index: A new chemical index of weathering. Sediment. Geol. 55, 319–322. https://doi.org/10.1016/0037-0738(88)90137-6.

Hayashi, K.I., Fujisawa, H., Holland, H.D., Ohmoto, H. (1997). “Geochemistry of ~1.9 Ga sedimentary rocks from northeastern Labrador, Canada”. Geochim. Cosmochim. Acta. 61: 4115–4137.

Herron, M. M. (1988). “Geochemical classification of terrigenous sand and shales from a core or log data”. Sed. Petrol. 58: 820-829.

Holland, H.D. (1978). “The Chemistry of the Atmosphere and Oceans”. New York, Wiley. 351.

Hossain, Z. M. H., and Roser, B. (2006). “Major and trace elements analysis of Tertiary sedimentary rocks from the Sylhet Basin, Bangladesh”. Geoscience Rept. Shimane Univ. 25: 49-59.

Hussain, M. F. and Bharali, B. (2019). “Whole-rock geochemistry of Tertiary sediments of Mizoram foreland basin, NE India: implications for source composition, tectonic setting, and sedimentary processes”. Acta Geochim. https://doi,org/10.1007/s11631-109-00315-3.

Ingersoll, R. V. (1978). Pertofacies and petrologic evolution of the Late Cretaceous forearc basin, Nothern and Central California. J. Geol. 68, 335–352.

Ingersoll, R. V., and Suczek, C. A. (1979). “Petrology and provenance of Neogene sand from Nicobar and Bengal fans, DSDP sites 211 and 218”. Journal of Sedimentary. Petrology. 49: 1217–1228.

Islam, M. J. and Rahman, M. J. J. (2009). “Geochemical Analysis of the Miocene Surma Group Sediments from the Meghna Gas Field, Bengal Basin, Bangladesh”. *Jahangirnagar University Journal of Science*. 32 (1). 29-46.

Jason, R. P., and Michael, A. V. (2003). “Chemical weathering indices applied to weathering profiles developed on heterogenous felsic metamorphic parent rocks”. Chemical Geology. 202: 397-416.

Johnsson, M. J. (1993). “The system controlling the composition of clastic sediments, in Johnsson, M. J., and Basu, A., eds., processes controlling the composition of clastic 172 sediments: Boulder, Colorado”. Geological Society of America, Special Paper. 284: 1-19.

Jinliang, Z., Xin, Z. (2008). “Composition and Provenance of Sandstones and Siltstones in Paleogene, Huimin Depression, Bohai Bay Basin, Eastern China”. J. China Univ. Geosci. 19: 252–270.

Karunakaran, C. (1974). *Geology and Mineral resources of the states of India*. Misc. Publ. Geol. Surv. India. 30(IV). 93-101.

Krishnamurthy, R. V., Bhattacharya, S. K. and Kusumgar, S. (1986). "Palaeoclimatic changes deduced from 13C/12C and C/N ratios of Karewa lake sediments, India". Nature. 323: 150–52.

Kroonenberg, S.B. (1992). Effects of provenance, sorting, and weathering on the geochemistry of fluvial sands from different tectonic and climatic environments. Proc. 29th Int. Geol. Congr. 69–81.

Laird, K. R., Cumming, B. F., Wunsam, S., Rusak, J. A., Oglesby, R. J., Fritz, S. C. and Leavitt, P. R. (2003). "Lake sediments record large-scale shifts in moisture regimes across the northern prairies of North America during the past two millennia". Proc. Natl. Acad. Sci. 100: 2483–2488.

Lallianthanga, R.K and Laltanpuia, Z.D. (2013). Landslide Hazard zonation of Lunglei town, Mizoram, India using High Resolution Satellite Data. *International Journal of Advance Remote Sensing and GIS*. 2(1), 148-159.

Lalmuankimi, C., Tiwari, R. P., Jauhri, A.K. and Ralte, V. Z. (2010). "Foraminifera from the Upper Bhuban Formation of Mizoram". Journal of the Paleontological Society of India. 55(1): 71-75.

Lalmuankimi, C., Kumar, S., Laldinpuia and Tiwari, R. P. (2011). "Geochemical study of upper Bhuban sandstone in Muthi, Mizoram, India". *Sci Vis Jour*. 11 (1). 40-46

Lalmuankimi, C. (2013). Geochemical study on Upper Bhuban shale in Aizawl district of Mizoram, India: an implication of chemical weathering, geochemical classification, tectonic setting, and provenance. *Sci Vis*. 14 (1), 18-27

Lalnunmawia, J., and Lalhlimpuii, J. (2014). "Classification and provenance studies of the sandstones exposed along Durtlang road section, Aizawl, Mizoram". Science Vision. 14(3): 158-167.

Le Maitre, R.W. (1976). “The chemical variability of some common igneous rocks”. J. Petrol. 17: 589–598.

Long, X., Yuan, C., Sun, M., Safonova, I., Xiao, W., Wang, Y. (2012). Geochemistry and U-Pb detrital zircon dating of Paleozoic graywackes in East Junggar, NW China: Insights into subduction-accretion processes in the southern Central Asian Orogenic Belt. Gondwana Res. 21, 637–653. https://doi.org/10.1016/j.gr.2011.05.015

Ma, S., Li, J., Wang, L. (2021). Provenance, tectonic setting and source-area paleo weathering of the Upper Paleozoic sandstones in the northwestern Ordos Basin, China: evidence from whole-rock geochemistry. *Carbonates Evaporites* 36, 64 (2021). https://doi.org/10.1007/s13146-021-00729-2.

Mannan, A. (2002). *Stratigraphic Evolution and Geochemistry of Neogene Surma Group, Surma Basin, Sylhet, Bangladesh*. 2, 59-113.

McLennan, S. M. (1989). “Rare earth elements in sedimentary rocks: influence of the provenance and sedimentary process”. Geochemistry and Mineralogy of Rare Earth Elements. 21: 169-200.

McLennan, S.M, and Taylor, S.R. (1991). “Sedimentary rocks and crustal evolution: tectonic setting and secular trends”. Journal of Geology. 99: 1–21.

McLennan, S.M., Taylor, S.R., McCulloch, M.T., and Maynard, J.B. (1990). “Geochemical and Nd-Sr isotopic composition of deep-sea turbidites: crustal evolution and plate tectonic associations”. Geochimica et Cosmochimica Acta. 54: 2015–2050.

McLennan, S.M, and Taylor, S.R. (1991). “Sedimentary rocks and crustal evolution: tectonic setting and secular trends”. Journal of Geology. 99: 1–21.

Mc Lennan, S. M., Hemming, S., McDaniel, D. K. and Hanson, G. N. (1993). “Geochemical approaches to sedimentation, provenance, and tectonics In Johnsson, M. J., and Basu, A. (Eds), Processes controlling the consumption of clastic sediments”. Geological Society of America, Spec. Paper. 284: 21-40.

Middleton, G. V. (1960). “Chemical composition of sandstones”. Geological Society of America. Bulletin. 71: 1011-1026.

Mitchell, A. H. G. (1993). Cretaceous – Cenozoic tectonic events in the Western Myanmar (Burma)-Asia region. J. Geol. Soc. London, 150, pp.1089-1102.

Mitchell, A. H. G., Reading, H.G. (1986). Sedimentation and tectonics. Sedimentary Environments and Facies (Reading, H. G., ed.). Blackwell Scientific Publications.

Mongelli, G., Critelli, S., Perri, F., Sonnino, M., Perrone, V. (2006). “Sedimentary recycling, provenance and paleo weathering from chemistry and mineralogy of Mesozoic continental redbed mudrocks, Peloritani mountains, southern Italy”. Geochem. J. 40: 197–209.

Najman, Y., Garzanti, E. (2000). Reconstructing early Himalayan tectonic evolution and paleogeography from Tertiary foreland basin sedimentary rocks, northern India. Bull. Geol. Soc. Am. 112, 435–449. https://doi.org/10.1130/0016-7606(2000)1122.0.CO;2.

Nandy, D. R. (1982). Geological Set Up of the Eastern Himalayas and the Patkai - Naga-Arakan-Yoma (India – Burma) Hill ranges in relation to the Indian Plate Movement. Misc. Publ. Geol. Surv. Ind., 41: 205 - 213.

Nesbitt, H. W. (1979). “Mobility and fractionation of rare earth elements during weathering of a granodiorite”. Nature. 279: 206-210.

Nesbitt, H.W., Young, G.M. (1982). Early proterozoic climates and plate motions were inferred from the major element chemistry of lutites. Nature 299, 715–717. https://doi.org/10.1038/299715a0

Ohr, M., Halliday, A. N. and Peacor, D. R. (1994). “Mobility and fractionation of the rare earth elements in argillaceous sediments: implications for dating diagenesis and low-grade metamorphism”. Geochim. Cosmochim. Acta. 58: 289-312.

Parker, A. (1970). An Index of Weathering for Silicate Rocks. Geol. Mag. 107, 501–504. https://doi.org/10.1017/S0016756800058581

Pearson, K. (1895). Contributions to the Mathematical Theory of Evolution. II. Skew Variation in Homogeneous Material. Philos. Trans. R. Soc. A Math. Phys. Eng. Sci. 186, 343–414. https://doi.org/10.1098/rsta.1895.0010.

Periasamy, V. and Venkatashwarlu, M. (2017). "Petrography and Geochemistry of Jurassic Sandstones from the Jhuria Formation of Jara dome, Kachchh Basin, India: Implication for Provenance and Tectonic Setting". Journal of Earth System Science. 126(44): 1-20.

Pettijohn, F. J. (1975). "Sedimentary rocks, 3rd ed. Harper and Row, New York". 624-629.

Pettijohn, F.J., Potter, P. E. and Siever, R. (1973). Sand and Sandstone. Springer Verlag, New Work.

Plank, T., Langmuir, C.H. (1998). The chemical composition of subducting sediment and its consequences for the crust and mantle. Chem. Geol. 145, 325–394. https://doi.org/10.1016/S0009-2541(97)00150-2.

Rahman and Mc Cann. (2011). "Sandstone diagenesis of the Neogene Surma Group from the Shahbazpur Gas Field, Southern Bengal Basin, Bangladesh". *Austrian Journal of Earth Sciences* Vol. 104(1), 1-13.

Rahman, M. J. J. and Suzuki, S. (2007). "Geochemistry of sandstones from the Miocene Surma Group, Bengal Basin, Bangladesh: Implications for Provenance, tectonic setting, and weathering". *Geochem. Jour*. 41. 415-428.

Rahman, M.J.J., Faupl, P., Alam, M.M. (2009). Depositional facies of the subsurface Neogene Surma Group in the Sylhet Trough of the Bengal Basin, Bangladesh: Record of tidal sedimentation. Int. J. Earth Sci. 98, 1971–1980. https://doi.org/10.1007/s00531-008-0347-7.

Rai, J., Malsawma, J., Lalchhanhima, C., Lalnuntluanga, P.,.,Ralte, V. Z. and Tiwari, R. P. (2014). "Nannofossil Biostratigraphy from Bhuban Formation,

Mizoram, Northeastern India, and its paleoenvironmental interpretations". Special publication of the Paleontological Society of India. 5: 121-134.

Rajkonwar, C., Tiwari, R. P., Ralte, V. Z. and Patel, S. J. (2014). "Additional Ichnofossils from Middle Bhuban unit, Bhuban Formation, Surma Group (Lower to middle Miocene), Mizoram and their environmental significance". Special publication of the Paleontological Society of India. 5: 257-271.

Raju, A. T. R. (1968). Geological evolution of Assam and Cambay/Basins of India. *Am. Assoc. Pet. Geol. Bull*., 52**:**2422-2437.

Ralte, V. Z. (2012). "Heavy mineral analysis of Tipam sandstone near Buhchang village, Kolasib district, Mizoram, India". Sci Vis. 12(1): 22-31.

Rintluanga, Pachuau. (1994). "Geology of Mizoram (1st edition)", New Aizawl Press, Chandmari, Aizawl. 54.

Rose, N. L., Boyle, J. F., Du, Y., Yi, C., Dai, X., Appleby, P. G., Bennion, H., Cai, S. and Yu, L. (2004). "Sedimentary evidence for changes in the pollution status of Taihu in the Jiangsu region of eastern China". Jour. Paleolimnol. 32: 41–51.

Roser, B.P., and Korsch, R.J. (1986). "Determination of tectonic setting of sandstone mudstone suites using SiO_2 content and K_2O/Na_2O ratio". Journal of Geology. 94: 635–650.

Rowley, D.B. (1996). Age of initiation of collision between India and Asia: A review of stratigraphic data. Earth Planet. Sci. Lett. https://doi.org/10.1016/S0012-821X(96)00201-4.

Roy, K. D., Rahman, Mostafizur Md. and AktherSarmin. (2006). "Provenance of exposedTipamsandstoneformation, Surma Basin, Sylhet, Bangladesh." J.Life Earth Science. 1(2): 35-42.

Rudnick, R.L., Gao, S. (2003). 3.01 - Composition of the Continental Crust, Treatise on Geochemistry. https://doi.org/http://dx.doi.org/10.1016/B0-08-043751-6/03016-4.

Saeed, N. E., Barzi, M. H. and Armstrong-Altrin, J. S. (2011). “Petrography and geochemistry of clastic sedimentary rocks as evidence for the provenance of the lower Cambrian Lalun Formation, Posht-e-badam block, Central Iran”. Jour. Of African Earth Sciences. 61: 142-159.

Sarkar, K. and Nandy, D. R. (1977). Structures and Tectonics of Tripura - Mizoram area, India. Geol. Surv. India. Misc. Publ., 34(1): 141 - 148.

Sarma, J. N., and Chutia, A. (2013). “Petrography of sub-surface Tipam sandstone formation of a part of Assam basin, India”. Global Research Analysis. 2(2): 112-113.

Sarma, J. N., and Chutia, A, (2013). “Petrography and heavy mineral analysis of Tipam sandstone exposed on the Tipam hill of Sita Kunda area, Upper Assam, India”. South East Asian Journal of Sedimentary Basin Research. 1: 28-34.

Schoenborn, W.A., Fedo, C.M. (2011). “Provenance and paleo weathering reconstruction of the Neoproterozoic Johnnie Formation, south-eastern California”. Chem. Geol. 285: 231–255.

Seiver, R. (1979). Plate tectonic controls on diagenesis. Journal of Geology, 87: 127-155.

Sengupta, S. (1966). “Geological and geophysical studies in the western part of Bengal Basin, India”. Am. Assoc. Pet. Geol. Bull. 50: 1001-1017.

Sengupta, S. (1994). “Textbook on Sedimentology”. Oxford Publication, New Delhi. 314319.

Singh, Y. R., Sijagurumayum, U. and Guruaribam, V. (2011). “Paleoecology of the Upper Bhuban and Tipam sediments of Mizoram, India- Palynological evidence”. Himalayan Geology. 32(1): 57-62.

Slack, J.F., and Stevens, P.J. (1994). “Clastic metasediments of the Early Proterozoic Broken Hill Group, New South Wales, Australia: geochemistry, provenance,

and metallogenic significance". Geochimica et Cosmochimica Acta. 58: 3633–3652.

Shrivastava, B. P., Ramachandran, K. K. and Chaturvedi, J. G. (1979). "Stratigraphy of Eastern Mizo Hills". *Bull. ONGC*. 16(2). 87-94.

Taylor S.R, McLennan S.M. (1985) The continental crust: its composition and evolution. Blackwell, Oxford, pp 1–311.

Suttner, L. J., Basu, A. (1981). Climate and the origin of quartz arenites. J. Sediment. Petrol. 51, 1235–1246.

Suttner, L.J., Dutta, P.K. (1986). Alluvial sandstone composition and paleoclimate, I. Framework mineralogy. J. Sediment. Petrol. https://doi.org/10.1306/212F8909-2B24-11D7-8648000102C1865D.

Tiwari, R. P., Rajkonwar, C., Lalchawimawii, Lalnuntluanga, P., Malsawma, J., Ralte, V. Z. and Patel, S.J. (2011). Trace fossils from Bhuban Formation, Surma Group, (Lower to Middle Miocene) of Mizoram and their palaeoenvironmental significance. Journal Earth System Science, 120(6), pp. 1127 - 1143.

Tiwari, R. P. and Mehrotra, R. C. (2000). "Study of fossil wood from the Tipam Group (Neogene) of Mizoram, India". Tertiary Research. 20(1-4): 85-94.

Tortosa, A., Palomares, M., Arribas, J. (1991). Quartz grain types in Holocene deposits from the Spanish Central System: some problems in provenance analysis. Geol. Soc. London, Spec. Publ. 57, 47–54. https://doi.org/10.1144/GSL.SP.1991.057.01.05

Uddin, A and Lundberg, N. (1998). "Unroofing history of the eastern Himalaya and the Indo-Burma Ranges: Heavy-mineral study of Cenozoic sediments from the Bengal Basin, Bangladesh". Journal of Sedimentary Research. 68: 465-472.

Uddin, A., Lundberg, N. (1999). A paleo-Brahmaputra? Subsurface lithofacies analysis of Miocene deltaic sediments in the Himalayan-Bengal system,

Bangladesh. Sediment. Geol. 123, 239–254. https://doi.org/10.1016/S0037-0738(98)00134-1.

Uddin, A., and Lundberg, N. (2003) “Miocene sedimentation and Subsidence during Continent-Continent Collision, Bengal Basin, Bangladesh”. *Sedimentary Geology.*164: 131-146.

Uddin, A., and N. Lundberg. (2004), Miocene sedimentation and subsidence during a continent-continent collision, Bengal basin, Bangladesh, Sediment. Geol., 164, pp. 131 – 146.

Weltje, G.J. (1994). Provenance and dispersal of sand-sized sediments: reconstruction of dispersal patterns and sources of sand-sized sediments by means of inverse modeling techniques. Geol. Ultraiectina.

Wilde, P., Hunt, M. S. Q., and Erdtmann, B. D. (1995). “The Whole-rock Cerium anomaly: a potential indicator of eustatic sea-level changes in shales of the anoxic facies”. Sedimentary Geology. 101: 43-53.

BRIEF BIO-DATA

PERSONAL DETAILS: -

Name : K. LALDUHAWMA

Address : VENGLAI, LUNGLEI

Mobile No. : 9863224814/8787332182

E-mail id : duhawmakhawlhring290@gmail.com

Father's Name : K. LALTAWNA (L)

Mother's Name : C. LAWMKIMI

Marital Status : MARRIED

State of domicile : MIZORAM

Nationality : INDIAN

Category : SCHEDULED TRIBE

EDUCATIONAL QUALIFICATIONS: -

Sl.No.	Examination passed	Year	Board/University	Division	Percentage
1	HSLC	1991	MBSE	I	63 %
2	PU (Science)	1994	NEHU	II	47.30 %
3	B.Sc.	1997	NEHU	I	64.50 %
4	M.Sc.	1999	MYSORE UNIV.	I	77.10%
5	NET	2011	CSIR-UGC	-	-
6	Ph.D. Course Work	2017	MZU	A	6.63 SGPA

PERFORMANCE:

PUBLICATIONS

1	Depositional Environment and Diagenetic Process of Bhuban Sandstone: Constraints from the Petrographic Characteristics. Indian Journal of Science and Technology. 2023;16(SP1): 208–218
2	Petrographic characterization and diagenetic impact on Bhuban Sandstone of Surma Group, Aizawl, Mizoram: implications for provenance, tectonic setting, and reservoir quality. Journal of Sedimentary Environments. Received: 5 April 2023 / Revised: 19 November 2023 / Accepted: 20 November 2023

PRESENTATIONS

1	Petrographic approach of Bhuban formation exposed in the southern part of Surma Basin, Mizoram to constrain the Provenance, Tectonic settings, and Paleoclimatic conditions. National Conference on Emerging Trends in Environmental Research (NACETER) (31 Oct – 2 Nov 2019)
2	Depositional environment and diagenetic process of Bhuban sandstone: Constraints from the petrographic characteristics. Mizoram Science Congress (MSC), (24 – 25 Nov. 2022)

SEMINAR/TRAINING etc. ATTENDED

1	Five-day online Faculty Development Program on "New Pedagogies: Creative Learning & Creative Teaching – A Futuristic Approach" (Dashmesh Khalsa College, Ziragpur)
2	Three-day National Workshop on "Landslide hazard in Southern Mizoram". (MIRSAC, DGMR, LGC & GSM)
3	Emerging trends in Environmental Research (Dept. Of Environmental Science, PUC, Aizawl, Mizoram).
4	Fighting floods for survival in South Asia (Dept. of History, Govt. Zawlnuam College)
5	Impact of Covid 19 on migrant workers, employment & economy: Special reference to Mizoram (IQAC Govt. T. Romana Collge & MYC, Mizoram)
6	Learning in the 21st century (Govt. Serchhip College & HATIM, Mizoram)
7	Understanding our Rivers of Hilly Region and its Conservation (Conducted by Mizoram University).
8	Capacity building for SWAYAM Course & MOOCs – A different educational space (Conducted by Mizoram University)
9	One week international webinar on Natural Disasters with special emphasis on earthquakes and their implications (IQAC, Govt. Champhai College)

10	Earthquake versus Landslide with special reference to Mizoram (Conducted by Mizoram University)
11	Towards inclusive innovations and network-based entrepreneurship (Dept. of Management, Mizoram University)
12	Recent Earthquake in Indo-Burmese Ranges (Dept. of Geology, PUC)
13	New Education Policy 2020 and Higher Education in India (Dept. of Education, Govt. Zawlnuam College)
14	Faculty Development Programme on Moodle Learning Management System (Govt. Zirtiri Residential Science College)
15	One week national webinar on 'Motivation and Techniques in Research' (Govt. Hnahthial College)
16	Online Interdisciplinary Refresher Course on Environmental Studies and Disaster Management (UGC, HRDC, Mizoram University)
17	EDC Mizoram District Innovative Challenge on Business Solution to Sustainable Development Goals (Planning & Programme Implementation, Govt. of Mizoram and Lunglei Government College)
18	Webinar on Earth Day 2021 (DST, Govt. of Mizoram and GSM)
19	Mizoram Science Congress 2022 (MISTIC, MAS, MSS, STAM, GSM, MMS, BIOCON & MITS)
20	Webinar on Unconventional gas Reservoirs: Exploration, Extraction Methods and Challenges in India (Dept. of Geology, Mizoram University)
21	Improving livelihoods and addressing climate change through community-based natural resources management: Experience from Guatemala & Research Opportunities for NE India (Mizoram University & University of Minnesota)

PARTICULARS OF THE CANDIDATE

NAME OF THE CANDIDATE	:	K. LALDUHAWMA
DEGREE	:	Doctor of Philosophy
DEPARTMENT	:	Geology
TITLE OF RESEARCH	:	'PETROLOGY, PROVENANCE AND DEPOSITIONAL ENVIRONMENT OF BHUBAN FORMATION IN AND AROUND LUNGLEI TOWN, LUNGLEI DISTRICT, MIZORAM'
DATE OF ADMISSION	:	19th August 2016

APPROVAL OF RESEARCH PROPOSAL: -

1	DRC	:	21st April 2017
2	BOS	:	2nd May 2017
3	SCHOOL BOARD	:	4th August 2017

MZU REGISTRATION NO.	:	1607309
Ph.D REGISTRATION NO. & DATE	:	MZU/Ph.D/1043 of 31.05.2017
EXTENTION (IF ANY)	:	No.16-2/MZU(Acad)21/70-71, 25th Feb. 2022

HEAD
DEPARTMENT OF GEOLOGY
MIZORAM UNIVERSITY

ABSTRACT

PETROLOGY, PROVENANCE AND DEPOSITIONAL ENVIRONMENT OF BHUBAN FORMATION IN AND AROUND LUNGLEI TOWN, LUNGLEI DISTRICT, MIZORAM

AN ABSTRACT SUBMITTED IN PARTIAL FULFILLMENT OF THE REQUIREMENTS FOR THE DEGREE OF DOCTOR OF PHILOSOPHY

K. LALDUHAWMA

MZU REGISTRATION NO.: 1607309

Ph.D. REGISTRATION NO.: MZU/Ph.D./1043 of 31.05.2017

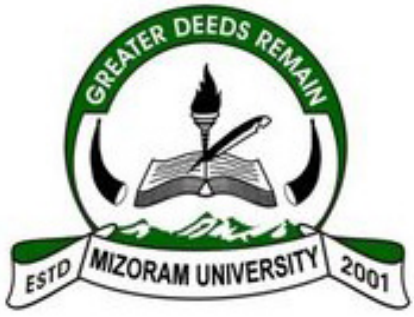

DEPARTMENT OF GEOLOGY

SCHOOL OF EARTH SCIENCES AND NATURAL RESOURCES MANAGEMENT

MAY, 2024

PETROLOGY, PROVENANCE AND DEPOSITIONAL ENVIRONMENT OF BHUBAN FORMATION IN AND AROUND LUNGLEI TOWN, LUNGLEI DISTRICT, MIZORAM

BY

K. LALDUHAWMA

DEPARTMENT OF GEOLOGY

NAME OF SUPERVISOR

Dr. V. VANTHANGLIANA

Submitted

In partial fulfillment of the requirement of the Degree of Doctor of Philosophy in Geology of Mizoram University, Aizawl.

ABSTRACT

The Miocene succession of the Bhuban formations belonging to the Surma Group is well-exposed in Mizoram. The vast majority of the rocks of Bhuban formations are composed of sandstone, siltstone, mudstone, and their various combinations. The study area covers the whole of Lunglei town and its surrounding areas. It is covered within the Survey of India Toposheet Nos. 84B/9 and 84B/13 and falls within the coordinates of 22°45’0” N latitudes to 23°0’0” N and 92°20’30” E to 92°51’30” E longitudes.

In this present work, various methods and techniques of sedimentary analyses like petrography and geochemistry are used to decipher the mode of formation, provenance, depositional history, tectonic setting, paleoclimatic condition, and nature of weathering. The present research work aims to establish the petrochemical characteristics of the main litho-unit belonging to the Bhuban formation in and around Lunglei Town and to explore provenance characteristics, depositional environment, and tectonic settings. The current study also attempts to explore the burial history of rocks where detrital sedimentary materials resulting from the disintegration of pre-existing rocks consolidated or lithified into sedimentary rock.

The study area is constituted by a repeated succession of arenaceous and argillaceous in various proportions belonging to the Middle Bhuban and Upper Bhuban formations of the Surma group. With gradational and transitional contact the upper Bhuban formation is underlain by the middle Bhuban formation. Shale and siltstone are the important rocks in the middle Bhuban formation, whereas, the dominant rock type of the upper Bhuban formation is sandstone which is mostly encountered along the limbs of anticlines. Sandstones exposed in the study area vary from fine grey, fine to medium brown color alternated with various proportions of clay and silt size particles of shales. The southern part of the town and its adjoining areas are dominated by argillaceous rocks of the Middle Bhuban formation which is characterized by occasional sandstone beds with thick shale beds. Most of the shales are grey, olive green to yellowish brown in color and exhibit spheroidal pattern and

fissility. Frequent occurrences of silty shale beds and silty sandstone beds with thin lamination of sandstone beds are encountered throughout the middle Bhuban formation.

A total number of 37 (thirty-seven) samples of Bhuban sandstone from the study area are accounted for petrographic analysis. The framework grains are mainly quartz, feldspars, and rock fragments. Other detrital components include micas like muscovite and biotite.

Cementing materials identified are argillaceous, siliceous, calcite, and ferruginous cement. The petrographic study reveals that the framework grains are represented by moderately sorted, angular to sub-rounded, and medium to fine-grained textures. The most common type of detrital component is quartz, and non-undulose monocrystalline quartz is the most abundant type. Feldspar grains in the studied sandstones are angular to sub-angular in which potash feldspar dominates over plagioclase feldspar. Both sedimentary and metamorphic rock fragments are identified in the studied samples where the former is identified by their sedimentary character and the latter is identified by preferred orientation and high-order interference color. Important rock fragments reported include chert, shale, slate, and schist.

Mica commonly occurs as elongated, slender, flaky minerals showing cleavages. Muscovite and biotite are the two important mica observed in the present study area. Muscovite being more resistant to chemical alteration is more common than biotite. Authigenic and detrital bended mica flakes are also commonly observed. The cementing materials frequently observed in the examined sandstones are mainly siliceous, calcareous, ferruginous, and argillaceous cement.

The concentration of major oxides in Bhuban sandstones of Lunglei roughly corresponds to the UCC except for depletion in Na_2O, CaO, and K_2O. The ratio of K_2O/Na_2O all greater than 1 (>1) is also consistent with the petrographic data. When correlating major oxides against Al_2O_3, Bhuban sandstones of Lunglei show a negative correlation with SiO_2 and a positive correlation with K_2O, Fe_2O_3, and TiO_2. X-ray diffraction analysis of shale samples shows an intense peak in Quartz,

cristobalite, and muscovite. Among the clay minerals, chlorite and illite are prominent although overshadowed by the intense peak of quartz.

The UCC normalized trace element pattern shows narrow compositional changes for Nb, Pb, Zr, Mg, La, Ce, Sc, Ni, and Cr. In comparison with UCC, the Bhuban sandstone samples are enriched in Si, and Rb, as well as depletion of Ca, Th, Na, Ba, and Fe. Among the High Field Strength elements (HFSE), the depletion of Th, Y, and Ti may be associated with the source rocks. The common occurrence of K-feldspar, mica, and clay minerals may account for the high Rb level in the Bhuban sandstone.

The Chondrite normalized REE pattern of the Bhuban samples shows enrichment of LREE (La-Gd) and depletion of HREE (Tb-Lu) with negative Eu anomaly. The REE pattern of Bhuban sandstones of Lunglei is nearly identical to the UCC patterns. The extremely uniform REE pattern of the samples may suggest that the derivation of sediments has a certain homogeneity.

The provenance analysis for the Bhuban sandstones of Lunglei has been carried out using petrographic modal data and geochemistry. The different quartz varieties of Bhuban sandstones within the study area indicated their derivation from granitic rocks and middle to upper-rank metamorphic rocks. The modal analysis also suggested that the sediments are transported for a moderate distance or reworking of sediments. In addition, the sediments are immature and derived from the continental block provenance. However, the C-N-K ternary plots indicated the sediments came from granitic terrain. Based on the TiO_2 vs Ni bivariate plot and La-Th-Sc ternary plot, the Bhuban sandstone of the study area is an acidic rock derivation and intermixing of granite and granodioritic source rocks. When the Bhuban sandstone samples are plotted in the bivariate diagram of Zr/Sc vs Th/Sc, it can be inferred that most of the Bhuban sandstones retained their original composition, however, some samples are sourced from recycled sediments.

Different classification schemes are employed to classify the Bhuban sandstones within the study area. The Q-F-L and Q-F-R ternary plot demonstrates that most of the samples in the study area are sublitharenite, with few subarkose.

However, major element geochemistry suggested that the sandstones are litharenite, lithic sandstone, and greywacke.

To ascertain the depositional environment and the degree of weathering of the sediments for the Bhuban sandstones in the study area, a variety of ternary and bivariate plots are utilized. All the discrimination plots indicated that the Bhuban sandstones of Lunglei are deposited under humid to semi-humid climatic conditions in low-relief areas (plains). The degree of weathering for the sandstone of the study area is assessed using the ternary plot of Nesbitt and Young (1982) and different weathering parameters. Based on the analysis, the sediments are chemically immature to mature and have undergone mild to moderate weathering.

The tectonic setting of the Bhuban sandstones in the study area is represented using the petrographic modal data. All the analyzed samples showed a quartzose recycled and craton interior in the QFL and QmFLt ternary plots. Texturally immature sediments are also advocated by the abundance of rock fragments and angular to sub-angular detrital grains. However, the discrimination diagram using geochemical data indicated an active continental margin tectonic setting for the Bhuban sandstones of Lunglei.